Weather Forecasting for Soaring Flight

Technical Note No. 203

World
eteorological
rganization
her • Climate • Water

MO-No. 1038

Weather • Climate • Water

Weather Forecasting for Soaring Flight

Prepared by

Organisation Scientifique et Technique Internationale du Vol à Voile (OSTIV)

WMO-No. 1038

World Meteorological Organization
Weather • Climate • Water

2009 edition

WMO-No. 1038

Chairperson, Publications Board
World Meteorological Organization (WMO)
7 *bis*, avenue de la Paix
P.O. Box 2300
CH-1211 Geneva 2, Switzerland

Tel.: +41 (0) 22 730 84 03
Fax: +41 (0) 22 730 80 40
E-mail: publications@wmo.int

ISBN 978-92-63-11038-1

CONTENTS

FOREWORD

The key importance of soaring flight skills was recently highlighted in the media through the successful emergency "landing" over the Hudson River of an airliner which had fully lost its power. It is remarkable that the pilot involved in this emergency was also an experienced glider pilot, thereby underscoring the potential benefits of extending these skills to aviation as a whole.

The second edition of WMO Technical Note No. 158 *Handbook of Meteorological Forecasting for Soaring Flight* was released in 1993 as WMO-No. 495. From that time, significant changes have occurred in soaring flight forecasting, in particular since Numerical Weather Prediction has considerably progressed towards the spatial and temporal resolutions required to generate important physical variables needed for non-powered flight, such as climb rates and their temporal and spatial distributions.

Data volume from numerical weather prediction centres to pilots has increased significantly and improved predicted weather interfaces are now accessible to pilots. Available weather information and forecasts further support pre-flight decision-making and, reciprocally, flight recorders are contributing quantitatively to prediction improvement.

Accordingly, the International Scientific and Technical Soaring Organisation (OSTIV - Organisation Scientifique et Technique Internationale du Vol à Voile) meteorological panel, under the chairmanship of Mr Hermann Trimmel, took the initiative to produce this update in order to document progress achieved.

The following experts have contributed their knowledge, experience and time to this publication: René Heise (Germany), Wolf-Dietrich Herold (Argentina), Rolf Hertenstein (United States), Edward Hindman (United States), Olivier Liechti (Switzerland), Erland Lorenzen (Germany), Christof Maul (Germany), Daniel Murer (Switzerland), Beda Sigrist (Switzerland) and Hermann Trimmel (Austria). To make the publication truly international, the following experts served as reviewers: Zafer Aslan (Turkey), Tom Bradbury (United Kingdom), Dan Gudgel (United States), Joerg Hacker (Australia) and Bernt Olofsson (Sweden).

Mr Olivier Liechti has served as working group chairman and Mr Edward Hindman as editor. The European Cooperation in Science and Technology (COST) generously provided support to working group sessions and the NMSs of Germany and Switzerland kindly hosted the meetings. The final document has been reviewed by the WMO Commission for Aeronautical Meteorology (CAeM).

The aim of this Technical Note is to provide the reader an internationally agreed set of guidelines for meteorological forecasting in soaring flight and related activities. As pointed out in the Introduction, this includes forecasters at busy aerodrome meteorological offices routinely receiving enquiries from pilots, as well as those detached on the field to provide forecasting support during contests and shows.

WMO is therefore pleased to make this highly relevant publication available to the wider soaring flight community.

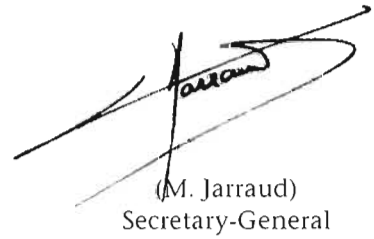

(M. Jarraud)
Secretary-General

INTRODUCTION

This publication has been prepared for everyone who is concerned with the meteorological support for gliding. This includes designers of pilot self-briefing systems and those who provide forecasts for pilots, as well as contest briefings. The publication is designed to help meteorological forecasters and pilot briefers respond to the requirements of glider flight operations.

A phenomenological description of atmospheric processes relevant to soaring presents the meteorological background for gliding activities. Convection is by large the most frequently used source of lift for gliders. The dynamical sources of lift are less frequent. They do, however, provide the opportunities for extremely fast and long flights. Soaring flight is occasionally limited by meteorological hazards.

A technical description of gliding and soaring flight is presented so that the impact of weather on feasibility, timing, range of operations and safety in soaring may be appreciated.

The classical forecasting framework of routine analysis and interpretation of prognostic charts must be extended to the smaller-scale features relevant to soaring. More and more numerical analysis and forecasting techniques that address these features are appearing. Soaring forecasts for both thermal and dynamic lift require a certain spatial and temporal resolution in order to be useful for meteorological flight planning. This publication addresses those issues.

The presentation of high-resolution weather forecasts to pilots is a challenging task. It is supported by new concepts, personal computers and the Internet. Sophisticated self-briefing systems have been developed: pilots may use high-resolution soaring forecasts for establishing flight plans for individual tasks. Personal briefings, however, are still appreciated by task-setters and pilots at soaring competitions. Preflight decision-making is supported by high-resolution forecasts and by the monitoring of weather observations in almost real time.

Finally, recorded flight data are presented that reveal the flight altitudes used, the climb rates achieved and the position of the updraughts. The data support both the development and the quality of numerical models for the prediction of soaring conditions. The simulation of documented soaring flights with the predicted weather demonstrates the skill of the state-of-the-art techniques in numerical weather prediction. Such simulations contribute quantitatively to the improvement of the numerical models.

CHAPTER 1

ATMOSPHERIC PROCESSES ENABLING SOARING FLIGHT

Whenever a glider deviates from a descending flight governed by the aerodynamic characteristics inherent in its design, atmospheric processes are at work. As it is the goal of glider pilots to use these processes to prolong the flight time and to increase the altitude or distance flown, it seems appropriate to begin this note with a description of the atmospheric processes relevant to soaring flight, which are the processes that produce rising and sinking air, or updraughts and downdraughts.

Note: In this publication rising air can take the names updraught, updraught rate, lift, climb, climb rate and lift rate. Typically, the rates refer to the speed a glider is moving away from the Earth's surface or the reading from the on-board vertical speed instrument (called the variometer). The other terms refer to the speed at which the air is rising. But a glider is always falling through the air due to its weight. Thus, in the case of rising air, the variometer reading is always slightly lower than the actual vertical air speed.

1.1 OVERVIEW

Updraughts in the atmosphere can be either of a convective (thermal) nature or driven by the horizontal flow deflected by terrain (Figure 1.1). For thermals to develop, solar radiation is needed as a main source of energy. Orography is the trigger for dynamically induced slope updraughts on the windward side, whereas on the lee side rotors and waves can develop in certain conditions. A horizontal flow of air above the convective boundary layer (CBL) may produce thermal waves as a combination of the two basic types of lift. The atmospheric flow patterns that can lift a glider are numerous; nature still has rich opportunities to surprise us.

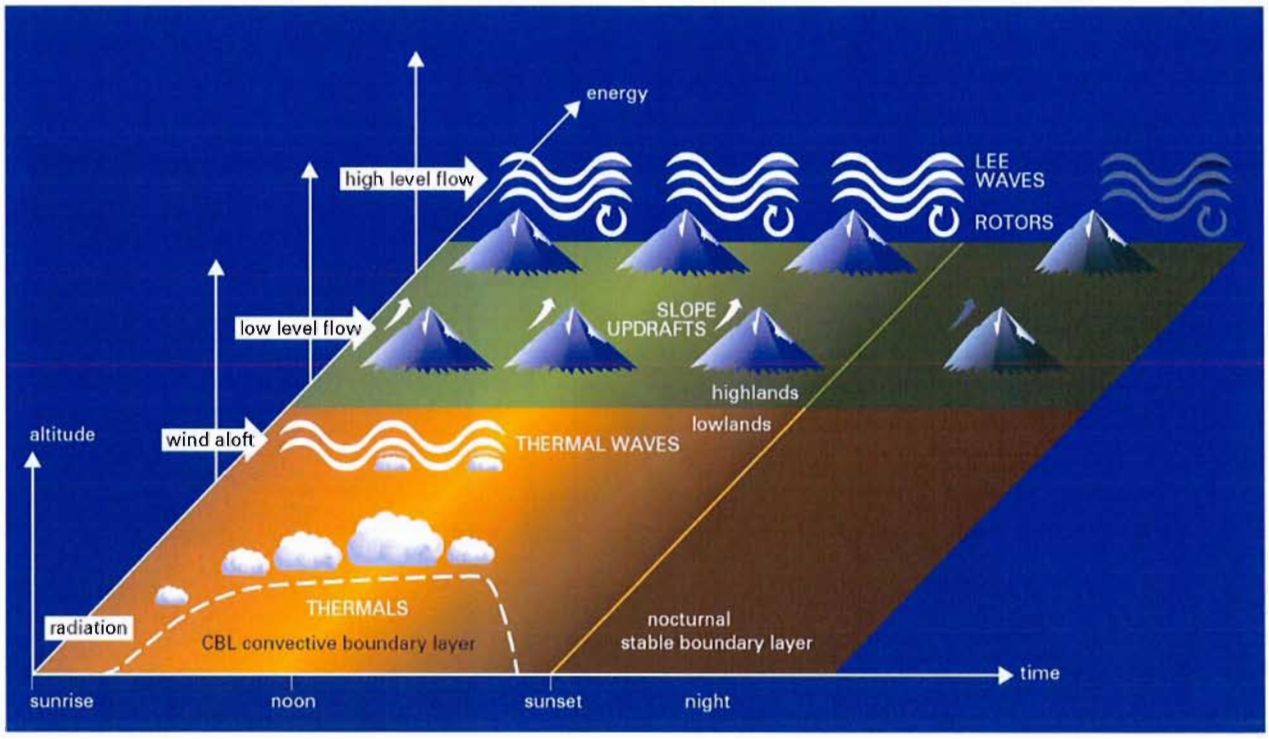

Figure 1.1. Principal sources of energy for gliding. The complex four-dimensional phenomena in nature are reduced here to a sketch, in which the main regimes are separated in a symbolic manner. The x-axis displays time and illustrates the lifetime of the updraughts in a diurnal cycle. The y-axis displays energy source and the z-axis displays altitude. Solar radiation produces thermals which, in turn, may interact with the upper-level winds to produce thermal waves. Low-level flow can be deflected by orography producing slope updraughts and high-level flow can favour lee waves.

Nowadays, thermals are the most common type of lift used for cross-country flights. For record flights, however, dynamic lift aligned in waves, in rotors and along ridges is much more favourable.

Different kinds of lift may be used in a single flight. It can be an unforgettable experience to climb in waves early in the day, use thermals later on and then return to dynamic lift in the evening. Dynamic lift also exists during the night, but flights are doubtful for safety reasons.

Each type of lift can be described in terms of its approximate horizontal extension and lifetime. Figure 1.2 presents the scales of the fundamental types of updraughts for gliding.

1.2 CONVECTIVE LIFT

1.2.1 Introduction

Convection is defined as heat transfer through vertical mass motions. When air is heated sufficiently from below or is cooled from above, rising and sinking convective currents are produced. Buoyancy is the force that causes the convective currents; it results when less dense air is adjacent to more dense air. Soaring pilots are interested in the relatively small-scale rising convective currents called thermals (Figure 1.3), which are microscale buoyant elements embedded within a mesoscale CBL.

Note: In this publication the CBL depth is defined as the distance between the surface and the tops of unsaturated thermals (so-called "blue thermals"). In the case of saturated thermals (that is, cumulus clouds), the CBL depth is the distance between the surface and cloud base.

Thermal forecasting requires an analysis of the atmospheric stability and knowledge of the environmental lapse rate. Examples are shown later in section 3.3.1, but first we will explore some characteristics of thermals.

1.2.2 Thermal size and strength

Thermals cover a broad spectrum of sizes and strengths, with characteristics varying from day to day, diurnally and by region. For instance, late-morning thermals are often small and weak, then become larger and stronger during midday and weaken towards evening, while remaining relatively large. Thermals tend to be stronger and more turbulent in desert and mountain areas, while they are weaker but more symmetric and manageable in the lowlands.

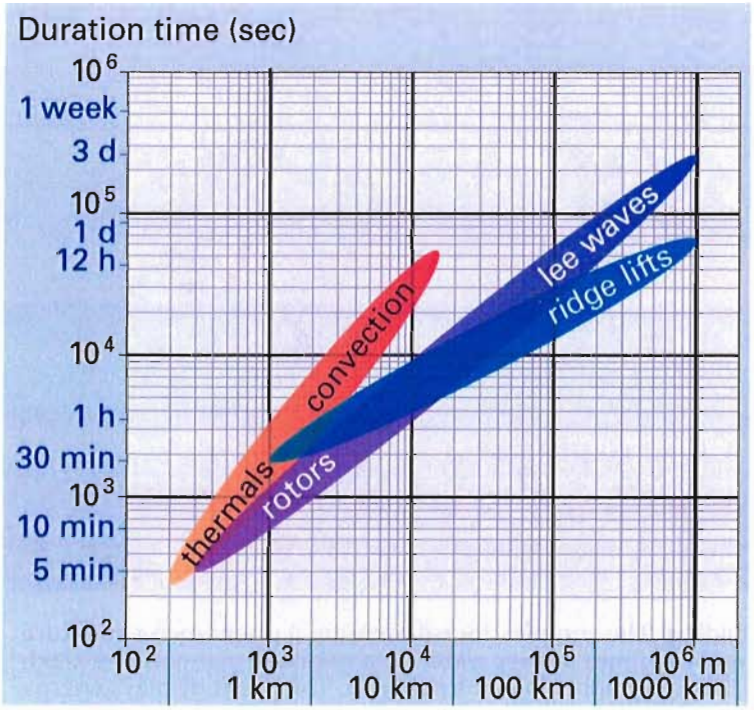

Figure 1.2. Scales of the patterns of atmospheric lift

Figure 1.3. A pilot's view of cumulus produced by vigorous thermals

Visual indicators of thermals include dust devils, haze domes (pre-cumulus clouds), cumulus clouds, as well as circling birds or gliders, all of which indicate a limited size. Individual thermal updraughts do not encompass broad areas as do other updraught types (for example, mountain lee waves). Turbulent eddies of many sizes constitute the CBL; thermals form a subset of these.

A typical thermal cross-section diameter is on the order of 150 to 300 metres, although individual specimens vary considerably from the norm. Fortunately for soaring pilots, the radius of turn of a circling glider falls into this range. A glider at a true airspeed of 98 km/h (50 knots) with a 40° bank angle flies a circle with a diameter of about 170 metres (550 feet). Thermals can be weak enough to be of little or no use to soaring pilots.

The strength of thermals depends on the air mass characteristics, the landscape and available insolation. Average thermal conditions vary from region to region. A low-lying soaring site at high latitudes might normally find thermals in the range of 1 to 2 metres per second (m/s), while thermals of 4 or 5 m/s would be rare. By contrast, at a desert site, 5 m/s thermals are common during summer months. In a given thermal-soaring season (spring through fall), every thermal-soaring site experiences days on which thermal strength is weak, and other days on which thermals are strong.

Thermal height and strength tend to be correlated. The higher thermals go, the stronger they are. The strongest thermal updraughts occur at a height about midway through the CBL and decrease in the upper third of the CBL.

Days with cumulus have relatively more moisture in the air. Moist air is more buoyant than dry air; hence, days with cumulus tend to have stronger thermals.

1.2.3 Distribution and life cycle of thermals

Field studies have shown that when CBLs are between 600 and 1 200 metres deep, the ratio of thermal spacing to CBL depth is about 1.5. On days with deep CBLs (1 800 to 3 000 metres above ground level, or AGL), the ratio increases to 5 or 10, and sometimes greater. As a general rule, the deeper the CBL, the greater the spacing between thermals.

Once away from the strong sinking air at the edge of thermals, the CBL is characterized by broad areas of weak downdraughts. Evenly spaced thermals typically occur over relatively uniform flat terrain, and in fairly light winds. Thermal and sink distributions may be highly variable, and sometimes large areas are void of thermals. Sought-after organized lines of lift can also form, however. Here we briefly list several factors that can modify thermal distribution:

(a) Surface features (terrain characteristics, moist soils, lakes);
(b) Extensive cloud cover from overdevelopment (such as merging or deepening of cumulus), fronts or thunderstorms;
(c) Ridges or mountains (especially under windy conditions) and mountain lee waves;
(d) Lines or zones of converging air (such as sea breezes) and cloud streets.

Figure 1.4 shows a time-height section of thermals passing a vertically pointing detector located over flat farmland. Occasional large, strong thermals pass over the detector, for example, at around 1.30 p.m. and 2.30 p.m. local time (LT). Smaller, weaker thermals are also noted, for example, at around 2.50 p.m. LT. At other times, small eddies appear, which would be of no use to a soaring pilot.

The thermal lifespan is on the order of 10 or 20 minutes, depending on many factors. These include the wind speed at the surface and aloft (wind shear), shading effects from higher clouds, as well as soil characteristics and moisture content of the ground.

The near-surface buoyant air may not be large and uniform. Instead, many small pockets of buoyant near-surface air may merge into a larger plume above about 200 metres. This view is based primarily on the experience of soaring pilots – thermals are often too disorganized to use below 200 or 300 metres (safety concerns aside).

1.2.4 Diurnal variation of thermals

A typical thermal soaring day starts with thermals that are weak and extend only to 300 to 600 metres AGL. As the day progresses, thermals become stronger and extend higher. Figure 1.5 shows a morning temperature and dewpoint sounding with a surface inversion up to 200 m and an elevated inversion (2°C temperature increase) between 1 000 and 1 100 m. As the surface heats during the day, thermals form, as shown by successive dry adiabats (lines describing the temperature of the thermal) corresponding to increasing surface temperatures. Insolation also evaporates soil moisture and convection mixes it vertically. Initially, the depth of convection is limited to 1 000 m by the elevated inversion. After noon the surface temperature

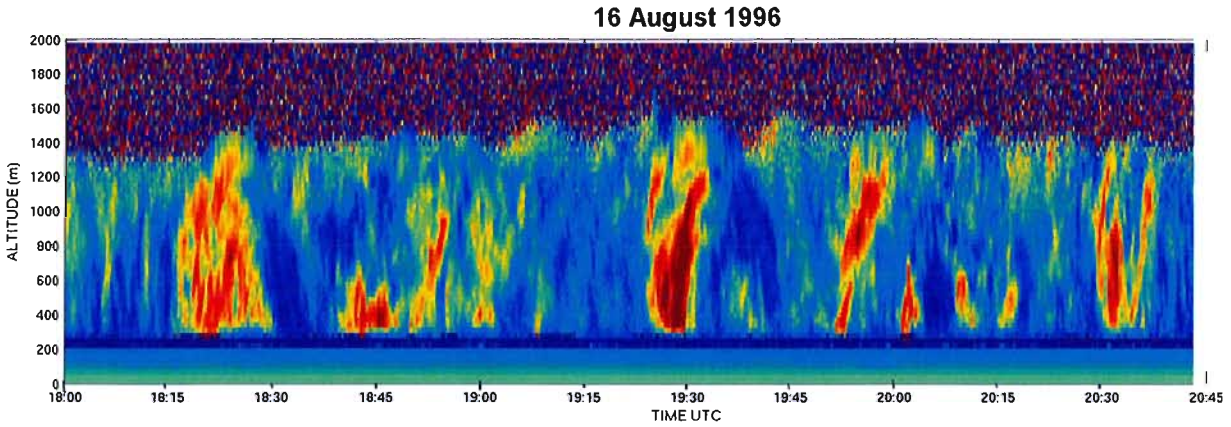

Figure 1.4. Height-time section of vertical velocities in a summertime CBL using LIght Detection And Ranging (LIDAR) measurements. Orange and red areas are thermals passing the LIDAR site, while blues and greens are regions of sink. Note: Local time (LT) is UTC – 5 hours.

warms sufficiently so that thermals become stronger and extend higher (right panel). The best climb rates persist for several hours after the highest solar elevation and thermal strength declines only after the insolation decreases markedly towards the end of the day. In this example, the air is dry enough that cumulus clouds never develop.

On another typical day, a nearly dry-adiabatic lapse rate and almost uniform moisture with height develop in the CBL as the surface warms. Thermals at first may not extend high enough to form cumulus, as shown in Figure 1.6. After 10 a.m. the surface temperature has warmed sufficiently for thermals to ascend high enough to form cumulus clouds (grey shading in the right panel). Thermal strength and the height of the cumulus cloud base increase along with additional daytime surface heating. If more moisture is present, low-based cumulus clouds form as soon as convection begins, with the cloud base gradually rising during the day.

At times, a moist layer coincides with an inversion layer. When this occurs, any cumulus that form tend to "spread out" into stratocumulus, rather than dissipating (Figure 1.7). Under moister conditions, the stratocumulus clouds develop rapidly, shutting off further insolation for hours and hinder-

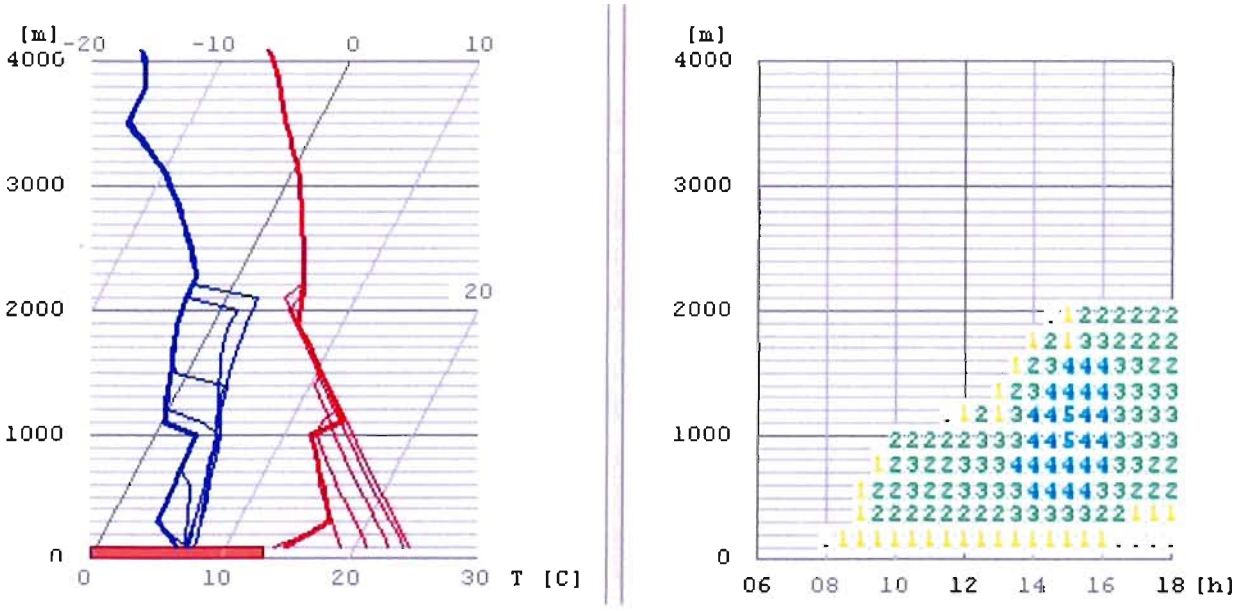

Figure 1.5. Diurnal evolution of thermal activity under dry conditions. The left panel shows a thermodynamic diagram with initial temperature (thick red line) and dewpoint (thick blue line) soundings. Thin lines show how the CBL is modified due to diurnal heating. The right panel shows the diurnal variation in thermal strength (m/s) as a function of height. Note: Time is local time (LT) and the surface is at 100 m (brown box) on this and Figures 1.6 through 1.8.

ing any further increase in thermal strength. If the stratocumulus is thick and widespread enough, it can reduce surface heating sufficiently so that thermals no longer form.

Cooling aloft will decrease the stability of a layer, enhancing thermal activity. Too much cooling aloft combined with surface heating can destabilize a deep layer and lead to deep convective clouds, along with showers or thunderstorms (Figure 1.8).

In the past, thermodynamic diagrams using data from one or more atmospheric sounding(s), along with local knowledge and synoptic observations, formed the basis of thermal forecasting (WMO/OSTIV, 1993). In recent years tools using output from numerical models have been developed. Soaring forecast products based on numerical model output have simplified the forecast process and have added significantly more spatial and temporal detail.

1.2.5 Factors influencing thermals

1.2.5.1 Solar heating

Buoyancy is achieved either by heating (through insolation, for example) or by adding moisture (through evaporation, for example) to an air parcel. The best thermals form when insolation heats the

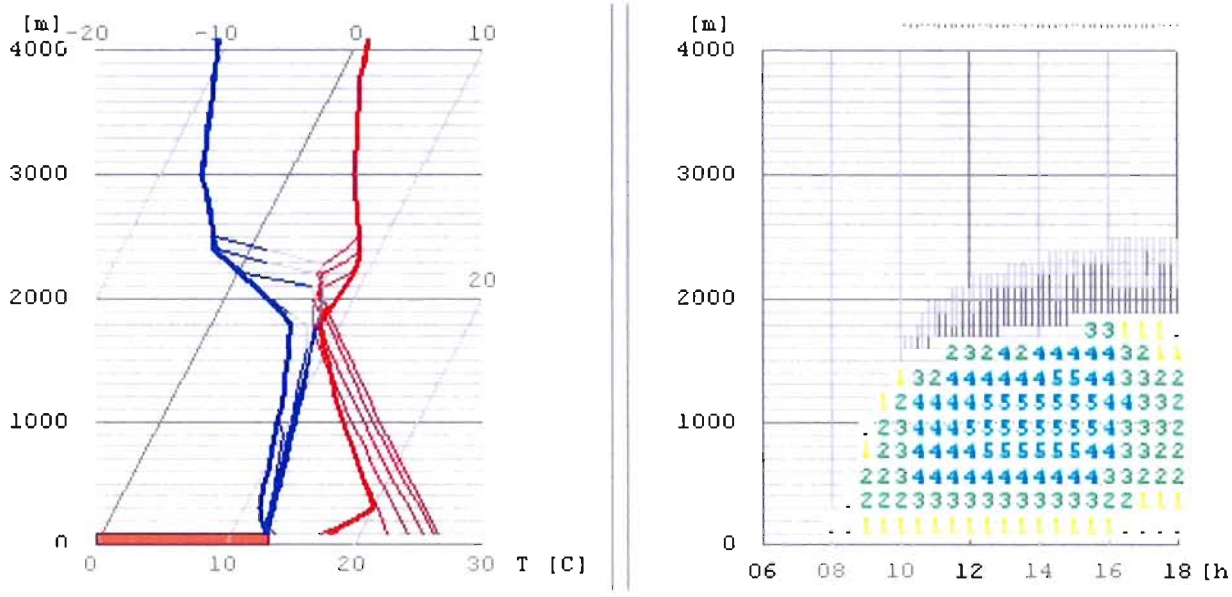

Figure 1.6. As in Figure 1.5, except for a different morning sounding scenario with more moisture in lower levels and no inversion at 1 000 m. As the CBL depth increases, cumulus clouds develop (the cloud base is at the level where the thermal temperature and dewpoint are almost identical), as indicated by the grey shading in the right panel. The grey shading indicates the liquid water content, and the largest values are found at the top (the same shading appears in Figures 1.7 through 1.10).

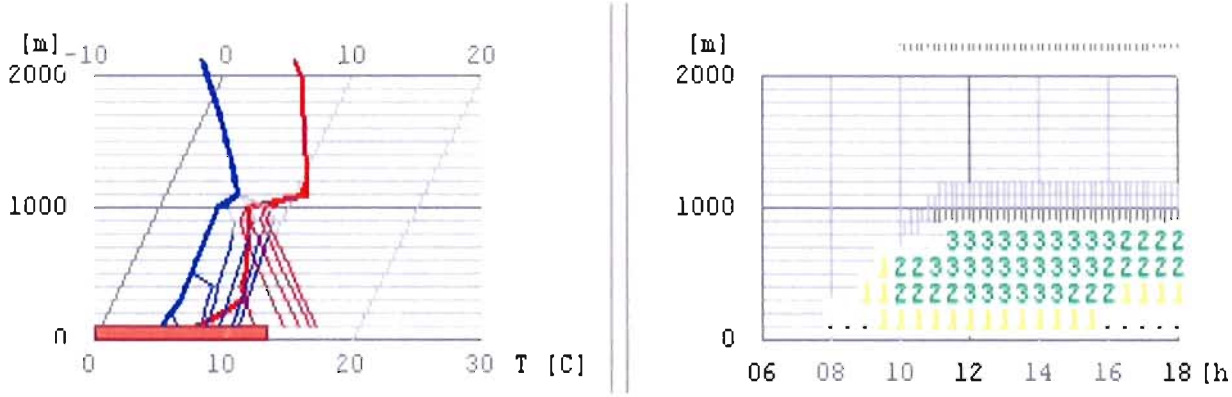

Figure 1.7. As in Figure 1.5, except for a scenario with a moist layer coinciding with a stronger (4°C) temperature inversion based at 1 000 m. This leads to a condition known as "spread-out", in which cumulus clouds form a widespread layer of stratocumulus clouds, hindering or even completely halting further thermal development.

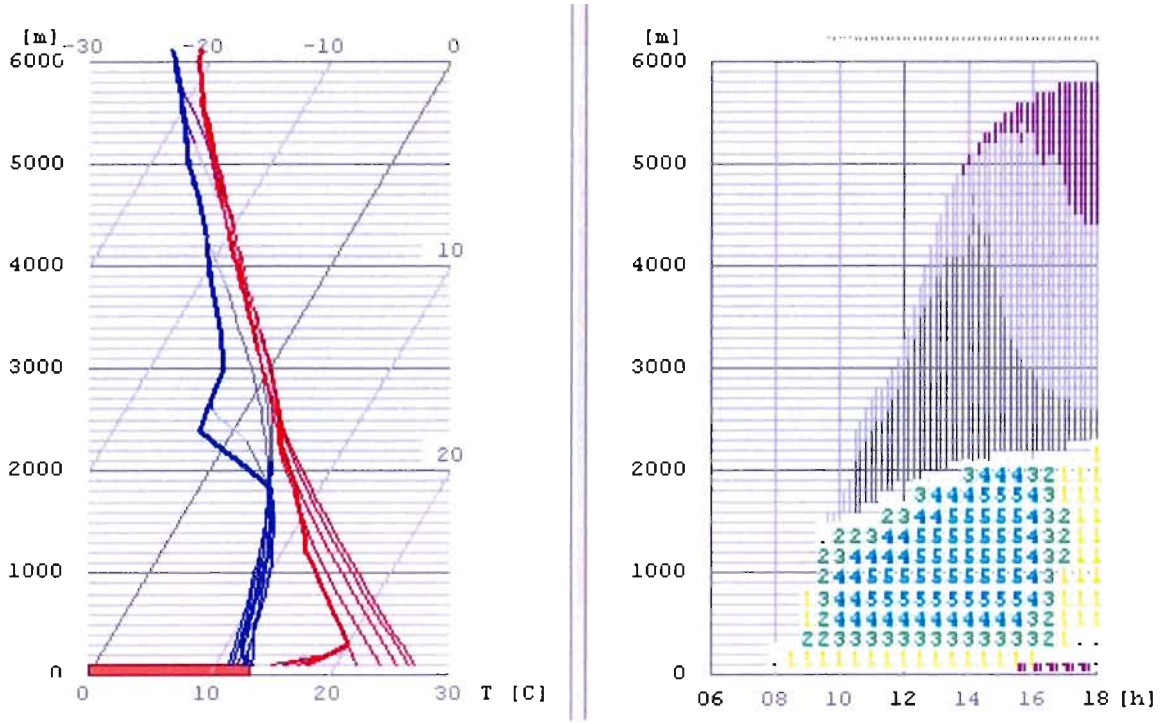

Figure 1.8. As in Figure 1.5, except for a scenario with less stability aloft, leading to overdevelopment and showers

ground, which in turn heats the overlying air. Heating of the ground is most efficient when insolation strikes the ground perpendicularly. Thus, the elevation angle of the sun is important for thermal formation and depends on latitude, season and time of day. Strong thermals are more likely to form in low or mid-latitudes, during the summer season and during the afternoon.

Anything that attenuates the insolation will reduce the strength of, or potential for, thermals. Examples are man-made pollution or heavy smoke from natural fires. An efficient natural attenuator is any kind of cloud. High, thin cirrus may only have the effect of minimally reducing thermal strength. On the other hand, a thick layer of stratus or altostratus can diminish insolation enough to eliminate the day's thermal activity completely.

Surface characteristics are important. Each soil and vegetation type has a characteristic albedo. Surfaces with high albedo (such as snow) will reflect rather than absorb the insolation, thereby decreasing surface heating. Low-albedo surfaces (for example, certain bare soils or rocky outcroppings) reflect little, and efficiently absorb the insolation, leading to favourable surface heating. Moist surfaces produce poor thermals, since much of the insolation goes to drying, rather than to heating, the surface. Homogeneous surfaces of any kind over large areas are less conducive to thermal production than areas consisting of a variety of surface albedos. Inhomogeneous surface characteristics lead to increased frequency of thermal activity. This may be due to microscale convergence on scales of a few tens of metres, which acts as a thermal trigger.

1.2.5.2 Temperature aloft

Relatively cool temperatures aloft are needed as well. It follows that warming temperatures aloft will hinder thermal activity. Warming aloft can occur on the synoptic scale, for instance, with building high pressure aloft. Local diurnal circulations near topography can also warm the air aloft over nearby valleys or plains.

1.2.5.3 Inversions

Inversions frequently form aloft, especially when associated with building high pressure. The most notable effect of inversions is to limit the height of the underlying CBL, thus marking the approximate maximum thermal height. Depending on the height and strength of an inversion, full development of thermals may be temporarily limited or the limit may persist the entire day. Such inversions may also enable the development of cumulus, but prevent their development into thunderstorms.

1.2.5.4 Elevated terrain

Elevated terrain in mid-latitudes favourably affects thermal development in many ways. First, insolation will strike sun-facing slopes at a more-nearly perpendicular angle compared to adjacent valleys or plains. This leads to more intense heating along sun-facing slopes. Thus, mountains, ridges and even small hills will produce thermals earlier in the day and later in the afternoon. On the other hand, valleys and other lowlands are ideal for the formation of night-time inversions. After sunset, dense radiatively cooled air sinks down the sides of hills or mountains, pooling in the valleys below. It can take many hours of heating during the morning before cool valley air completely erodes, delaying the onset of thermals over the valley floor. Elevated terrain also drains water, which then collects in adjacent relatively moist valleys. The drier slopes and peaks heat more efficiently, giving stronger thermals and producing them earlier in the day. In contrast, mountainous regions receive more precipitation. This, combined with higher-reaching thermals, means that mountainous regions are more likely to produce cumulus clouds than adjacent lowlands. Elevated terrain is also more likely to produce deep convective clouds and showers, or to produce them earlier in the day. An example of the evolution of an atmospheric temperature profile with an elevated thermal source is shown in Figure 1.9. A comparison of this figure with Figure 1.8 illustrates the earlier onset of showers.

In mountainous terrain at lower latitudes (such as northern Australia), soaring conditions are often better over the flat areas. One reason is that the sun angle is so high that sloping terrain does actually decrease the sun's incidence angle. Another reason is that cloud sometimes forms over the flat areas, which normally have slightly more vegetation, rather than over the bare desert mountains with less vegetation. The lift over the mountains can be stronger, but even the slightest development of cloud helps identify the location of thermals.

1.2.5.5 Complex terrain

Complex terrain also influences thermal production due to the Valley Volume Effect (Steinacker, 1984; Whiteman, 2000). Figure 1.10 illustrates the diurnal cycles of thermals over flat and complex topography resulting from the same initial conditions (sounding) and insolation. The effect produces larger temperature ranges in valleys than over plains.

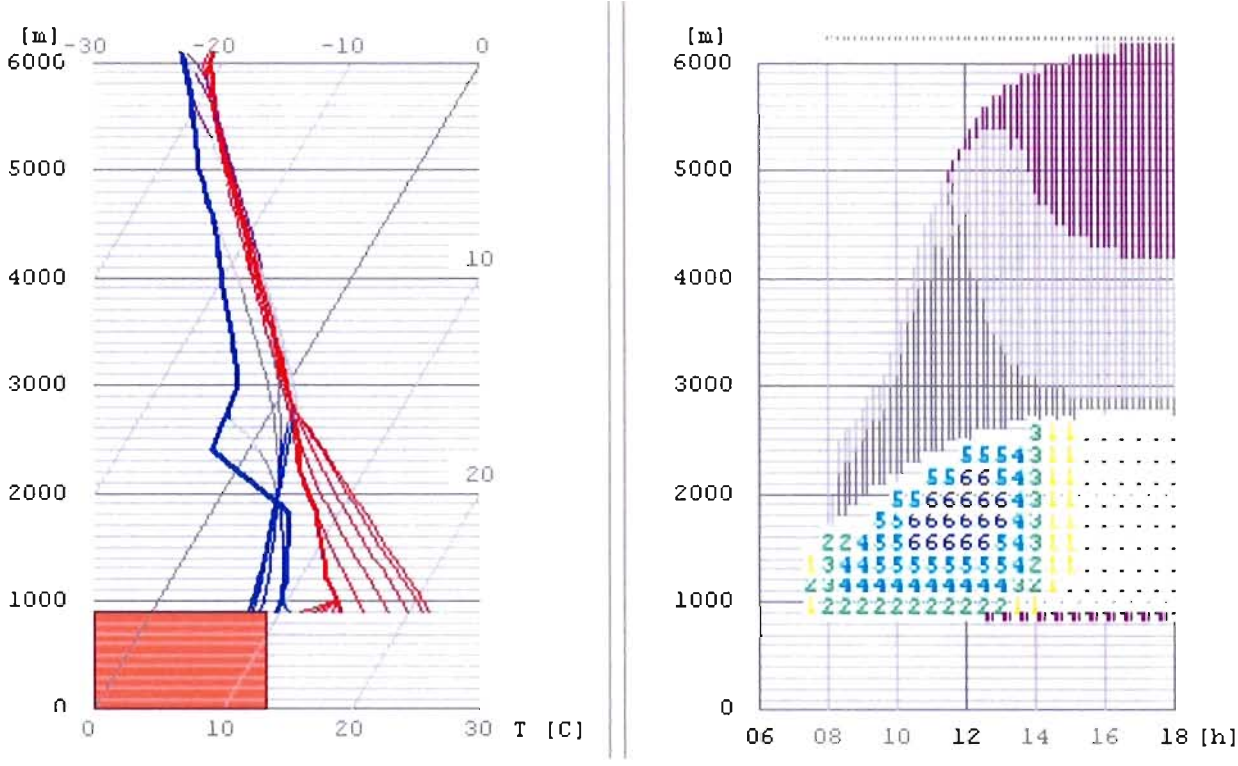

Figure 1.9. Enhanced thermal strength due to a convective source region over elevated terrain (900 m mean sea level (MSL)) leading to overdevelopment and showers earlier in the day

1.2.5.6 Wind

Winds influence thermals over flat or hilly terrain. Calm conditions lead to thermals that are relatively easy for soaring pilots to use. Light winds, less than 5 m/s, are also conducive to good thermal conditions and appear to increase thermal frequency by aiding the initial impulse (the trigger mechanism). Moderate winds of 5 to 15 m/s distort thermals, especially at levels below about 600 m AGL, making them difficult to use. On the other hand, moderate winds typically organize convection. Strong surface winds create a great deal of mechanical turbulence and will break up thermals, making them difficult to use. Surface winds stronger than approximately 20 m/s are enough to disrupt thermal activity entirely.

Winds aloft are also a factor. As long as the vertical shear (wind speed or direction change with height) is not too large, thermals will rise into layers with quite strong winds. When the vertical shear is moderate (for example, 5 m/s over 300 to 600 m), thermals are likely to become rough and difficult to use. Turbulence production by large shear (for example, 10 m/s over 300 to 600 m) is enough to disrupt thermals rising into that layer. Strong winds aloft above a capping inversion create the possibility of thermal waves.

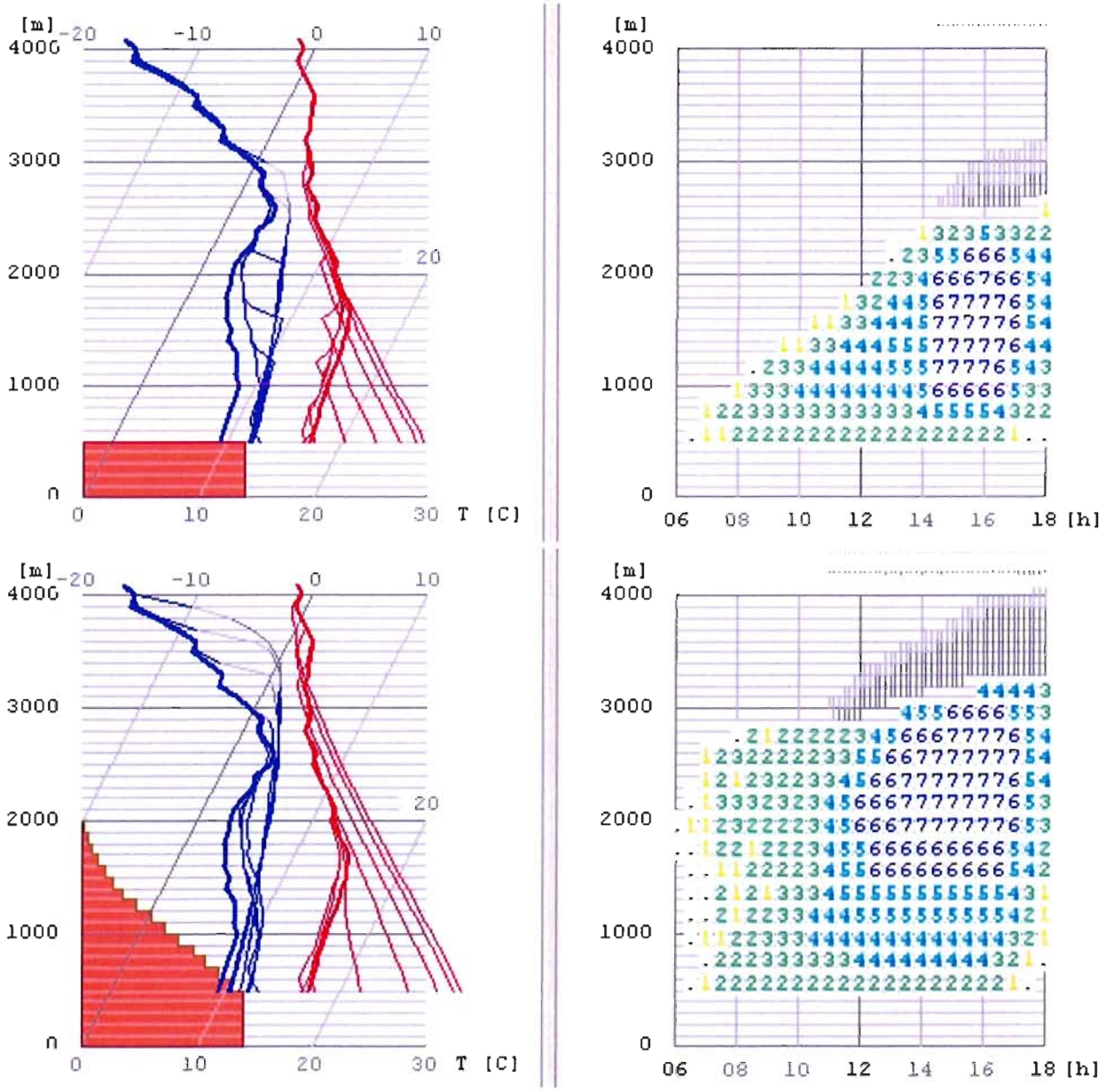

Figure 1.10. Enhanced thermal strength due to the Valley Volume Effect (see text). The left panel shows topography along one side of a valley (500 m – 2 000 m MSL).

Cool or stable low-level air can drift with the wind. Thus, some landforms can reduce or eliminate thermal activity, for example, downwind of large lakes or wet irrigated areas. These "dead air" regions are revealed by cloudless areas in an otherwise cumulus-filled sky.

1.2.5.7 A general comment

There is a significant difference between convective soaring conditions in Australia and Europe. In Europe the best conditions are often on the day after the cold front passage, while in Australia, the best day normally is the day just before the cold front passage, or even better, the day of the cold front passage (provided the passage happens in the evening or night). In simple terms, this probably means that in Europe, the change in the lapse rate (or stability) is the deciding factor, while in Australia the deciding factor is the extreme heating of the underlying surface (and the consequently increasing temperatures in the surface layer).

1.2.6 Organized convection

Cumulus clouds, and the thermals that form them, are often distributed across the sky without a recognizable pattern. Horizontal spacing of randomly spaced thermals is typically 2.5 or 3 times their height. Thermals can become organized into lines or areas of lift along convergence zones, form long so-called cloud streets or align with elevated terrain.

1.2.6.1 Convergence

Convergence is the coming together of currents causing an updraught. In this section, we are interested in convergence occurring on scales large enough to enhance and organize convection, that is, tens or even a few hundreds of kilometres. A well-known example of a convergence zone is the sea-breeze front (see, for example, Bradbury, 2000). The boundary between two air masses acts as a focus for strong and closely spaced thermals. The air on the water side of the front is often so stable that no thermals (or clouds) can form. Convergence lines also form where there is a discontinuity in temperature between two air masses, without a notable wind shift. Temperature discontinuities and convergence zones can also occur along the edge of a cloud layer that is causing an extensive shadow or a moist area, perhaps due to localized precipitation on the previous day.

1.2.6.2 Cloud streets

In breezy conditions, cumulus clouds sometimes align in regularly spaced parallel bands called cloud streets, thermal streets or cumulus streets (Figure 1.11). Individual cloud streets can extend 100 km or more. Typical spacing between cloud streets is about three times the height of cloud base. Cloud streets are parallel to the wind direction in the CBL layer. Cloud streets form best over relatively flat terrain. Typical conditions include wind speed increasing by 5 to 10 m/s between the surface and cloud base, ideally with constant wind direction through the CBL. A wind speed maximum is found in the middle or upper part of the CBL. The CBL is usually capped by an inversion or by a stable layer. It is worth noting that dry thermal streets can form when the wind and stability are favourable, but moisture is lacking so that cumulus clouds do not form.

1.2.7 A pilot's view: a flight in thermal lift

The forecast conditions were not ideal, but we had only two options: either to start our six-day soaring safari today, or to forget it altogether. For the following day a hot and humid air mass was expected to move in from the south-west with the accompanying haze, late thermal development and high risk of heavy thunderstorms later in the day. As we assembled our gliders, it seemed as if the precursor of that weather system was already having an effect: it felt hot and the sky looked a pale blue. Shortly after noon no clouds were to be seen in the vicinity of the airport. Over the mountains, hardly 50 km to the north, however, increasing moisture at altitude had already caused partial overdevelopment of the few cumulus clouds.

Figure 1.11. Cloud streets aligned along the wind direction in the CBL

As soon as I stuffed my toothbrush and sleeping bag behind the seat, I rolled the glider out to the runway. Nobody wanted to take off into cloudless conditions around the airfield, so I got a tow right away. "Go north, and I'll release when I think I can make it to the clouds", I told the tow pilot. As we headed north and climbed through the haze layer at 1 000 m, I could see the first shower under one of the fat cumulus congestus over the highest point of the mountains. After release I glided cautiously towards the least-developed cumulus in the entire pack of dense clouds, hoping to get there before it dumped its load of water.

As I climbed slowly, I saw that the clouds to the west appeared to be ones shooting up most rapidly. Farther east I was able to penetrate the shower line. After another 30 km the cloud base rose from 1 700 m mean sea level (MSL) to nearly 2 000 m, visibility was better and none of the cumulus clouds showed exceeding vertical development. I followed a line of clouds, which was the result of a convergence: the early thermal development over the high hills drew in air from the wide basin in the east and the lower river valley to the west. Along the line of collision of those two currents, strong updraughts bubbled up and formed a highway in the sky, which made for fast cruising. As I approached the end of this run, still close to cloud base, I swung around to the upwind side of the last cumulus to avoid getting sucked into its white belly. And, lo and behold, rather than hitting descending air found so often next to a well-developed updraught, I continued to climb. Soon I found myself 200 m above cloud base, at some distance from the white stuff. What a rare view. It felt like soaring the ridge lift on a snowy slope. Most likely, a wind shear in the upper part of the convection layer had triggered this flow pattern with its increase in wind speed with altitude.

Much too soon this exhilarating part of the flight came to an end and I entered the typical setup of a promising thermal day. Good-looking clouds with dark, flat bottoms scattered almost evenly across the sky in front of me. Climbs of 3-4 m/s alternated with fast cruise of 160 km/h and made for excellent progress. Two hours later another range of hills came into view, the highest ridge reaching just about 1 000 m. The stronger thermal conditions typical for hilly terrain manifested themselves in a markedly higher cloud base and more vertical development of the cumulus clouds. I sped up to get as quickly as possible to the promising conditions ahead. The first climb confirmed my expectations: the variometer needle swung around the 5 m/s mark, and when I stopped climbing to proceed north-east I was at almost 3 000 m. Two more boomers like this one and I was at the end of the ridge. I turned toward a more easterly course and headed out over the adjoining plain. As its elevation was only about 150 m MSL, I was at roughly 2 800 m AGL, a rare situation in this part of the world. The air mass ahead was different: a change in visibility and hardly any cloud were a sign of drastically reduced humidity. As much as I enjoyed the view, I missed the clouds as makers of updraughts. After a long glide I found the next thermal at an altitude of about 1 200 m MSL. I barely managed to extract a paltry 1.5 m/s. The blue conditions lived up to their reputation: the updraughts were weaker, reached to lower top altitudes and, on top, were more difficult to find. This was going to be the slow part of the flight.

It was a blue line on the map that appeared to make yet another change in convective characteristics: shortly after I crossed a big river, the blue of the sky deepened, the visibility seemed to be unlimited and in the distance I saw a small cumulus floating high over a green forest. I made one more cautious climb in the blue before I dared to glide out to the little cloud. It didn't disappoint. A constant climb at almost 3 m/s brought me up to 2 500 m. No problem to get centred properly in this updraught, it was a wide and quietly rising column of air: a surprisingly strong evening thermal! It was almost 6 p.m. and my goal was an easy final glide away. After landing I quickly checked my flight recorder: 620 km distance, it displayed. What a wonderful flight!

1.3 RIDGE LIFT

Ridge soaring (also called slope soaring) was the first source of rising air used by glider pilots to maintain or gain altitude, allowing flight for extended periods. Today, ridge soaring still provides a consistent source of lift in hilly or mountainous terrain when winds are favourable. Ridge soaring is useful over the full spectrum of soaring flight – from basic training to contests and record flying.

1.3.1 Mechanism

Ridge soaring is the easiest form of lift to visualize and understand. Air approaching a wide barrier with enough speed will be forced over it, creating an updraught (Figure 1.12). Glider pilots simply use the vertical component of the wind (updraught) created as the wind is deflected by the barrier. The barrier could be a cliff, ridge or mountain.

The distribution of updraughts along the slope depends on the wind speed and direction, stability of the air and nature of the slope itself (its shape and texture). Unfortunately, these details are often difficult to quantify. Knowledge of local soaring experts provides valuable input to the weather forecaster.

1.3.2 Meteorological factors

Wind is the critical meteorological ingredient for slope soaring. For moderate slopes (about 30°), a minimum wind speed of about 5 m/s blowing towards the ridge is needed. Stronger winds produce stronger updraughts, but also create stronger turbulence, especially close to the slope and on the lee side.

Ideally, the wind direction should be perpendicular to the ridge. Wind directions within 10° or 20° of perpendicular also produce updraughts, but oblique wind angles are not useful. Even though a strong wind at an oblique angle should have a sufficient component towards the ridge, updraughts are doubtful. The reason is that as the wind angle deviates further from a direction perpendicular to the ridge line, there is an increasing tendency for the flow to deflect and run parallel to the ridge line. This process is more likely if winds aloft, as well as at the surface, are oblique to the ridge.

Stability of the air mass plays a secondary role. Stable layers offer more resistance to vertical displacements. Thus, a neutral or only slightly stable layer will be lifted over a barrier more easily, providing stronger and higher-reaching updraughts for ridge soaring.

Changes in wind direction with height force three-dimensional thinking, especially in regions of high and complex terrain. For instance, the wind at low levels might be channelled along the valley, while at mountaintop levels the wind is directed perpendicular to the mountains, producing updraughts there. Thus, in high, complex terrain it is important to be aware of wind direction and speed at all levels. In addition, waves excited by upstream terrain can cause turbulence or sink where ridge lift would otherwise be expected.

Three factors are important in determining whether flow will go over or around a barrier. First, the stronger the flow, the greater the tendency for air to go over, rather than around, the barrier. Second, air with neutral stability has a greater tendency to flow over a barrier; stable air tends to flow around a barrier (see also the concept of the dividing streamline (Whiteman, 2000)). Third, the flow tends to go over wide barriers, while it flows around small or narrow barriers. These factors are combined into one parameter called the Froude number, which takes a variety of forms. The most useful

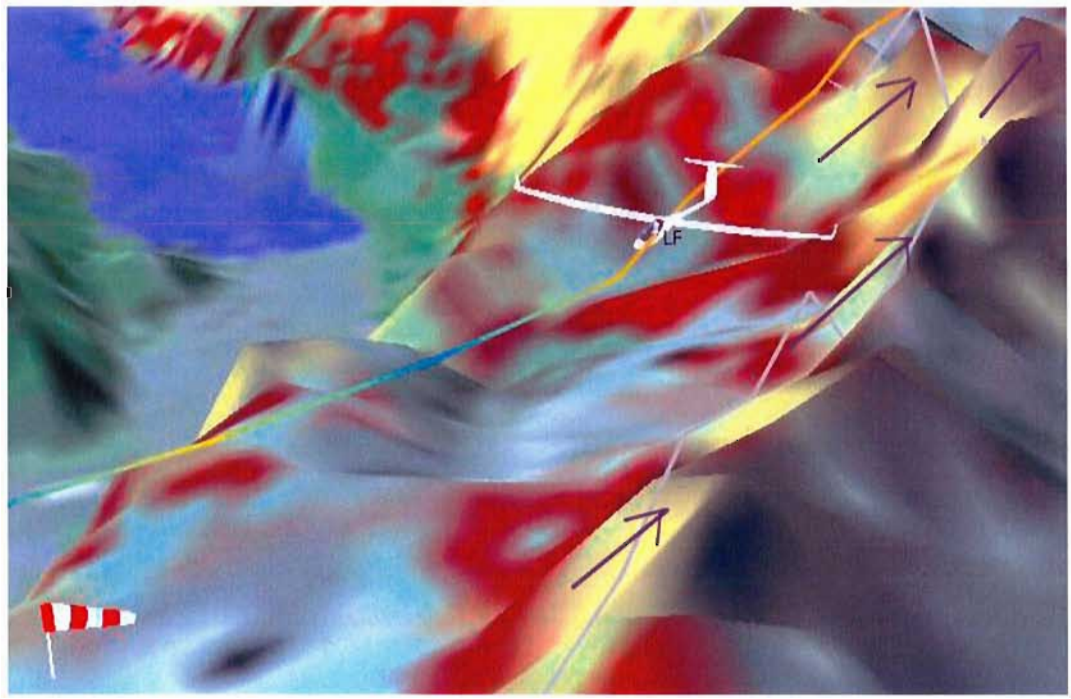

Figure 1.12. Wind blowing towards the rising terrain creates an updraught (arrows), called ridge or slope lift. Note: The grey line near the upwind ridge crest is the ground track of the glider.

definition for our purposes is: speed of the flow divided by the product of the flow stability and barrier length. Readers seeking a more theoretical treatment of flows around barriers are directed to many references on the Froude number in the literature (see, for example, Baines, 1995).

1.4 WAVE LIFT

Mountain lee waves were first explored by soaring pilots in the Riesengebirge of Poland during the 1930s (Dörnbrack and others, 2006). The waves were quickly recognized as a source for obtaining high altitudes, and by the early 1950s, glider pilots using mountain waves had reached the lower stratosphere. The world altitude record as of 2006 is 15 460 m. Observations have shown evidence of atmospheric waves extending to heights of 30 km. Mountain waves have also been used for many distance and speed records. Notable among these is the first soaring flight exceeding 3 000 km achieved in 2003. Mountain waves occur worldwide in the lee of small and large topographical barriers (Figure 1.13).

Figure 1.13. The pilot's view of a well-developed lenticular cloud with underlying lines of rotor clouds. These clouds are typically associated with the mountain wave.

1.4.1 Waves in the atmosphere: wind and stability

Many types of atmospheric waves are known to exist. The most common, called buoyancy waves (also called gravity waves), occur when air parcels are disturbed from an initial equilibrium level; oscillations about the equilibrium level result due to restoring buoyancy forces (Figure 1.14). Buoyancy waves can be excited by different phenomena, for instance, thermals encountering a stable layer. In this section, we consider only buoyancy waves excited by elevated terrain, from small hills and ridges to large mountain ranges. These are known as mountain waves, lee waves or mountain lee waves (Figure 1.15).

Lee waves occur only in atmospheric layers with a stable lapse rate. That is, in unsaturated air, the environmental lapse rate must be less than the dry-adiabatic lapse rate (10°C per 1 000 m). Scorer (1978) provides the theoretical framework for calculating lee waves.

The wind flowing over topography plays a vital role in two ways. The flow spilling down the lee slope of a ridge or mountain distorts a stable layer, exciting

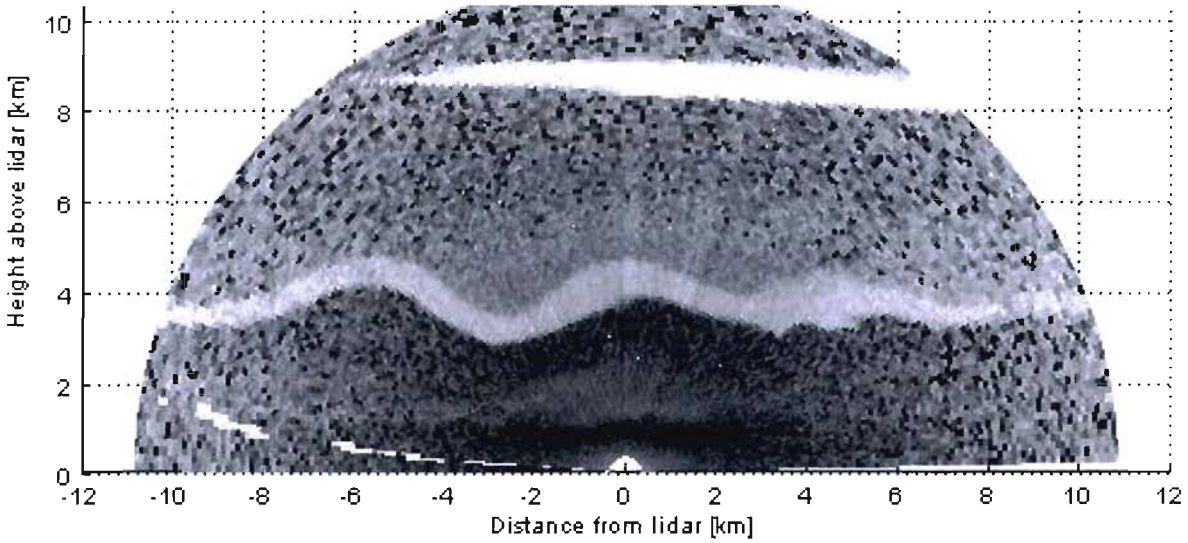

Figure 1.14. A vertical LIDAR scan of a wave (grey sinusoidal layer) downwind of the Sierra Nevada over the Owens Valley (USA) on 15 April 2006

waves downwind of the barrier. In addition, the wind provides the energy source for the wave updraughts, and is a determining factor in the mountain-wave structure.

Two parameters for describing the mountain lee wave are wavelength and amplitude. Wavelength (typically between 3 and 30 km for mountain waves) is determined mostly by the wind and stability profile. For a given stability profile, the stronger the wind, the longer the wavelength. For a given wind profile, the weaker the stability, the longer the wavelength. Wave amplitude depends on the wind and stability profile, as well as the steepness and height of the lee slope exciting the wave.

1.4.2 Idealized two-dimensional mountain-wave system

Given the almost infinite variety of the Earth's elevated terrain, along with ever-changing wind and stability profiles, we can expect tremendous variation in the atmospheric wave response. As a starting point, it is useful to consider a conceptual model, which, though simple, captures important features common to most mountain lee waves.

The right-hand panel of Figure 1.15 shows an idealized two-dimensional mountain-wave system. Along the lee slope, a dissipating cap cloud and a strong downdraught are found. The strength of the lee-slope downdraught is usually 5 to 15 m/s. In the region where the waves form, the air is usually laminar, providing smooth flight. Wave updraughts vary in strength; 5 m/s is common, and 15 m/s or more has been recorded in strong waves. Under some conditions, updraughts can be quite weak: 0.5 to 1 m/s. Wave downdraughts are stronger, but on the same order of magnitude as the updraughts.

The number of harmonics (wave crests or troughs) also depends on the wind and stability profiles. Figure 1.15 shows waves extending through much of the troposphere. Smaller topography can also excite waves that reach high altitudes. In the low-level turbulent zone, rotors (the main rotor is illustrated) often form under the wave crests. Rotors are discussed further in the next section.

It is important to note that all, some or none of the cloud forms shown in Figure 1.15 will occur in a wave event, depending on the amount and stratification of moisture.

The left-hand panel of Figure 1.15 shows a typical wind and temperature profile associated with mountain-wave conditions. The main features are winds increasing with height and increased stability in a layer near the mountaintop level.

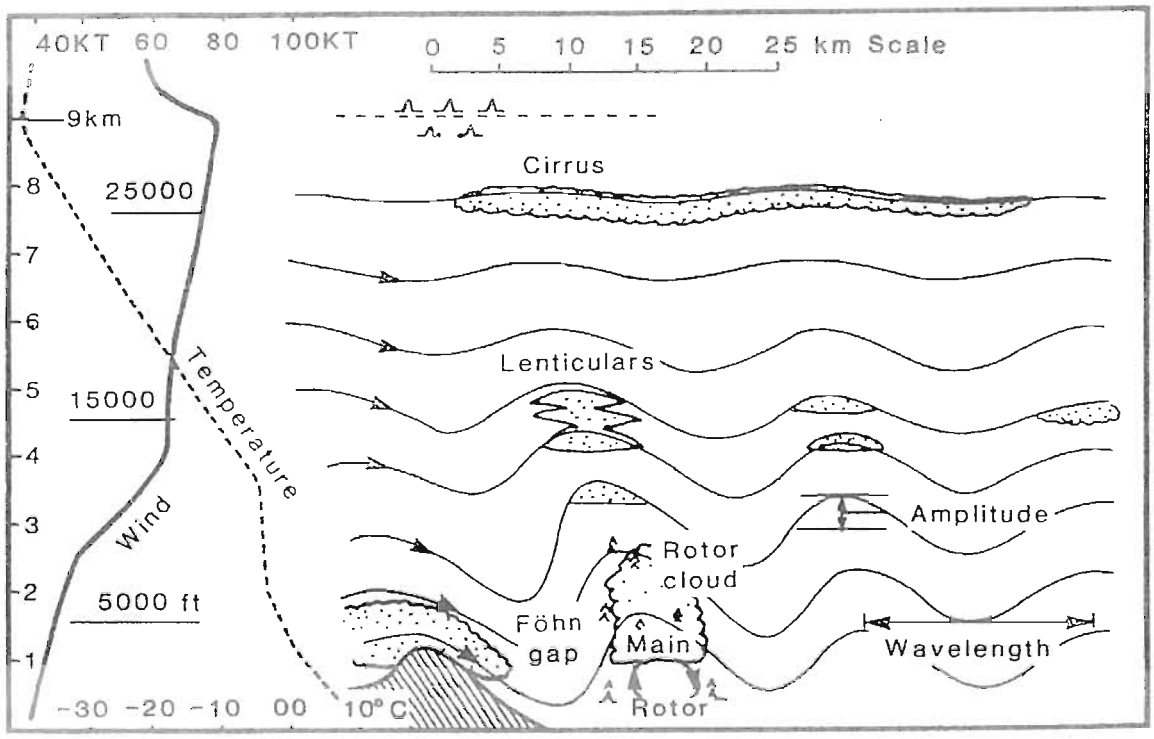

Figure 1.15. Idealized two-dimensional wave system with atmospheric wind and temperature profiles (left) and characteristic cap, roll and lenticular clouds and foehn gap (right)

1.4.2.1 Turbulence associated with mountain waves – Rotors and wave breaking

Turbulence below laminar flow is almost always found when mountain waves are strong enough to be useful to soaring pilots. Soaring pilots use the term rotor to refer to any turbulent air under the laminar wave flow.

Rotors are comprised of turbulent eddies on scales ranging from a kilometre or more to as little as 10 metres. Rotor turbulence can range from light to extreme, but is most often moderate to severe.

Clouds can form near the top of each rotor. In dry conditions, rotor turbulence occurs with little or no cloud at all. Even relatively small hills or ridges can produce severely turbulent rotors.

The current state of forecasting does not provide detailed forecasts of rotors, for example, how likely turbulent rotors are to be on a given day. We do know that rotors will almost certainly be present when conditions favour mountain waves. In addition, the strongest rotors occur in conditions favourable to high-amplitude waves and strong winds. Local knowledge of experienced soaring pilots is a valuable source of information that should not be neglected by forecasters.

Another source of turbulence associated with mountain lee waves is wave breaking, which occurs when the amplitude increases to the point that the wave overturns. Wave breaking often causes moderate to severe (and sometimes extreme) turbulence. Wave breaking can occur in layers with negative vertical shear, that is, wind decreasing with height. The tropopause and lower stratosphere are common wave-breaking regions. Wave breaking can occur at lower levels as well.

1.4.3 Variations from the idealized conceptual model

Wave responses can deviate greatly from the simple, two-dimensional conceptual model considered thus far. In this section, we present a small sampling of wave structures. To illustrate several flow regimes, we will at times make use of idealized, high-resolution numerical model simulations.

1.4.3.1 Effect of winds aloft

The vertical shear of the winds aloft has a profound impact on the wave structure. Figures 1.16 through 1.18 show results from simulations that differ only in the vertical shear above mountaintop level. Figure 1.16 shows a typical wave structure that occurs with weak shear, on the order of 10 m/s from mountaintop level to the tropopause. The wave structure is composed primarily of a vertically propagating mode. The wave response occurs mostly above the peak, and extends through the troposphere. Only minimal disturbed flow is noted downwind of the mountain.

Figure 1.17 shows the wave structure resulting from moderate shear, with winds increasing 20 m/s. Lee waves occur farther downwind of the mountain, especially at lower levels, with a longer wavelength aloft. The primary wave has a pronounced upwind tilt. This mountain-wave system shows both high-level vertically propagating and low-level trapped-wave modes, and is of interest to soaring pilots seeking maximum height or height gain. When clouds are present, the lower-level waves are marked by rotor clouds, while the upper level wave is marked by a single lenticular cloud (also called an arch cloud).

The final simulation (Figure 1.18) shows the effect of strong shear, with winds increasing to 45 m/s. The wave energy is largely trapped as seen by several waves forming in the lower troposphere and little disturbed flow at higher levels. When trapped waves form, soaring pilots can find updraughts far downwind of the mountain exciting the wave. Mountain-wave systems with trapped waves are useful for cross-country soaring.

1.4.3.2 Negative shear

It is possible, though much less common, for the wind speed to decrease with height. This is called negative shear, and it disrupts mountain-wave systems. Turbulence is likely if the negative shear is strong. If the wave amplitude is large, breaking waves can occur (Figure 1.19). Also, wave flow will be disrupted by a significant wind direction change with height.

1.4.3.3 Atmospheric jumps

Under certain conditions, a flow structure forms that is completely different from the vertically propagating or trapped waves considered thus far. This type of mountain-wave system is sometimes called an atmospheric jump, since it resembles the hydraulic jump long studied by the fluid-dynamics and engineering communities. Figure 1.20 shows an example of a simulated atmospheric jump. Downwind of the lee slope, one large wave updraught forms; there are no resonant waves. Under and downwind of the jump, rotors form.

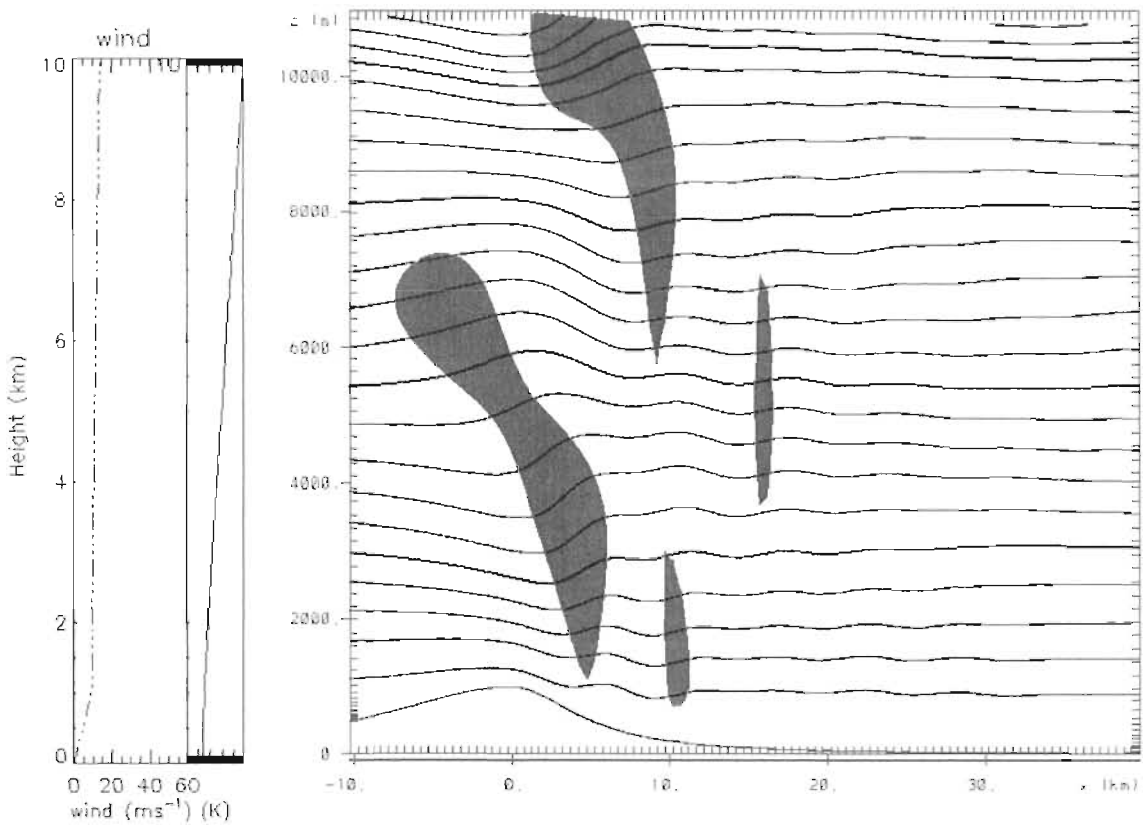

Figure 1.16. Isentropes (contours) and positive vertical velocity (grey shading) showing mostly vertically propagating waves from a numerical model simulation initialized with weak vertical shear of the wind above mountaintop level (right panel) Wind and potential temperature profiles (left panel)

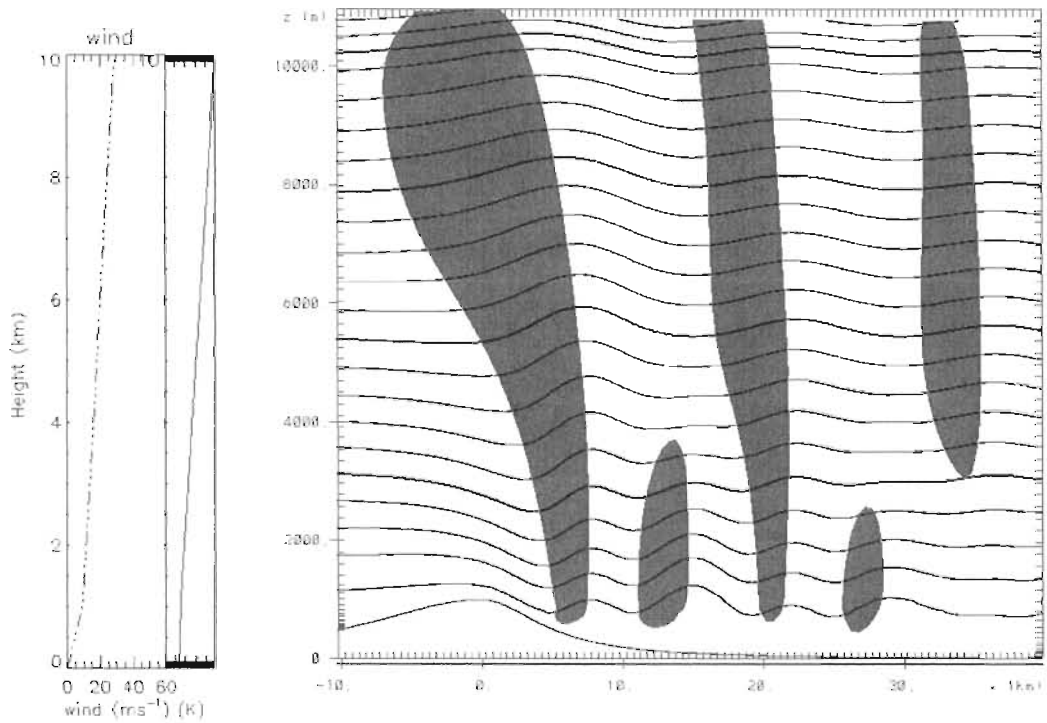

Figure 1.17. Isentropes (contours) and positive vertical velocity (grey shading) showing mixed-mode waves from a numerical model simulation initialized with moderate vertical shear of the wind above mountaintop level

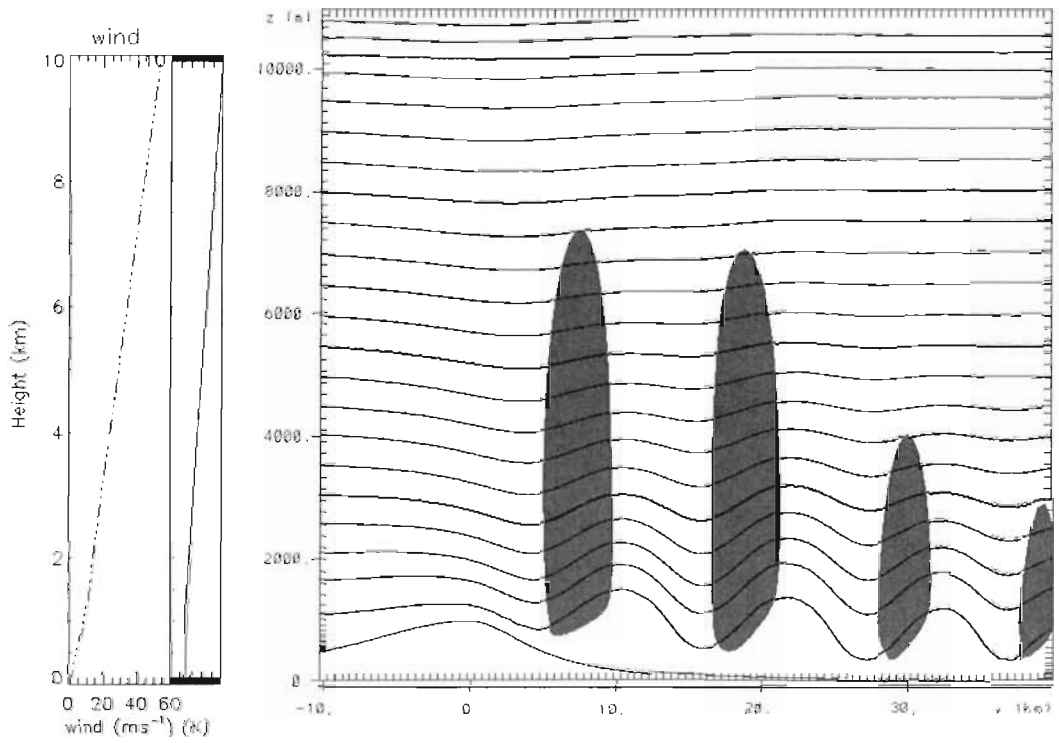

Figure 1.18. Isentropes (contours) and positive vertical velocity (grey shading) showing trapped waves from a numerical model simulation initialized with strong vertical shear of the wind above mountaintop level

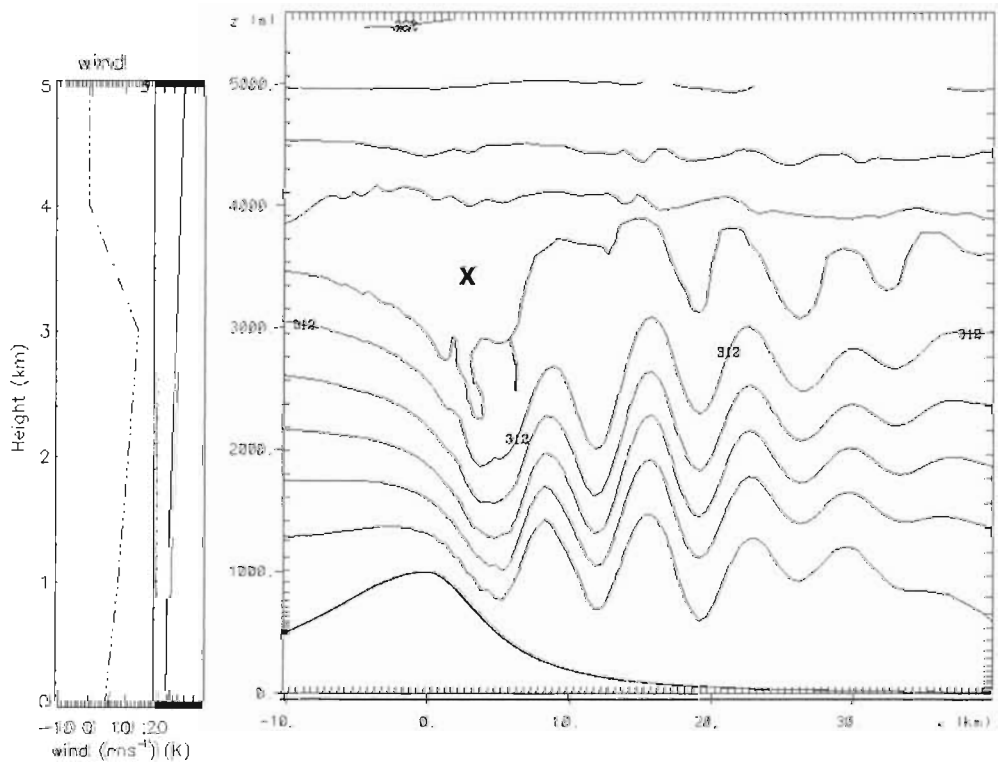

Figure 1.19. Isentropes (contours) showing a numerical model simulation initialized with negative vertical shear of the wind above 3.5 km, leading to wave breaking and turbulence (marked by the "X")

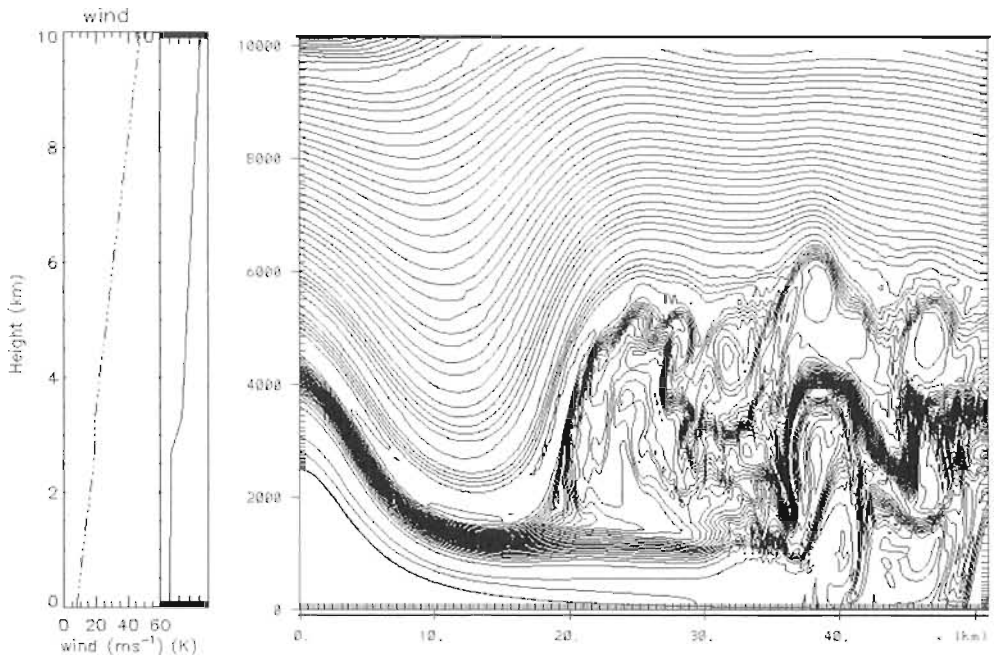

Figure 1.20. Isentropes (contours) showing a numerical model simulation of an atmospheric jump initialized with a high, steep lee slope and a strong near-mountaintop inversion

The atmospheric-jump rotor has no organized branches (such as the rotor in Figure 1.15 has); these rotors can extend much higher than the mountaintop and are usually far more turbulent than the trapped-wave rotors.

Atmospheric jumps are much less common than the more familiar trapped-wave systems. Little is known about specific conditions leading to atmospheric jumps rather than trapped waves. From numerical model studies, we know that they favour environments with strong near-mountaintop inversions and relatively weak vertical shear.

1.4.3.4 Effects of topography

Complex terrain can modify the wave flow in a process known as interference. In constructive interference, downwind waves are enhanced when the wavelength is in phase with the spacing between mountain ranges. By contrast, destructive interference leads to a destruction of downwind waves when the wavelength is out of phase with the spacing between the ranges. Real-world terrain leads to interesting wave responses: wave patterns can be transient and complex.

An isolated single peak can produce a different kind of mountain wave, as shown by the satellite photo in Figure 1.21. The peak is not a broad barrier, but it does disrupt the flow nonetheless. The best analogy to the wave produced by a single peak is the wake

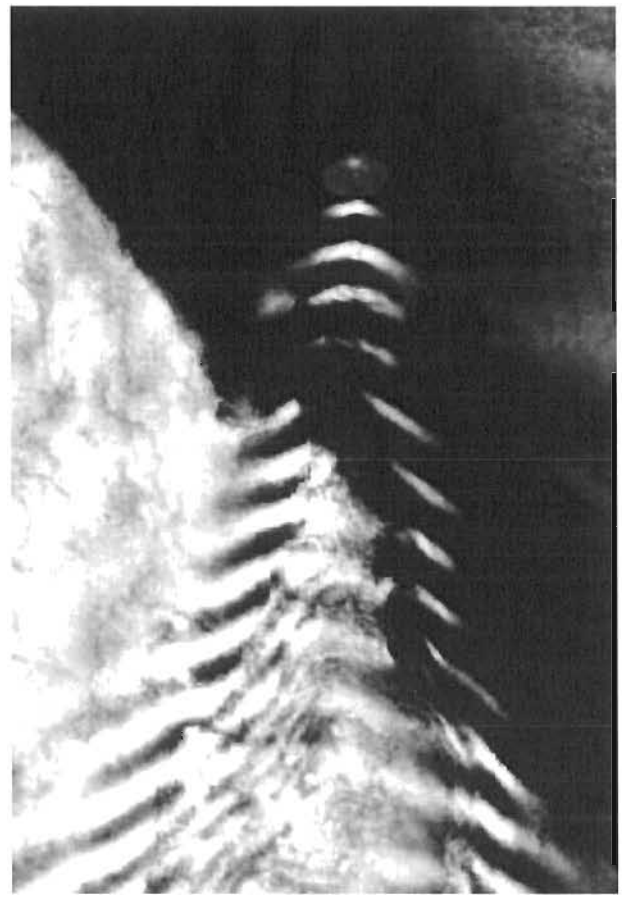

Figure 1.21. Satellite image showing the wave pattern downwind of an isolated island peak (Amsterdam Island in the Indian Ocean)

produced as a ship ploughs through the water. Pilots have reported usable wave updraughts from single peaks. In some cases, the lift is neither strong nor does it extend high above the peak. In contrast, pilot reports from the Andes indicate that the strongest lift is often found in the lee of large volcanoes.

1.4.4 A pilot's view: a flight in wave lift

The forecast for the next day looked promising. The airflow was supposed to cross the mountain chain almost perpendicularly, and the wind speed in the 24-hour model forecast showed 25 knots at 3 000 m, increasing to 40 knots at 7 000 m. A cold front was expected to pass at the end of the day.

I set my alarm clock to 4 a.m., 2 hours before sunrise. It takes time in the darkness to get everything ready: food, drinking bottle, three layers of warm clothes and special boots. The glider had already been prepared.

It was 6.05 local time, beginning of civil morning twilight, but the sun was still below the horizon. I was ready for take-off. During the ground roll, moisture started to condense on the canopy. I opened the ventilation to keep the runway in sight. Above the surface inversion, the sun rose over the horizon and completely dried the canopy. What a beautiful view! The morning sunshine illuminated the mountain ahead. The mountaintops were capped with a white cap-cloud and some cumulus fractus were seen on the lee side. This is the place to look for the lift associated with the rotor. The tow was through this turbulent air. I released at 1 200 m above ground in rotor turbulence: minus 4 and plus 8 m/s. New little roll clouds developing upstream provided sustaining lift; they had to be recognized and approached.

Suddenly, at 3 000 m, just above the mountain crest, the conditions changed. No turbulence, absolutely quiet air in this laminar flow. Good lift was contacted, a steady 5 m/s. To stay in the lift zone, I turned the glider into the wind; the flight position was kept always upwind of the leading edge of the lenticular cloud.

The position of the initial climb was abandoned at 6 000 m and the upwind edge of the well-marked wave clouds was followed crosswind to the first turning point. The outside temperature was now –25°C, and close to the clouds the canopy became sometimes covered with hoar frost. It was necessary to open the ventilation to reduce the hoar frost and improve forward visibility, but it was at the expense of a comfortable temperature.

The second turning point was far downwind. So at the first turning point, as much altitude as possible was obtained to minimize the altitude lost in the downdraught of the wave and to take advantage of the reduced density and the tailwind: the groundspeed exceeded 300 km/h! The sink rate in the downdraught was only 2 m/s, less than expected and smooth. After 20 km, the updraught of the second wave was encountered. This pattern was repeated several times and fortunately, the waves were marked with lenticular clouds. In the secondary and tertiary waves, altitude was gained by slowing down without turning into the wind.

Far downwind, the third turning point was reached at 5 500 m. The next leg back to the main ridge was oblique to the headwind. According to theory, the optimal flight path is a series of orthogonal glides. So the lines of lift were carefully followed during the crosswind glides. At the end of a wave cloud, a turn was executed directly into the headwind to get through the regions of sink into the next updraught as fast as possible. Step by step the main ridge came closer, but the glider came closer to the ground.

The steep slopes on the lee side of the mountains were expected to produce good lift in the primary wave. In the primary wave, a climb again occurred at 2, 4...6 m/s. The way back home was well marked with lots of wave clouds, perpendicular to the airflow at several levels. The sun sank close to the horizon, turning the clouds a spectacular orange-red colour.

Although the high wind speed required a remarkable crab angle, the ground speed was fast. But the indicated airspeed was carefully controlled. At higher altitudes the true airspeed is greater than the indicated speed, and at high speeds there are structural limitations because of flutter.

The closer the flight approached the airfield, the more clouds developed and the foehn gap (Figure 1.15) became smaller and smaller. Therefore, the air brakes were deployed immediately to get below the stratocumulus clouds filling the foehn gap.

After 14 hours of flight, a safe landing occurred back home. Some 30 minutes later, the cold front passed with an overcast ceiling and heavy rain.

1.5 COMBINED LIFT AND OTHER LIFT SOURCES

With the exception of convergence acting to organize convection, we have only discussed lift sources in isolation. In many cases, two or more lift sources exist at the same time, and processes even interact with each other.

A combination of elevated terrain, an environment with moderate winds and weak stability, along with sufficient insolation, leads to the simultaneous occurrence of ridge lift and thermals. This is useful to the soaring pilot since thermals often "cycle", that is, they cease to form for a period. When this occurs, soaring pilots can stay aloft using the ridge lift until thermals once again form.

In elevated terrain, in an environment with relatively strong winds aloft, along with weak stability and strong insolation in lower levels, waves can exist above an active CBL. Rough thermals typically will be found along the rising, upwind branches of rotors, possibly triggered by low-level convergence associated with rotors. Thus, an active CBL can provide a pathway for entry into the wave.

In addition to convergence, ridge and wave lift also can act as a thermal source region and organizer. Thermals will be best and more numerous where they coincide with the updraught regions of these other lift sources, and they will be suppressed in downdraught regions.

Both ridge and wave lift require elevated terrain and wind. The combination of lift sources provides soaring pilots a potential path into the wave from lower levels. In areas with complex terrain, an unfavourable phasing of waves excited by an upwind barrier can cancel lift on an otherwise lift-producing ridge.

An uncommon phenomenon sometimes occurs, in which convective cloud streets are aligned across one or more mountain ranges with mountain wave above, marked by lenticular clouds aligned parallel to the terrain. Hindman and others (2004) present an analysis of one such case.

In complex terrain, or in regions with elevated terrain bordering plains, it is possible for thermals, convergence and ridge and wave lift to exist on the same day. It is also possible for one lift source to exist during part of the day, while others are present during other times. An example (found during the fall and spring in areas with relatively low terrain) is wave during the morning hours and thermals in the middle of the day, followed by wave redeveloping as convection dies away towards the end of the day.

1.5.1 Convective waves

In flat terrain, waves can be excited above a CBL by thermals disturbing the overlying stable air, a phenomenon called convective waves. These form in an environment with a CBL capped by a strong inversion, along with relatively strong wind and shear in the stable air above. Convective waves are neither as strong nor reach as high as mountain waves, but they have been measured at heights many times the depth of the CBL (Kuettner and others, 1987). Convective waves can be randomly organized. Under certain conditions, however, the wind profile through the CBL is conducive to cloud streets. Long lines of convective waves can then form if the wind direction in the overlying stable air is perpendicular to that in the CBL.

1.5.2 Other possibilities

Another wave-like lift source is a travelling wave such as a bore. An example that has been used by soaring pilots is the Morning Glory of Australia (Pretor-Phinney, 2006). Occasionally, other occurrences of apparent travelling waves have been reported in the soaring literature.

Glider flight by dynamic soaring in a wind-shear situation is theoretically possible for gliders (Lissaman, 2007), but it is not practised.

We close this chapter by noting that the current state of our knowledge is incomplete. Over the past 80 or 90 years, soaring pilots have identified lift sources that can be categorized as convection, convergence, ridge, wave or some combination of these. It is not uncommon, however, for the soaring pilot to report lift with characteristics, or in a background environment, that does not fit our current conceptual models. It is possible that in the future, reports from soaring flights, combined with atmospheric research, will identify other, yet unknown, lift sources.

1.5.3 A pilot's view: a flight in combined lift

As we drove out to the airport, the sky offered a range of possible scenarios for our afternoon flight. There were cumulus clouds above the mountains, indicating thermal activity. There was a blustery wind coming from the west and shaking the motorglider in her tiedowns, so with the mountainous

terrain surrounding us, ridge lift was almost a given. And with wind and mountains, there's always a chance for lee waves.

When my pilot lined up the motorglider for take-off, the last wind check read 20 knots at 270 degrees. "I'll show you the Route of the Seven Lakes, from a ridge perspective", my pilot decided. Sure, this was Argentina, the mountains were the Andes – no point in chasing common thermals, when something much more indigenous to place and meteorological conditions was on the menu.

The popular sightseeing trip connects seven lakes with a road winding its way through a 90-km stretch of valleys and passes, some deep and narrow, others wide and open. It runs more or less north–south, so the adjoining ridges would be mostly perpendicular to the westerly winds, offering a good chance for decent ridge lift. To get to the beginning of our scenic flight, however, was a different story. We had to follow a valley more or less parallel to the wind, with little promise of encountering lift-producing slopes. After a climb to 2 000 m, which brought us 10 km closer to our starting point, we turned off the engine and pointed the nose into a sun-facing bowl with a small outcropping to the north. Mild turbulence indicated that the air was alive. A little searching and we found the sweet spot, where the wind hitting the small ridge and the thermal energy collected by the bowl collaborated to form an updraught, which lifted us at 2 m/s to the crest of Chapelco Mountain at 2 200 m. At the windward side of the plateau next to the summit, plumes of dust were kicked up and driven across, providing a first visible confirmation of the forecast wind.

We swung around to the steep west-facing slope and immediately felt the upward push of the ridge lift. No need to fly back and forth along the ridge to gain altitude – one slight pull up in the strongest part of the updraught and we were well above ridge line. In the steep valley below, the road meandered in wide S-turns between isolated mountains, short ridges and small contributing valleys. Seen from our vantage point more than 1 000 m above, this topography was anything but ideal for extended ridge soaring, where one looks for a long, smooth ridge running perpendicular to the prevailing wind direction, with essentially flat and unobstructing terrain upwind of its slopes.

Our ridge ended as valley and road headed in the first S-bend turning west. Rather than jumping to the next north-south slopes about 5 km ahead, and accepting the probable altitude loss due to lee effects of the mountains across the valley, we turned west, too, crossing road and valley while heading for a short, steep cliff pretty much parallel to the forecast wind direction. Amazingly enough, we found lift there. Not the powerful push we felt before, but enough to keep us at constant altitude, while cruising along at 150 km/h. What was going on? "Always fly the outer perimeter of a turn in the valley!" my pilot commented, as if talking to himself. Apparently, the complex, convoluted topography deflects the local flow so as to channel it into the direction of appropriately aligned parts of valleys, even if they run at 90 degrees to the main wind direction. And this was the perfect demonstration: coming from the north, the valley curved west before completing its S-turn and opening into a straight section heading south again. The ridge on its eastern flank rose to an almost constant altitude of about 2 000 m and obviously provided the deflecting barrier. If our channelling hypothesis was correct, then there wasn't much dynamic lift to be expected from its slopes, as most of the flow was not going to head uphill but rather "sideways", parallel to the valley floor (Figure 1.22).

And that was exactly what we found: no lift, just mild turbulence. We fell farther and farther below the ridge line. The valley widened and the middle part of the slopes was covered with dense forest. After an agonizingly long descent we suddenly felt a jolt. My pilot put the motorglider on its wingtip and muscled her into the tight core of a turbulent updraught. This was not the typical mountain thermal. "Probably a mix of thermal, ridge lift and rotor", he remarked, while trying to keep the airspeed between 130 and 150 km/h and maintaining a rather large distance to the slope. "This is a pretty dangerous combination if you're too close to the ridge", he continued. "If the rotor pushes the thermal just a little bit uphill, its downflow part sits right where one would expect ridge lift. Fly there and you're doomed!" We took the rough updraught just high enough to reach the next ridge farther south. On its smooth flank we encountered pure and strong uphill flow. Within a couple of kilometres we were well above crest line. Which is exactly what we needed: enough altitude to safely cross Lago Nahuel Huapi and reach the mountains on its south-western shore, about 15 km away.

The first ridge on the other side we hit, although perfectly perpendicular to a westerly flow, produced nothing but strong downwash.

"Channelling again", I said to myself, and searched for the telltale ripples on the surface of the lakes below to confirm my suspicion. And sure enough, the two small lakes pointing to the intersection of the corresponding valleys indicated two different wind directions, at almost 90 degrees to each other.

Somewhere out over the valley had to be one hell of a convergence. We kept pressing on. Opposite to the flanks of the volcano Tronador, we found turbulent ridge lift again. My pilot was surprised: "In this valley, ridge lift is often suppressed by the descending part of a wave system off the Tronador." Today, with its thermal instability, the wave had either not developed at all, or, more likely, did not reach down far enough to cause trouble at ridge level. We continued ridge running. Thirty kilometres ahead, we could already see the wide valley of El Bolson, the goal of our ridge mission. Its long, straight crest lines made it easy to locate the optimum flight track. With slopes rising at near-ideal angles and a wind speed of about 20 knots, the updraughts reached 4 m/s and a fast run took us to our turnpoint in no time.

A short distance farther south, we turned away from the ridge and headed for the black bottom of a well-developed cumulus. It provided us with a climb high enough to search for wave. A few circles later my pilot turned the motorglider away from the cloud into the blue sky. The variometer kept singing and soon we found ourselves at 4 000 m, all set for a return to Chapelco at flight level 130.

1.6 HAZARDS

Depending on the performance and structure of the glider, some meteorological conditions might be more dangerous to one kind of glider than another. For example, hang-gliders and paragliders are generally more exposed to hazards than gliders, mainly because of their limited speed and strength with respect to mechanical stress. Fortunately, meteorological hazards are infrequent, but they are difficult to forecast. Short-range considerations, nowcasting and careful monitoring of the actual weather, therefore, are important and helpful in identifying potentially hazardous situations.

Sometimes, good soaring conditions may turn quickly into dangerous situations if the following conditions exceed a certain limit:

(a) Instability of the atmosphere;
(b) Horizontal wind speed.

1.6.1 Thunderstorms

If an air mass is unstable and enough moisture is present, thunderstorms can be triggered either by solar heating or by synoptic features such as frontal systems, convergence lines, upper troughs and the like.

Hazards connected with thunderstorms are:

(a) Heavy turbulence and sudden wind changes close to the ground, even some kilometres away from the storm: the cold outflow may be invisible during the approach and take-off phases of a flight;

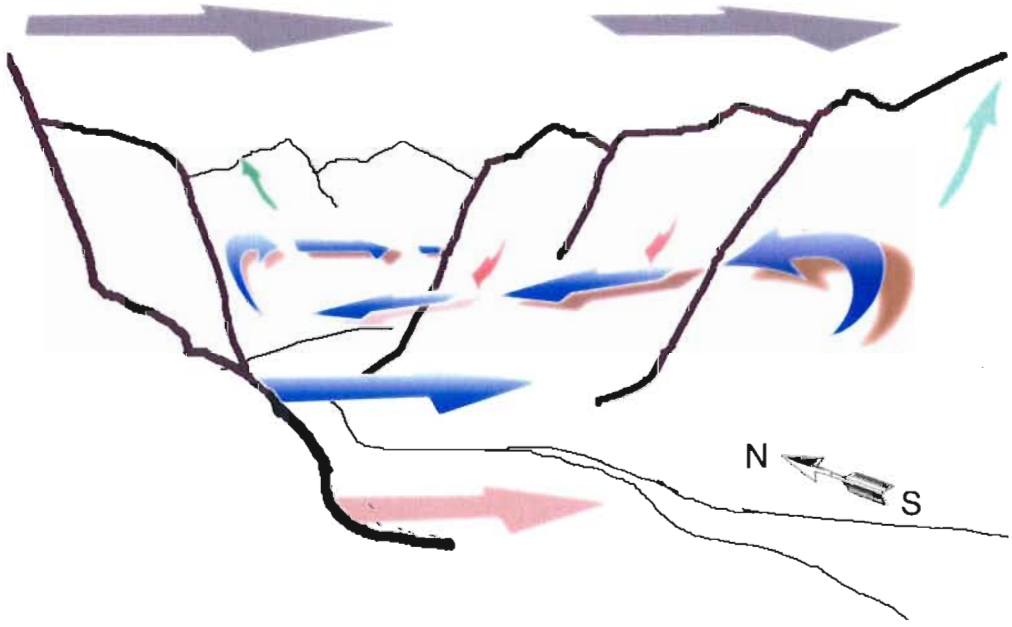

Figure 1.22. Channelling of flow in complex terrain

(b) Strong updraughts, whose climb rates can be so strong that the glider is sucked into the cloud. Paragliders and hang-gliders are especially susceptible;
(c) Strong downdraughts or downbursts: the sink rate can cause an unexpected outlanding in unsuitable terrain associated with dangerous surface wind conditions;
(d) Heavy precipitation, which can reduce the visibility rapidly;
(e) Hail, which can cause serious damage to the glider in the air as well as on the ground;
(f) Lightning, which may also strike at some distance from a storm. It is dangerous either to fly near or launch a glider in the vicinity of a thunderstorm;
(g) Tornadoes, which are often associated with extreme thunderstorms and can damage tied-down gliders, trailers and even hangars;
(h) Icing in a thunderstorm, which can be so strong that it becomes impossible to control the glider (in countries where cloud flying is permitted).

1.6.2 Strong winds and wind shear

Whenever there is a wind blowing, there are likely to be waves or slope conditions that glider pilots can enjoy. But if the surface wind or the winds aloft exceed certain limits, soaring flight becomes increasingly risky, depending on the type of glider. In addition, zones of significant wind shear or even a reversal in flow aloft can produce dangerous turbulence.

Hazards connected with strong winds are:
(a) Strong drift: in connection with lee-wave flow, little downwind drift may be noticed during the climb. But at the wave crest, the horizontal wind is strong and the sink rate increases downwind of the crest. This causes a strong unexpected drift downwind, especially for less-experienced pilots. The resulting rapid loss of height can be dangerous, depending on the terrain and the clouds below;
(b) Closing foehn gap (Figure 1.15): increasing moisture, especially if there is a frontal system approaching, can close the foehn gap rapidly. If the pilot is not aware of the changing cloud cover below, the pilot could be in a critical condition;
(c) Severe downslope winds: the flow down the lee slope may be much stronger than upstream of the ridge. Thus, flight in the lee of a ridge can cause rapid loss of altitude and terrain clearance;
(d) Rotors (Figure 1.15) with heavy turbulence make it sometimes impossible to control the glider;
(e) Wind shear on or near the ground below a rotor: sometimes moving eddies alter the low-level airflow. In foehn conditions, a cold pool of air near the ground and a strong wind above can produce a transition zone with a strong wind shear. In those conditions take-off or landing can become unsafe;
(f) Wave breaking: regions of wind shear, especially a reversed flow, may destroy the waves and produce heavy turbulence. (If not marked by clouds, this is called "clear air turbulence".) In these conditions, it can be difficult to keep the glider within design speed limits;
(g) Orographic effects: flows through gaps of mountains can accelerate the wind speed significantly (2–3 times more than the general flow). The resulting downdraughts, wind shear and turbulence can be serious.

CHAPTER 2

GLIDERS AND SOARING FLIGHT

GLIDERS

Gliding is a recreational activity and competitive sport in which pilots fly aircraft known as gliders. Properly, the term gliding refers to descending flight of unpowered heavier-than-air craft, while soaring is the correct term to use when the craft gains altitude or speed from rising air between phases of gliding, thus allowing prolonged flight.

Gliders with a high aerodynamic performance are sometimes called "sailplanes". The term "glider" also encompasses hang-gliders and paragliders. Like sailplanes, these can use updraughts to soar.

Most modern sailplanes are constructed of fibre-reinforced plastic (glass, carbon or Kevlar fibre). Older (vintage) sailplanes are made of metal or wood and fabric.

All sailplanes have ailerons, a rudder and elevator controls. They also have some form of spoilers or flaps to control the rate of descent for landing. Some high-performance gliders also have trailing-edge flaps to optimize the airfoil for different speed regimes.

Sailplanes do not necessarily have to be lightweight aircraft. Modern types are designed to carry water ballast (to increase the ratio of overall weight to wing area). This boosts the cross-country soaring speed by increasing the speed for any given glide angle/performance. This ballast can be jettisoned in weak updraught conditions to improve climb performance or before landing to avoid undue stress on the airframe.

For storage, transport between flights or retrieval after an off-(air)field landing, gliders can be dismantled, or derigged, and stowed in a trailer.

Hang-gliders and paragliders both started out as foot-launched gliders. They differ most distinctly in the design and construction of their wings. Paragliders have a wing consisting of two layers of fabric, connected in such a way as to form a row of cells whose shape is formed by the pressure of entering air. The wings of hang-gliders are predominantly fabric supported by a rigid aluminium or composite frame. In both gliders, the pilot sits or lies in a harness suspended from the wing. Due to their flexible design, both types are easier to (de)rig and transport than conventional sailplanes, but they are also more susceptible to adverse weather conditions.

2.1 CLASSES AND PERFORMANCE

For competition and records, gliders are classified according to several criteria, the most apparent being wing span. Table 2.1 contains typical characteristics of gliders, while Table 2.2 gives an overview of typical characteristics of sailplanes in the classes presently recognized by the International Aeronautical Federation (FAI) for international championships and world records.

Motorgliders can be operated in both an aeroplane mode and a glider mode. According to the prevalent mode of usage, they are grouped in two categories:

(a) Touring motorgliders, which are predominantly used for powered (cross-country) flight, in a similar fashion as small aeroplanes. Owing to their comparatively smaller fuselage, they carry at most two people. In connection with their larger wingspan, they have moderate soaring performance;

Table 2.1. Typical characteristics of gliders

Class	*Wing span*	*Empty weight*	*Gross weight*	*Best glide ratio @ speed*	*Min. sink rate*
Paraglider	10 m	8 kg	100 kg	1:8 @ 38 km/h	1.2 m/s
Classical hang-glider	11 m	32 kg	130 kg	1:13 @ 50 km/h	1.1 m/s
Rigid hang-glider	13 m	50 kg	150 kg	1:27 @ 65 km/h	0.7 m/s
Glider	15 m	230 kg	525 kg	1:46 @ 105 km/h	0.51 m/s

Table 2.2. Typical values for glider classes for international competition and world records

FAI class	*Wing span*	*Empty weight*	*Gross weight*	*Best glide ratio @ speed*	*Min. sink rate*
Ultralight class	13 m	110 kg	max. 220 kg	1:37 @ 85 km/h	0.60 m/s
World class	13.44 m	190 kg	300 kg	1:33 @ 80 km/h	0.64 m/s
Multi-seat class	20 m	420 kg	700 kg	1:45 @ 103 km/h	0.58 m/s
Club class	15 m	230 kg	525 kg	1:40 @ 90 km/h	0.58 m/s
Standard class	15 m	230 kg	525 kg	1:44 @ 95 km/h	0.55 m/s
15 m class	15 m	230 kg	525 kg	1:46 @ 105 km/h	0.51 m/s
18 m class	18 m	270 kg	575 kg	1:50 @ 105 km/h	0.45 m/s
Open class	No limit	480 kg	850 kg	1:65 @ 110 km/h	0.40 m/s

(b) Motorized sailplanes, which are sailplanes equipped with a small engine that can be retracted completely into the fuselage. They come in two variants:
   (i) Self-launch motorgliders, which have engines powerful enough to enable the aircraft to take off, climb repeatedly and thus cover moderate distances in non-soarable weather conditions;
   (ii) Motorgliders with sustainer engines that are less powerful and provide only limited climb performance. They are useful to avoid off-field landings or to continue a flight under marginal soaring conditions.

Many newer sailplanes, particularly in the 18-metre and open classes, are equipped with retractable engines, since their performance differs little from the non-motorized versions.

2.1.1 Straight-flight performance

The aerodynamic performance of gliders and sailplanes in straight flight is characterized by their speed polar $w(v)$, representing the dependence of the sink rate w on the airspeed v (Figure 2.1). The best glide ratio v_0/w_0 is obtained from a tangent to the speed polar. This best glide ratio v_0/w_0 and the corresponding speed v_0 are the major parameters for the classification of gliders and sailplanes (Irving, 1998; Liechti, 2001). A speed range from about 75 per cent (stall speed) up to 250 per cent of v_0 can be used.

In straight flight the glide ratio v/w decreases for speeds slower and faster than v_0 (Figure 2.2). At double the speed of v_0 the glide ratio is reduced to 50 per cent.

2.1.2 Climb performance

For a glider in steady circular flight, the sink rate w changes with the radius r of the turn (Thomas, 1999). Slow gliders can climb in quite narrow atmospheric lift patterns with diameters of 30 m to 50 m, while faster sailplanes need wider updraughts with diameters of about 150 m in order to gain altitude (Figure 2.3).

The typical sink rate in circular flight is between the range of 0.8 m/s and 1.2 m/s, and the minimum time needed for a full circle is between 10 s and 20 s. Atmospheric lift patterns must exceed all these threshold values in terms of size, strength and lifetime in order to allow gliders to climb.

Typically, convection generates a lift pattern of localized updraughts centred around a core. A parabolic lift profile with a core updraught of 3 m/s and a radius of 150 m describes a thermal of moderate strength quite well (Figure 2.4). Strong thermals are often wider, while weak thermals are more confined.

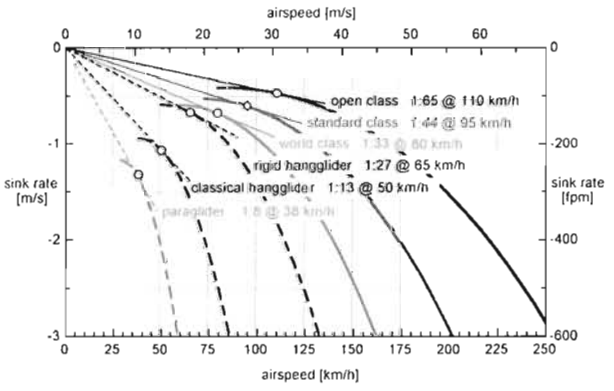

Figure 2.1. Speed polars of gliders and sailplanes in straight flight

A vertical displacement of the parabolic lift profile conveniently represents these typical properties of thermal updraughts. The lift distribution within actual thermals can be more complex.

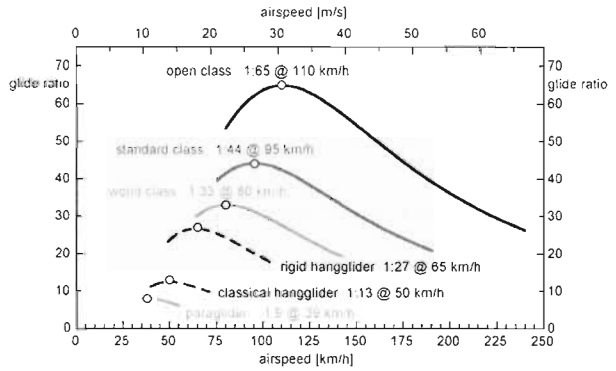

Figure 2.2. Glide ratio of gliders and sailplanes in straight flight

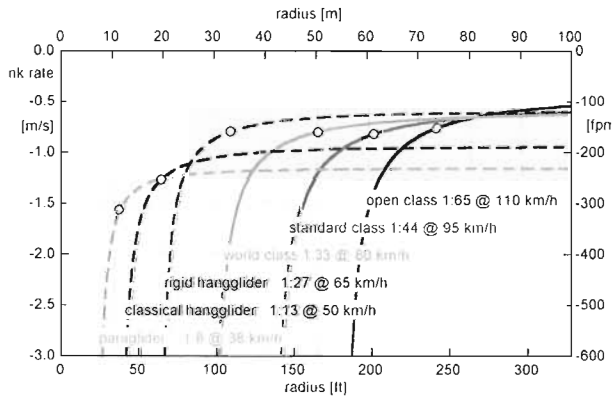

Figure 2.3. Sink rate of gliders and sailplanes in steady turn

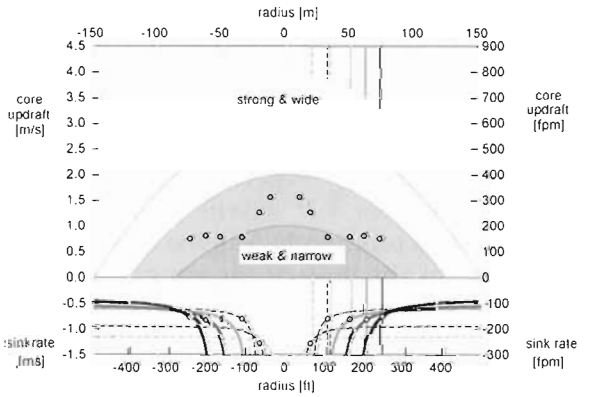

Figure 2.4. Parabolic lift profiles (top) and sink rate of gliders and sailplanes (bottom) in steady turn. Open circles refer to the optimum turn radius, the corresponding sink rate and the minimum required core updraught of a standard parabolic thermal.

A circling glider climbs when its sink rate is less than the updraught velocity. It is easier for light and slow gliders to climb when circling in weaker and more confined updraughts than it is for heavy and fast sailplanes. According to the standard parabolic lift profile, the minimum radii are 24 m, 32 m, 50 m, 62 m and 74 m for paragliders, hang-gliders and world-class, standard-class and open-class sailplanes, respectively. The core lift of the displaced standard parabolic lift profile must exceed 1.6 m/s for open-class sailplanes, whereas hang-gliders require at least 1 m/s.

2.2 CRUISING SPEED

The spatial distribution of updraughts can be localized or extended. This has an effect on the average cross-country speed of a glider (Ragot, 2004).

2.2.1 Localized lift

Lift is considered localized if the horizontal extension is only slightly larger than the diameter of a circular flight track, as is typical for convection. With a pattern of localized updraughts, gliders have to climb in circling flight and switch to straight flight to cover distance, at the expense of the gained altitude.

The average cross-country speed in localized lift is obtained from the distance flown and the sum of the times spent climbing and gliding back to the initial altitude. In flight, pilots optimize the average cross-country speed by adjusting the glide speed to the climb rate obtained when circling (Figure 2.5).

In strong and large-sized updraughts, high-performance sailplanes with water ballast reach a significantly higher average cross-country speed

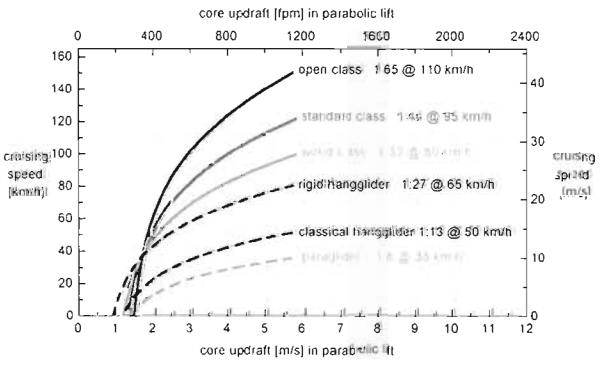

Figure 2.5. Average cross-country speed in localized updraughts

than light and slow gliders. In weak localized lift, however, light and slow gliders do better.

2.2.2 Extended lift

Patterns of extended lift are generated by wind, orography or both: examples are ridge lift, wave lift, convective rolls and convergence lines. Patterns of extended lift and localized lift can coexist in the atmosphere.

In an extended pattern of updraughts, gliders may cruise without circling and control altitude by adjusting the airspeed to the updraught. The average cross-country speed can be substantially higher in extended lift than in localized lift (Figure 2.6).

High-performance sailplanes need less extended updraught than gliders to maintain altitude in straight flight and they cruise at higher speeds.

2.3 GROUND SPEED

The ground speed is a combination of the average cross-country speed and the drift caused by the wind (Figure 2.7). The ground speed is anisotropic with wind: the minimum ground speed is obtained for headwind tracks and the maximum for tailwind tracks. For crosswind tracks the ground speed is intermediate between tail- and headwind tracks. Paragliders and hang-gliders are more sensitive to wind than sailplanes because of their slower average cross-country speed. The ground speed is relevant for flight planning.

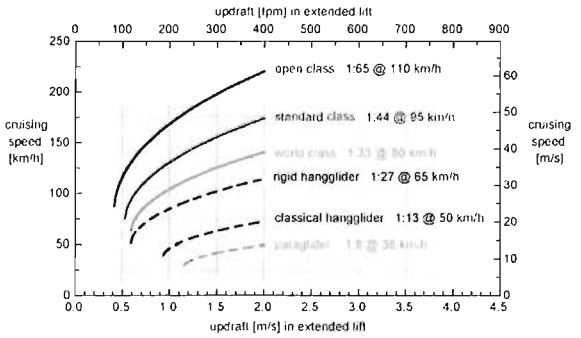

Figure 2.6. Average cross-country speed in extended updraughts

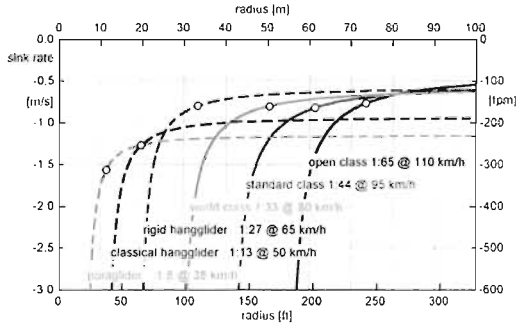

Figure 2.7. Wind drift and ground speed

2.4 EFFECTS ON PERFORMANCE

The speed polar is sensitive to changes in the air density, the wing loading (the weight of a sailplane divided by the wing area) and the wing profile (Thomas, 1999; Irving, 1998). The effects of reduced air density on the flight polar $v(w)$ become significant at high flight levels. Both the airspeed v and the sink rate w increase with reduced air density ρ, where ρ_0 is density at sea level (Table 2.3):

Table 2.3. Increase in airspeed as a function of altitude

Altitude (m)	*3 000*	*5 000*	*7 000*	*9 000*
ρ/ρ_0	0.74	0.60	0.48	0.38
$(v/v_0)^{-1}$	+16%	+29%	+44%	+62%

The increased airspeed is favourable for cruising. In circular flight, however, the radius increases with reduced air density and the increased radius for circling requires larger lift patterns for climbing. The increased minimum speed also leads to longer runs for take-off and landing. The maximum speed of a glider (V_{ne} = velocity never exceed) is defined because of structural limitations (flutter).

An increase in the wing loading has the same effects on the flight polar as a decrease in air density. In competitions with high-performance sailplanes, water ballast is used to increase the wing loading up to 50 per cent in strong weather.

The aerodynamic performance of a sailplane wing suffers $\sqrt{\frac{\rho_0}{\rho}}$ when the laminar airflow becomes partly turbulent due to insects that accumulate on the nose of the wing. Rain drops produce a similar effect.

2.5 INSTRUMENTATION AND EQUIPMENT

Sailplanes, motorgliders, ultra- and microlight gliders and hang-gliders typically have an airspeed indicator, altimeter, a particularly sensitive

rate-of-climb and descent indicator (variometer) and a magnetic compass. Some also have instruments for flying in non-visual conditions, such as an artificial horizon. Often these basic instruments are supplemented (Figure 2.8) by sophisticated electronic gear to calculate optimum speed to fly from measured achieved climb rates and the speed polar.

Most gliders used for cross-country flight carry a navigation system consisting of a global positioning system (GPS) receiver and a moving map display. This system records position (latitude, longitude, altitude) with typical GPS resolution (5–50 m) at intervals ranging from a few to several tens of seconds. For flight documentation, these data can be stored on a digital device for the duration of the flight. They can also be fed into an on-board navigation computer to derive and display wind information and guidance for final glides.

In addition to the flight instruments, sailplanes often carry equipment to address the needs of flights in special conditions. Radios and, occasionally, transponders provide communication with other aircraft, as well as with air traffic control, and are necessary for access to certain types of airspace. An oxygen system including bottle, pressure valve and face mask is mandatory for flight at high altitude. For world altitude record attempts, pressure suits are required as the present record in absolute altitude stands at more than 15 km.

Anti-collision or proximity-alert devices can be found in an increasing number of gliders. Based on transmitting and receiving GPS position data, these units generate an audio-visual alarm whenever the flight path of a glider is extrapolated to intersect with that of another glider or a known obstacle within a speed-dependent time window.

As even small irregularities on the laminar airfoils of modern sailplanes can inflict heavy performance penalties, all contamination, particularly at the wing leading edge, is unwanted. Consequently, many of the sailplanes used in competition are equipped with so-called bug wipers, which are small plastic bows that conform to the shape of the airfoil and drag a thin nylon thread spanwise across the leading edge, thus scraping off small insects.

SOARING FLIGHT

Most flights in gliders are prolonged flights in which, after an initial altitude gain accomplished by several methods of take-off, a climbing phase using various types of updraughts is followed by a descent, giving up altitude to cover distance. Instructional flights are mostly descent-only flights in fairly close range of an airfield. Soaring flight is usually conducted in visual meteorological conditions (VMC).

Figure 2.8. Instrument panel of a self-launch glider: airspeed indicator (1), magnetic compass (2), anti-collision alert (3), variometers (4), altimeter (5), radio (6), engine control unit (7), GPS navigation computer (8), transponder (9), moving map display (10)

2.6 PROCEDURES AND OPERATIONS

2.6.1 Ground handling

In preparation for flight, gliders may have to be rigged and pushed or towed to a take-off position. Most gliders can be rigged and prepared for take-off in about 10–30 minutes. Rigging a sailplane primarily involves attaching the wings and elevator to the fuselage, connecting controls and adding water ballast, if applicable and desired. Taxiing patterns and tie-down procedures are similar to those of general aviation, except that the aircraft are moved about usually by towing them by car. Derigged hang-gliders and paragliders packed in their bags can be carried, at least a short distance, by one person. They are usually rigged close to a launch position. Rigging may be impossible on exposed sites in fresh or gusty winds.

2.6.2 Take-off

The most common and widespread method for launching a glider is to tow it with a powered aircraft (aerotow) up to a height where the pilot releases the towrope and starts gliding. For sail-

planes, 600 m above ground is a widely used release height, especially in competitions. During the ground run along the runway, directional control, especially of heavily ballasted sailplanes, can be difficult in crosswinds of more than 20 km/h. Aerotowing (usually by microlight aeroplanes) from flat sites is increasingly used for hang-gliders as well.

Winch launch is another popular launch method. A winch pulls in a cable of fixed length between 800 and 1 200 m, hauling the glider up to release heights of usually 250 to 500 m. The winch is often mounted on a mobile chassis to accommodate different take-off directions for optimum headwind components. Hang-gliders can also be winch-launched. Occasionally a car replaces the winch, pulling the glider up to release height. This method requires powerful cars and long airfields.

Historically, elastic ropes (bungee cords) have been used to catapult a sailplane, mostly from the ridge of a hill into the upslope airflow. This works reasonably well for slow-flying, lightweight vintage gliders. Hang-glider or paraglider pilots achieve the same effect by running down a hill slope or a specially built ramp or launch pad. This foot launch is the most common method in hang-gliding and also for foot-launched ultra- and microlight gliders.

2.6.3 Flight

After launch, the pilot must find lift for the sailplane to gain altitude. Once sufficient altitude has been gained, the sailplane glides to an area where a usable updraught is expected for the next climb. Meteorologically, flight time is limited by the duration of usable lift.

2.6.4 Final glide and landing

For a high-performance sailplane, the approach can be a long and very shallow glide – for example at an angle of about 1 degree, from an altitude of 2 000 m and a distance of more than 100 km from the intended landing site. The pilot can monitor this so-called final glide by the use of a final-glide calculator, which uses position data from a GPS navigation system, measured airspeed and stored glider performance data.

For sailplanes, approach and landing technique is similar to that of powered aircraft. It is preferable to land into wind as gliders have only limited control for cross- or downwind landing. Due to being unpowered, a glider cannot compensate for loss of airspeed resulting from low-level wind shear or turbulence without steepening its glide path, thus compromising its ability to reach a certain landing spot. Therefore, the last part of an approach to landing is at a speed which the pilot anticipates to be sufficient for coping with adverse low-level flow phenomena.

Approach and landing are similar in principle for ultra- and microlight gliders, hang-gliders and paragliders, but distances, time and airspeed are progressively reduced. These gliders are also more sensitive to turbulence and wind shear.

2.7 TYPES OF FLIGHT

2.7.1 Instructional and local flights

Instructional flights are conducted in order to learn and practise the control of a glider within its flight envelope. The goal of these flights is primarily to get a glider license or rating. They take place in a practice area close to an airfield. Take-off decisions are made for the most part on the basis of meteorological conditions observed by the pilot or instructor.

2.7.2 Cross-country flights

Once a flight reaches a position from which a return to the take-off airfield necessitates an additional climb, it is called a cross-country flight. For such flying, pilots need route or area forecasts for planning purposes. To optimize progress and flight safety, they constantly adapt their flight tracks to changing meteorological conditions.

2.7.3 Competition flights

Formal world and international championships in all established air sports are regulated and authorized by the FAI. National and regional contests in principle follow the same rules, which are occasionally adapted to accommodate lower levels of pilot experience.

Competition gliding usually comprises a number of tasks in which pilots accrue points. The tasks normally entail flying around or along courses via turnpoints. Points are awarded for speed and distance achieved. With the exception of Grand Prix-style competitions, only one task per

competition class or group is set on a competition day.

Characteristic distance and time ranges for competition flying in sailplanes, hang-gliders and paragliders are related to the meteorological conditions. Usable altitudes are increasingly limited by airspace restrictions, and not necessarily by the height ranges of updraughts. Cloud flying is usually not permitted in championships.

International sporting events are organized under the rules of the FAI. The different competitions, the classes (Table 2.2) and tasks are defined in the FAI Sporting Code (Table 2.4).

2.7.4 Record flights

Record flights are individual efforts and often need personalized meteorological support. Successful record attempts for speed, distance or altitude will most likely make use of wave and, occasionally, convective updraughts. For the latter, atmospheric motion is the major limiting factor (duration, strength and alignment of thermals). For wave flights, however, aerodynamic engineering becomes the major limiting factor (maximum airspeed, flutter). Record attempts in wave lift require specialized meteorological services, which might also have to address logistical and operational aspects of high-altitude flight.

Table 2.4. International gliding sporting events

FAI competitions	*Short description*	*Tasks*	*Meteorology*
Sailplane Grand Prix	Max. 20 pilots; one class; duration 8 days; 7–10 events/year in different places all over the world	Speed tasks with "regatta start" and a number of turnpoints, designated by the organizer	Meteorological information has to be prepared by the organizer for the task-setter and the pilots Pilot's decision game only during flight
Championships World, continental, national, regional	Up to 120 pilots in different FAI-classes Open, 18 m, 15 m, standard, world, club and 20 m multi-seat class	(a) Racing tasks; the organizer sets a number of turnpoints in a sequence which the pilot has to pass through (b) Assigned area task (AAT); (speed and distance) the pilot has to achieve the highest speed and/or the greatest distance in an assigned area, designated by the organizer	Meteorological briefing for the task-setter and the pilots by the organizer The task-setter is able to select the type of task and adjust it to the uncertainty of the weather situation (for example, AAT when showers or thunderstorms are expected) The pilot decides his individual start time and in ATT the distance of his flight as well. Meteorological support from a team meteorologist can be helpful
Online contest OLC Classic and IGC-OLC world league	Cross-country flights are documented worldwide on the Internet and ranked every day and every year, also special speed competitions for clubs of specified airfields	Free selected turnpoints during flight as a polygon Sprint task in a 2.5-hour period with up to 3 turnpoints	Meteorological flight planning by the pilot before and during the flight
Barron Hilton Cup	2-year period; winners of 5 geographic regions are invited to a soaring week at Barron Hilton's ranch	The longest triangular flight in a region. The course must be declared in advance by the pilot	Meteorologically based decision before the flight

CHAPTER 3

WEATHER FORECASTS

Weather forecasts are based on observations and measurements that define the state of the atmosphere. The atmosphere changes over time according to physical laws. Numerical models represent these laws with a limited spatial and temporal resolution in order to allow computers to calculate the atmospheric changes. The scales of the updraughts relevant to soaring are at and below the resolution limits of today's operational weather forecast models. Thus, special techniques are needed for soaring forecasts. Particular methods are also in use for the presentation of these forecasts to pilots.

3.1 OBSERVATIONS AND MEASUREMENTS

The basis for every weather forecast and warning is the information on the actual state of the atmosphere. The main observation and measurement systems are (Figure 3.1):

(a) Conventional observations and measurements;
(b) Ground-based remote sensing;
(c) Satellite-based remote sensing.

The following is a list of the observations and measurements that are used operationally (here "wind" always denotes horizontal wind speed and direction):

Figure 3.1. Meteorological observations and measurements are used to define the initial atmospheric state for numerical model forecasts.

(a) Land stations and ships (wind, visibility, station pressure, temperature, humidity and precipitation);
(b) Buoys (pressure, humidity and wind);
(c) Radiosondes (vertical profiles of wind, temperature and humidity);
(d) Aircraft (wind, temperature);
(e) Wind profilers (vertical profiles of wind);
(f) Ground-based radars (precipitation analyses derived from reflectivity of radar radiation);
(g) Satellites (cloud types, cover, movement, development, dissipation).

Systems used experimentally in preparation for their operational use include:

(a) Ground-based Doppler radars (vertical profiles of wind);
(b) Vertical profiles of temperature from radio acoustic sounding systems (RASS);
(c) Indirect sounding systems via satellites (temperature profile and integrated water vapour in a vertical column).

The above-mentioned data are not nearly sufficient to determine the initial state accurately enough, however. There are large data gaps, especially over the oceans and polar regions. The three-dimensional measurement of the wind field and the humidity is particularly incomplete. Numerical weather prediction is, therefore, an under-determined initial value problem. This is one of the reasons that the weather forecasts are not always correct.

3.2 NUMERICAL WEATHER PREDICTION

3.2.1 General

The simulation of atmospheric processes on a computer, with the aim of deriving future developments based on the current state, is known as numerical weather prediction (NWP). With the exception of extremely short forecast periods (hours, for example), most numerical weather forecasts are produced for the next two to ten days.

Such simulations are feasible because atmospheric processes – and thus the development of the weather – can be described by physical laws. The

mathematical formulation of these laws leads to a set of equations that describe the temporal change in the atmospheric-state variables (such as pressure, wind velocity and temperature). Unfortunately, the mathematical form of these equations is so complex that an exact (analytical) solution is not possible. They can, however, be solved approximately by means of numerical processes.

The numerical solution of the model equations requires, as a first step, the definition of the model grid. This is complicated by the fact that the spatial and temporal structure of the weather processes in the atmosphere is variable. Thus, in addition to the large-scale distribution of high- and low-pressure areas (with characteristic dimensions of some 1 000 km), which determine the general weather situation, there are also small-scale phenomena, such as thunderstorms (with the characteristic dimensions of tens of kilometres), which can have a dramatic influence on weather. Consequently, the most accurate model grid resolution possible is necessary.

The demand for a global model area with, at the same time, finer resolution of the grid, is in conflict with the finite capacity of the computer available. As the computing effort increases with the number of grid points, a forecast for a period of several days has to be completed within a few hours of computing time. Furthermore, the number of model grid points is strictly limited, even for the largest computers. The computers currently used in routine operation at many of the world's meteorological services solve this problem by using a higher-resolution (regional) model (RM) with a mesh size of 5–10 km, embedded in a global model (GM) with a mesh size of 25–60 km (Figure 3.2).

The larger-scale state variables of the corresponding GM prognosis are given at the edge of the RM during the forecast. In a further computer run, a local model (LM) with a mesh size of 2–4 km can be embedded in the lower-resolution RM. The state variables of the corresponding RM prognosis are then given at the edge of the LM during the course of the forecast.

3.2.2 Data assimilation

Mathematically speaking, numerical prediction is an initial value problem: define the state of the atmosphere at each grid point (x, y, z) at an initial time (t). At present, intensive research and development are being carried out in the field of four-dimensional data assimilation, since a more precise and detailed definition of the initial state is expected. The combination of improved assimilation procedures with additional observations and measurements made in previously data-sparse areas has been the main reason for the improvements achieved in large-scale global NWP during the last 10–15 years. This approach is expected to result in further improvements of forecast quality.

3.2.3 Parameterization

In order to solve the equations of an NWP model, a spatial and temporal grid has to be defined. A direct forecast in the model grid is possible only for such processes that have characteristic dimensions of at least double the distance between the grid points. Even in the relatively fine-mesh grid of a convection-resolving model, it is not possible to directly simulate all important small-scale processes. One example is the turbulent exchange of momentum, heat and water vapour between the ground and the lowest layers of the atmosphere. The related processes have typical dimensions of only a few metres. The transports take place by means of molecular processes exactly at the earth's surface. The most important of small-scale processes are shown in

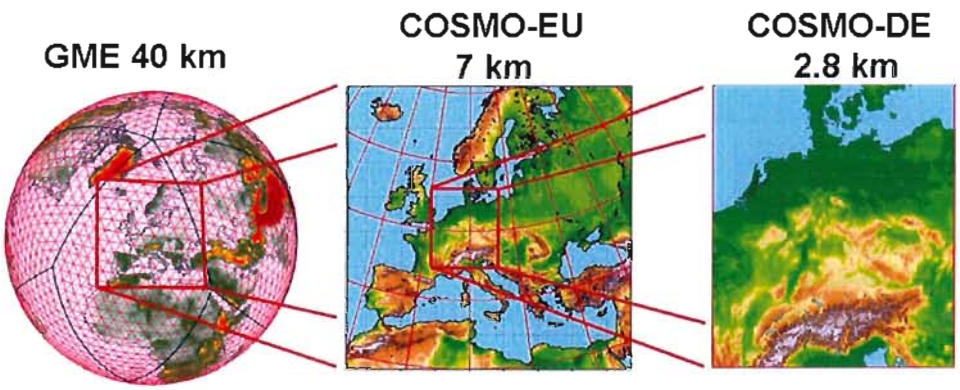

Figure 3.2. The model chain at the German Weather Service: left, the global model (GM); centre, the regional model (RM); and, right, the local model (LM)

Figure 3.3. All these processes defy direct simulation in the model grid. In relation to the model grid they are subgrid-scale processes, as opposed to the grid-scale processes that can be simulated directly. The scales of the parameterized processes are separate from those of the directly simulated processes (scale separation). In spite of their small dimension, they must not be neglected. This is immediately clear with regard to the formation of precipitation.

In addition, intensive interaction occurs in the atmosphere among all processes, even when they have completely different characteristic dimensions. This is why simulation of the subgrid-scale processes is important for the correct simulation of the grid-scale processes in the NWP models. Therefore, they must not be neglected. They are taken into account by means of so-called parameterizations.

First, a parameterization is the description of a subgrid-scale process using the grid-scale state variables at the model grid points. Second, a parameterization is the determination of the temporal changes in the state variables on the basis of the process. For example, the following processes are parameterized in most NWP models (the examples below are from the German Weather Service (DWD) models):

(a) Radiation;
(b) Grid-scale precipitation, cloud microphysics;
(c) Formation of showers and thunderstorms (deep moist convection; in the LM, for example, this is simulated directly as a grid-scale process);
(d) Formation and dissipation of clouds;

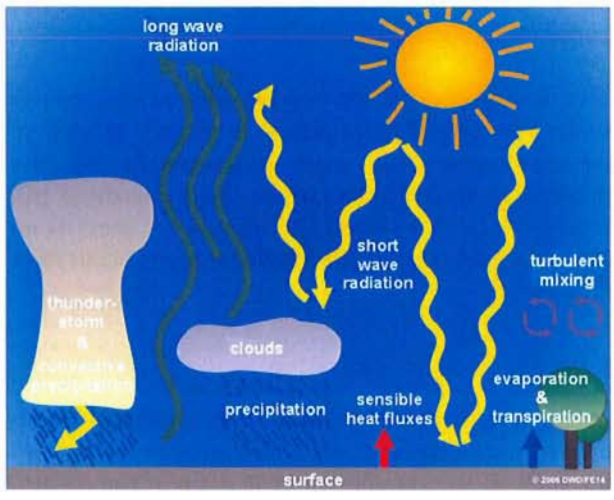

Figure 3.3. The most important processes that must be parameterized in numerical models of the atmosphere

(e) Turbulent exchange of momentum, sensible and latent heat fluxes between the earth's surface and the atmosphere;
(f) Subgrid-scale orographic effects (mainly from mountains), which, among other things, cause waves in the atmosphere and thereby exert a decelerating effect on the flow at high altitudes (only in the GM; in the RM and the LM, these waves are resolved by the model grid and therefore are simulated directly as grid-scale processes);
(g) Processes in the uppermost soil layers;
(h) Change in the thickness and temperature of sea ice;
(i) Changes in the temperature of lakes (not yet operational).

3.2.3.1 Convective parameterization schemes as an example

The main objective of the schemes for convection is to provide tendencies to grid-scale prognostic variables such as temperature and humidity, which result from coherent but subgrid-scale processes associated with condensation in cumulus clouds and their interaction with the environment. At the same time, these schemes determine the amount of convective precipitation generated by such clouds.

In order to establish the existence of convective clouds within a particular model grid box at a given time within the forecast, the first step of any convection scheme consists of a virtual parcel ascent, which typically uses characteristic properties of near-surface air based on the grid-scale thermodynamic variables. Frequently, this near-surface air is perturbed slightly in an attempt to emulate possible subgrid-scale variations. In stable atmospheric conditions, the lifting of such a parcel will be terminated by a lack of buoyancy with regard to the properties of the environmental air aloft. If, however, unstable conditions allow a dry adiabatic lifting due to positive buoyancy of the parcel until a cumulus condensation level is found, the first model level where this occurs is considered to be the "convective cloud base height" in the NWP models. From that level upwards, the parcel ascent follows a moist adiabat and the thermodynamic properties of the parcel are adjusted to account for the latent heat released by the condensation process. At this stage, the effects of lateral entrainment and detrainment are not considered, that is, the exchange of cloud air with the environment is ignored and the ascent continues until a cloud top is found, which is the level where the parcel is no longer buoyant with regard to the environment.

Since most NWP models employ a bulk mass-flux convection scheme, some determination of convective cloud type must be made in order to determine essential cloud properties, such as lateral entrainment coefficients. The cloud-base mass flux is derived from the total moisture convergence, that is, the sum of surface evaporation and the horizontal convergence of moisture. The distinction between shallow and deep convection is based on the relative role of the surface evaporation and the horizontal convergence of moisture. Alternative approaches, such as the approach used in the NWP model of the European Centre for Medium-Range Weather Forecasts (ECMWF), determine the cloud-base mass flux for deep convection on the basis of convective available potential energy (CAPE) integrated over the cloud layers, and distinguish between various convection types mainly on the basis of cloud thickness. Even though CAPE is not used directly in the parameterization schemes employed by the NWP models of the DWD, it is computed and can be used as a diagnostic product that carries information about the atmospheric stability simulated by the model. Once the cloud type and associated properties are defined, the parcel ascent is repeated with due regard for the effect of mixing through lateral entrainment and detrainment on the cloud properties, and a revised cloud top is determined.

The vertical profiles for updraught and downdraught mass flux are determined from the cloud-base mass flux and the lateral entrainment and detrainment coefficients. Tendencies of the various thermodynamic model variables are obtained from the divergence of the respective vertical fluxes computed on the basis of the updraught and downdraught mass flux. The cloud condensate content determined for the updraught after consideration of lateral and cloud top detrainment is converted to precipitation in deep convective situations, but may evaporate partially or completely in the sub-cloud layer.

The parameterization scheme itself requires no explicit determination of cloud cover at any model level. Convective clouds, just like other forms of subgrid-scale clouds, however, are an important atmospheric constituent for the radiative transfer computations in particular. A convective cloud fraction for each layer is diagnosed empirically based on the vertical extent of the convection, and it is provided to model users.

The parameterizations contained in the models are constantly being monitored by verification of the forecast results. If this shows indications of unsatisfactory results, or if improved methods are offered in literature, the existing methods are modified or replaced. The modification of an existing parameterization generally means an improved definition of free parameters that appear in the method. Each change is followed by sophisticated quality control of the new version within the forecast model as a whole. This entails calculating forecasts with the modified model parallel to the operational model over a period of one to two months. Then the results of both versions are compared (verification) and both are compared with the actual weather. In the case of an overall positive result, the previous operational model is replaced by the modified model.

One of the most important differences between an RM and an LM is that the LM does not use a deep convection parameterization. Instead, the LM resolves the larger parts of convection with its whole life cycle, the generation of updraughts, the latent heat release, the formation of ice particles and the formation of a cold downdraught, which can generate gust fronts. Therefore, a better representation of convective gusts can be achieved. The travelling of such cells with the mean wind is simulated by the LM as well. A shallow convection parameterization scheme may be required for the smaller scales of convection. Such a scheme can transport moisture from the boundary layer to a height of about 3 km, and it can therefore avoid the overestimation of low cloud coverage. Without a deep convection parameterization, there seems to be a need for a faster-sedimenting ice phase. Thus, a microphysics scheme can be extended by a new precipitation class. The introduction of a detailed three-dimensional turbulence scheme with a full and more detailed soil model (Baldauf, 2004) could be a further improvement of the physics parameterizations.

The description of the topography of the earth's surface (external parameters) is closely related to parameterizations, and particularly to the modelling of the processes in the uppermost soil layers. Figure 3.4 shows the orography used in an LM. Steep slopes can be resolved more accurately (Figure 3.5).

3.2.3.2 Scale separation

An important prerequisite for the correct formulation of parameterizations is the clear separation of the scale of the model from the scale of the parameterized process. The processes must be considerably smaller, in spatial and temporal scales, than the model grid scale (at least double the grid-point

distance and double the length of the time step). This prerequisite is naturally fulfilled for molecular processes (radiation), and it is also true for the formation of precipitation and the turbulent exchange processes.

There are, however, processes that do not show a clear scale separation. This applies in particular to deep convection. With characteristic horizontal dimensions of only a few kilometres and a characteristic time of several hours, it is spatially still subgrid-scale for a global model (such as the DWD GM) and at least in the proximity of the resolved processes for a regional model (such as the DWD RM). Large convective elements (such as a thunderstorm) can be resolved in the LM, with its grid width of about 2.8 km.

When convection is temporally not subscale in any model, the prerequisite of scale separation is not fulfilled. For example, in the DWD GM and RM, the resolution is insufficient for an explicit simulation of convection (Figure 3.6). Experience has shown that, in spite of the lack of a clear scale separation, a parameterization of convection is necessary. The results are often not satisfactory, but without parameterization they would, as a rule, be worse. Only an LM allows, at least roughly, a direct simulation of showers and thunderstorms.

3.2.4 Application models

The output of the operational NWP models is used as input data for a large number of specialized

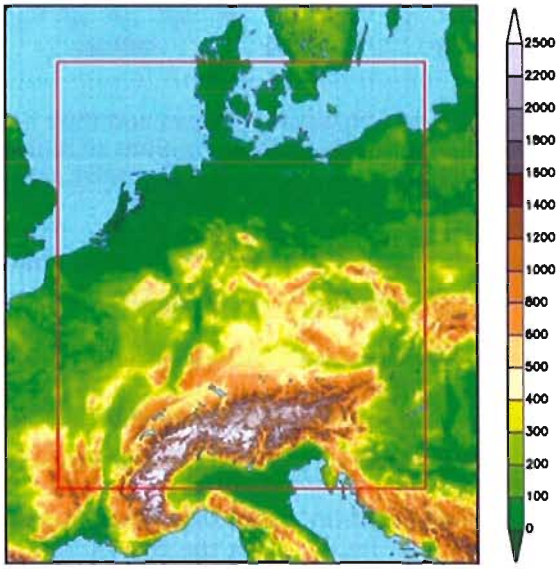

Figure 3.4. Mean elevation of terrain for the grid elements of the DWD local model (in metres as indicated by the colour scale). The brown box is the region of this model.

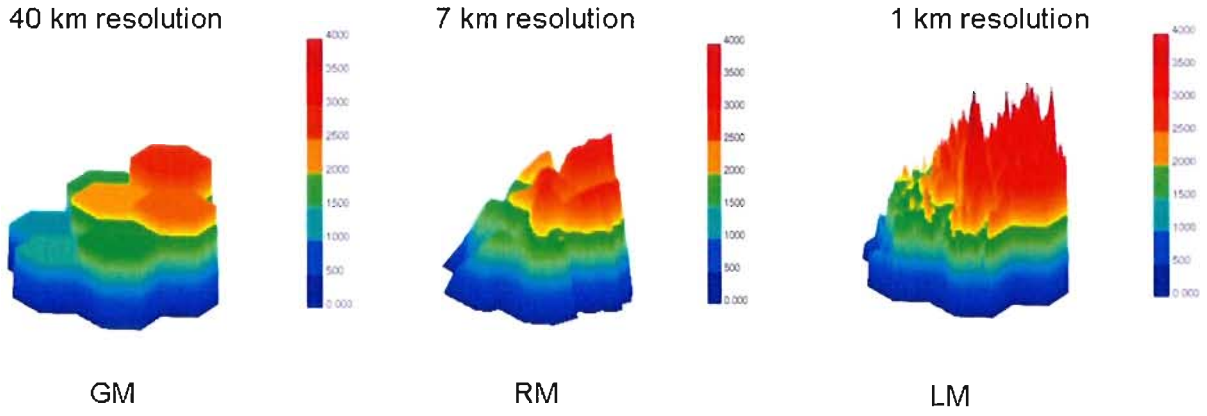

Figure 3.5. Picture of Mont Blanc area with three different model elements of the DWD LM (in metres as indicated by the grid-point resolutions. The true height of Mont Blanc of 4 807 m is reduced to values of < 2 500 m (GM), < 3 000 m (RM) and 4 000 m.

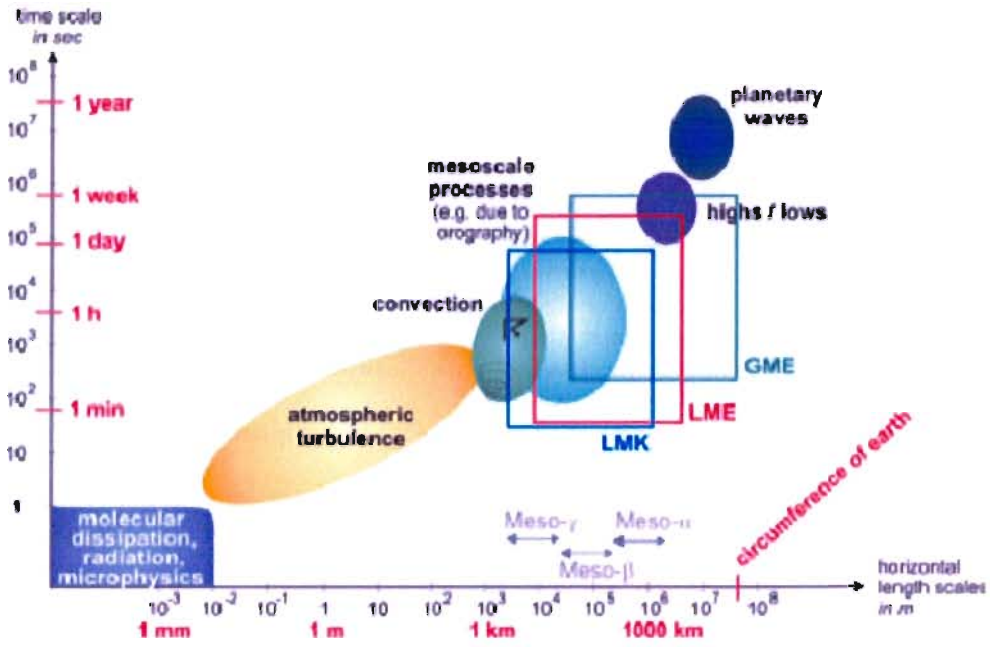

Figure 3.6. Scales of the major atmospheric physical processes and their resolution by the various DWD NWP models. For example, the GM completely resolves regions of high and low pressure, partially resolves orographic effects and does not resolve convection.

forecasts. A number of specialized forecasts for wind regimes, cloud (upper and lower boundaries), thermal lift and trajectories are distributed via self-briefing systems for use by glider pilots. In Europe, for example, one of the most important products for glider-pilot route forecasts is produced with the TOPTHERM/TopTask application model as part of the DWD pc_met online system. In the United States, glider pilots use an online system based on a variety of meteorological fields produced by post-processing results from NWP models of the National Centre for Environmental Prediction.

3.2.5 Model products

Numerical models calculate forecasts for the state variables of the model, which are the so-called prognostic variables. Each of these is subject to a prognostic equation, which means that the value of a variable at the end of a fixed short-time interval is calculated from the values that the variable in question and the other model variables have at the beginning of the said time interval. This procedure is repeated many times until a certain forecast date is reached. Not all of the meteorologically relevant parameters, however, are such prognostic variables. Therefore, for the model output, a variety of additional quantities are calculated diagnostically. This means that at certain times, the values of these quantities are deduced from the prognostic quantities already calculated for the respective time.

All the prognostic and diagnostic values exist everywhere in the model atmosphere as quasi-horizontal fields on the (two-dimensional) model grids lying over each other. The heights of these grids (model levels), however, are not constant in terms of space (or time, in the case of global models), but depend on the elevation of the terrain underneath (with the exception of model levels clearly above a height of 10 000 m). As this may complicate the interpretation of the fields, some of the meteorological values are interpolated for output into given levels of constant height or constant air pressure. Other values, notably those relating to ground-level parameters (such as precipitation reaching the ground) or quantities integrated over the vertical column (such as total cloud cover), are, by definition, available only as two-dimensional, horizontal one-level fields and need no further interpolation. As an exception, the surface pressure is extrapolated to mean sea level to identify regions of high and low pressure.

3.2.5.1 Direct model output

The simplest application is the graphical presentation of direct model output, for example, in the form of horizontal field distributions or time series (Figure 3.7).

Given a resolution of 2.8 km, the simulation of lee waves, which have a wavelength of about 10 km, is possible in an LM. In Figure 3.8, the predicted vertical velocity at a height of 3 000 m is shown. This pattern of up- and down-directed winds was predicted to be stable for several hours.

3.2.5.2 Interpretation and verification

NWP models are only "models", despite their complex construction. They do simulate the essential atmospheric processes. But they cannot capture every detail in a complete and perfect way, because the weather system is a continuum and the models are not a continuum. Owing to the necessary numerical solutions and the parameterizations, uncertainties are inevitable in the calculation of the initial state and in the formulation of model equations. Since the atmosphere is a chaotic system, small uncertainties in the forecast system can lead to large discrepancies between reality and model results. We must accept these forecast errors, but we also have to recognize them by verification and to account for them by interpretation.

The aim of verification is to estimate forecast quality in a quantitative way and to systematize forecast errors. This serves two purposes: verification provides the model users with guidance for a meaningful interpretation of model forecasts, and it provides model developers with guidance for model improvements.

The aim of interpretation is an increase in forecast value for the user. The procedures can be fully automatic and can therefore process the direct model output to produce tailored products for various users (Figure 3.9).

Generally, interpretation can focus on two different aims:

(a) Deriving forecast variables that are not contained in the direct model output;

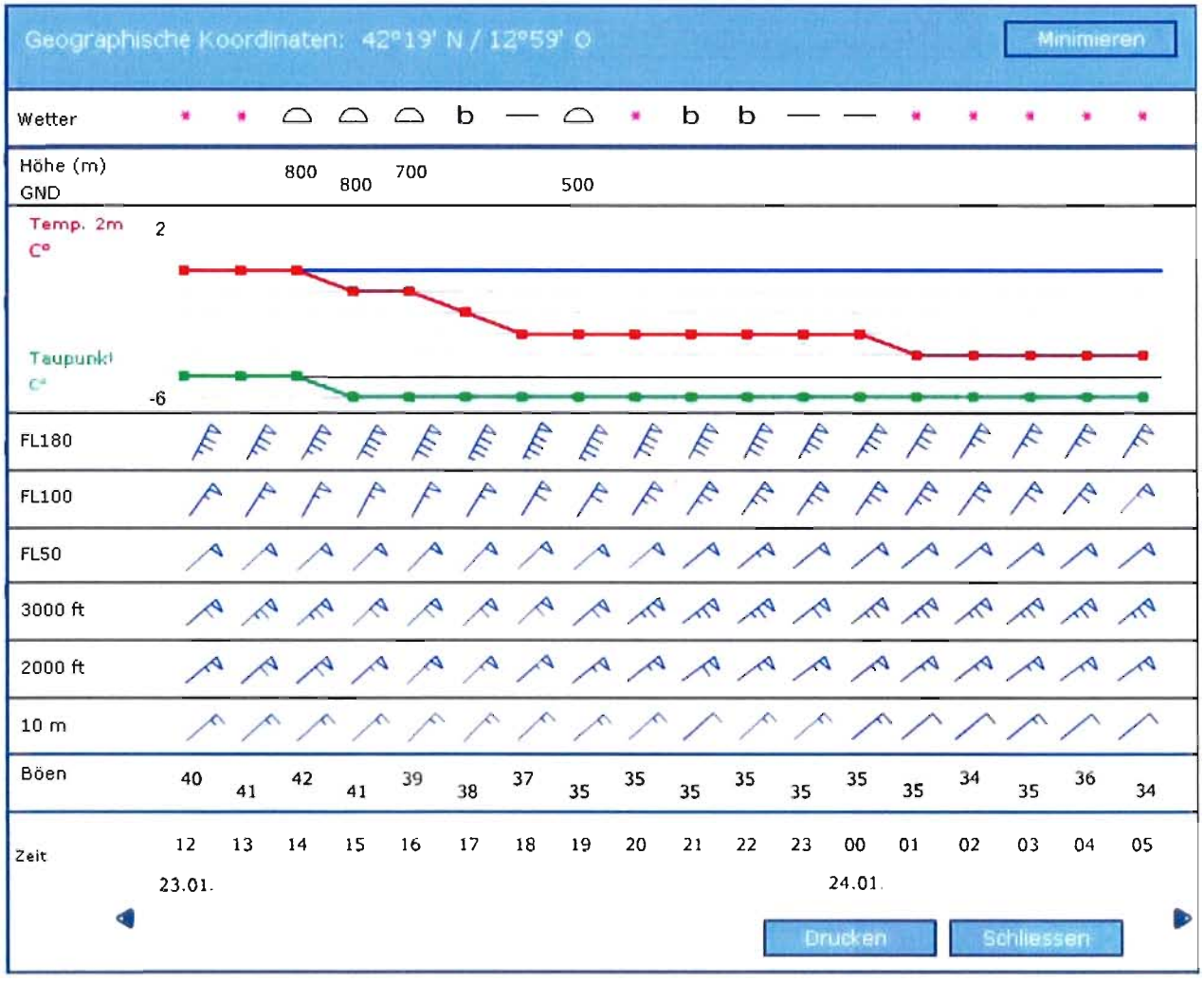

Figure 3.7. A meteogram: a predicted time series of meteorological variables

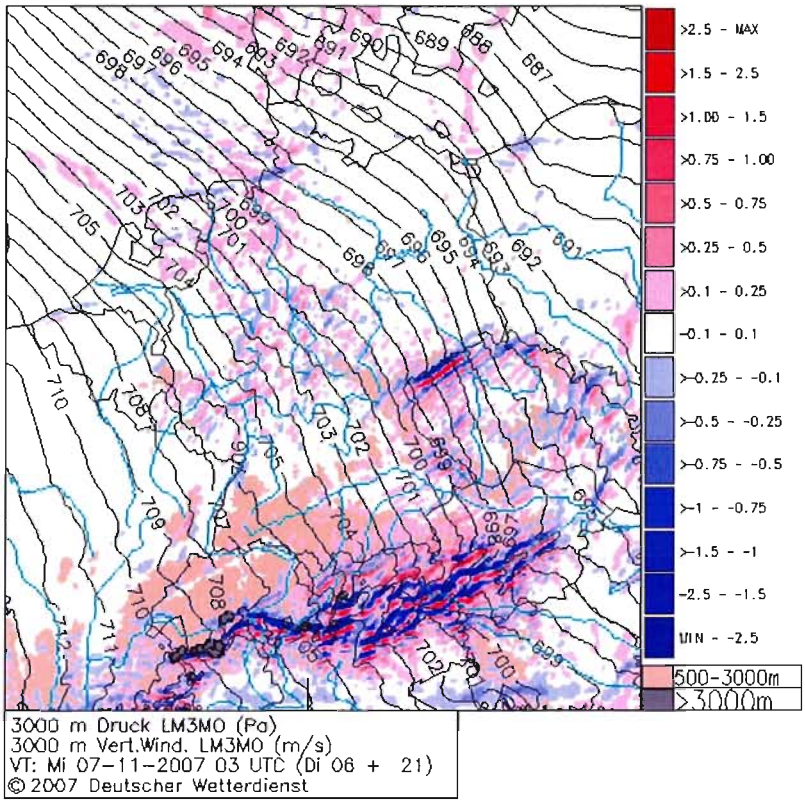

Figure 3.8. Vertical motion and isobars at 3 000 m above mean sea level in NNW flow over the Alps. Stationary patterns of updraughts (red) and downdraughts (blue) indicate mountain-wave activity.

(b) Correcting the direct model output on the basis of known forecast errors.

The development of interpretation procedures is based primarily on a retrospective comparison of model forecasts with actual weather. The long-term comparison produces a general relation between forecasts and actual weather, which is then applied to real-time forecasts. A variety of specific methods is available.

For example, the weather interpretation and the neighbourhood method derive forecast variables that are not contained in the direct model output. The weather interpretation is a heuristic expert system and derives a forecast of significant weather (such as thunderstorms); the neighbourhood method derives probabilistic forecasts.

Further expert systems are used for the automatic prediction of the risk of icing. The Model Output Statistics (MOS) method applies a statistical interrelation (of forecast errors, for example), which has been derived from a comparison between model predictions and actual weather over several years. For localized forecasts, MOS is used both as a

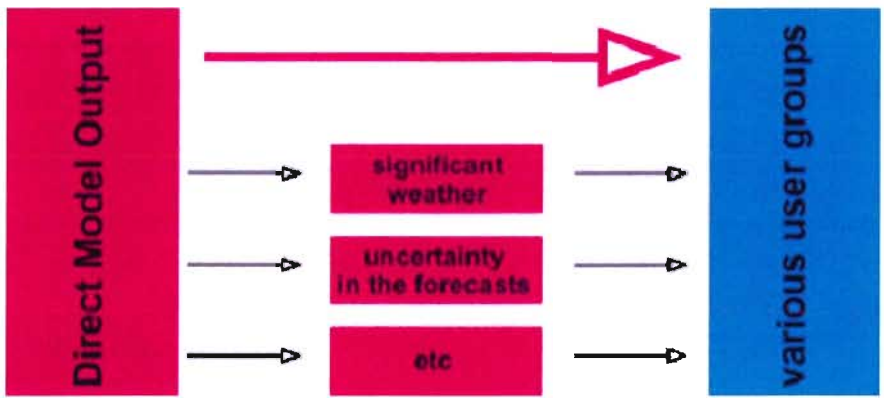

Figure 3.9. Automatic interpretation procedures supplement the direct model output for specific users.

correction of the direct model output and for the derivation of many supplementary forecast variables, such as those for advisories and warnings. A Kalman filter can also be applied for a correction of the direct model prediction (Kalman, 1960).

We offer below a detailed description of methods of weather interpretation:

(a) Direct model output:
  (i) The direct model output contains predictions of atmospheric variables such as wind, pressure, temperature and humidity. It does not contain a prediction of "significant weather", that is, weather events such as fog, drizzle, rain showers, snow showers and thunderstorms (Figure 3.10);
  (ii) Predictions of significant weather are added by the automatic weather interpretation. The procedure is empirical and accesses the direct model output of the NWP models. For the GM, RM and LM of the DWD, there is one operational procedure for each model. Significant weather is derived at each model grid point. At present, the weather interpretation distinguishes among 20 different events. They are expressed by a truncated version of the so-called SYNOP WW code for present weather;
  (iii) Direct model output can be post-processed to diagnose different cloud types (Figure 3.11), winds and precipitation (Figure 3.12) at one-hour intervals;

(b) Statistical interpretation (neighbourhood method):
  (i) High-resolution numerical weather prediction models derive forecast fields that are rich in spatial detail. The smallest scales of a forecast field are especially difficult to predict, however. Often it is not reasonable to focus on single grid points, because this part of forecast information is likely to be unreliable. In order to produce isolated grid-point forecasts in a meaningful way, the direct model output undergoes statistical post-processing. This is the so-called "neighbourhood method". The aim is not only a reduction in forecast uncertainty, but also an estimation of uncertainty in terms of probabilities. Two aims are pursued:
    a. Filtering of small-case structures;
    b. Derivation of exceedance probabiLities, for warning thresholds in particular (Figure 3.13).

The method defines a spatial-temporal neighbourhood around each grid point. If rain is forecast for, say, 30 per cent of the points within the neighbourhood, the probability of rain is set to 30 per cent at the central grid point. This method is efficient and relatively simple to implement, because it does not require ensemble simulations or long-term training data. But the method can be combined with such methods, if necessary.

3.3 SOARING FORECASTS

Weather forecasts for soaring assess the availability of updraughts useful for gliders. The duration, strength and height of the vertical currents are needed with specific resolutions. The onset and

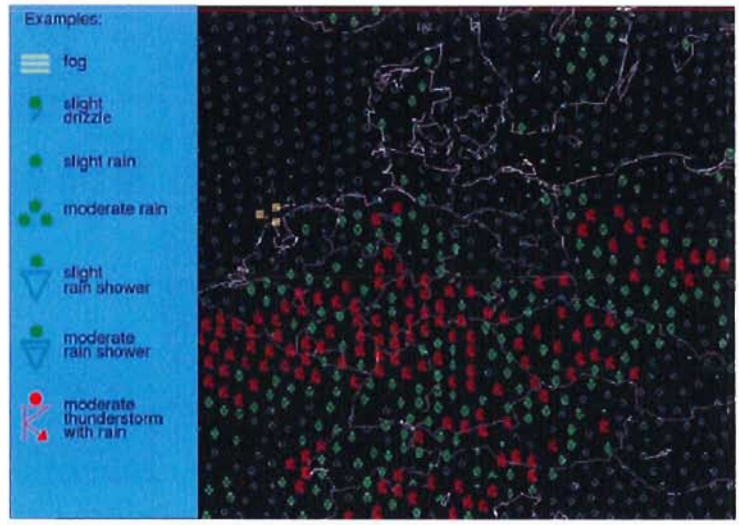

Figure 3.10. Prediction of significant weather derived from the direct output of the DWD regional model

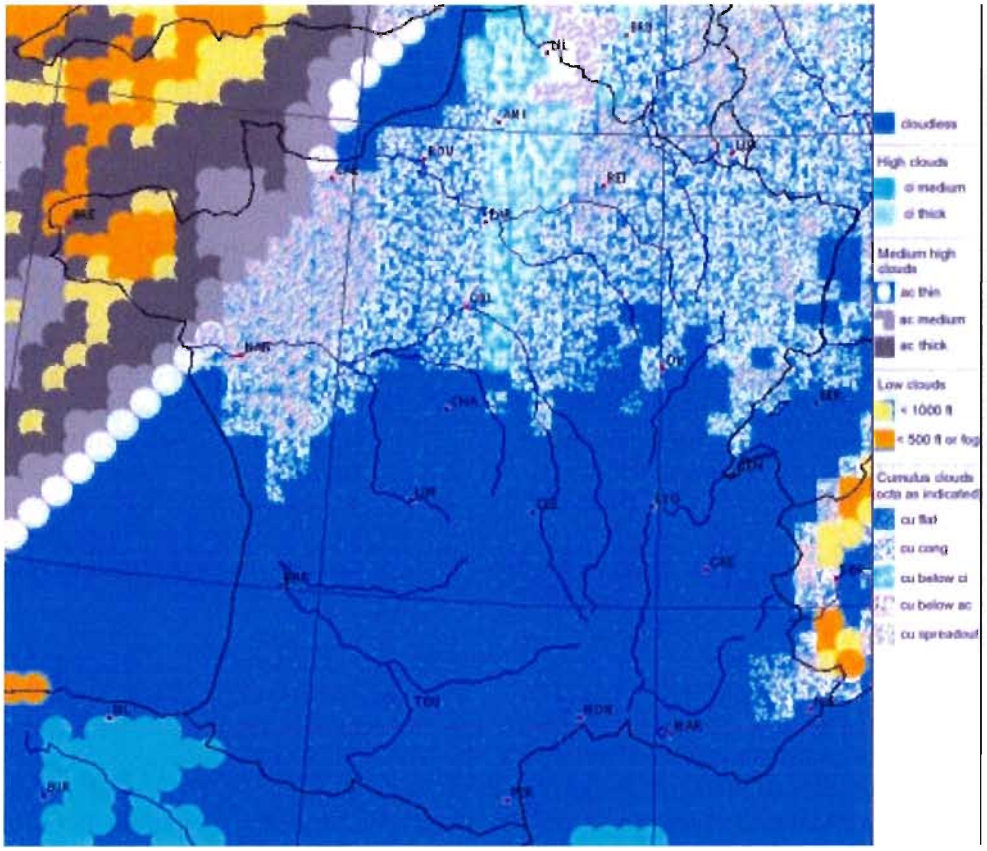

Figure 3.11. Convective and stratiform clouds at low, middle and high levels calculated from the grid-point data of a regional model

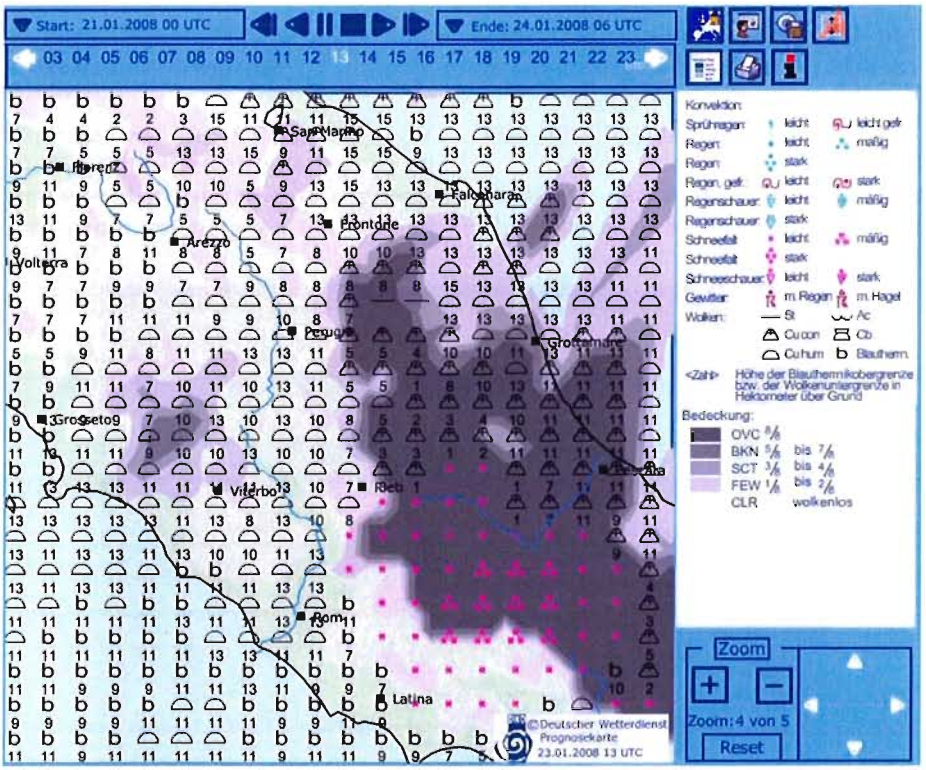

Figure 3.12. Convective and stratiform cloud cover at low, middle and high levels from the DWD regional model

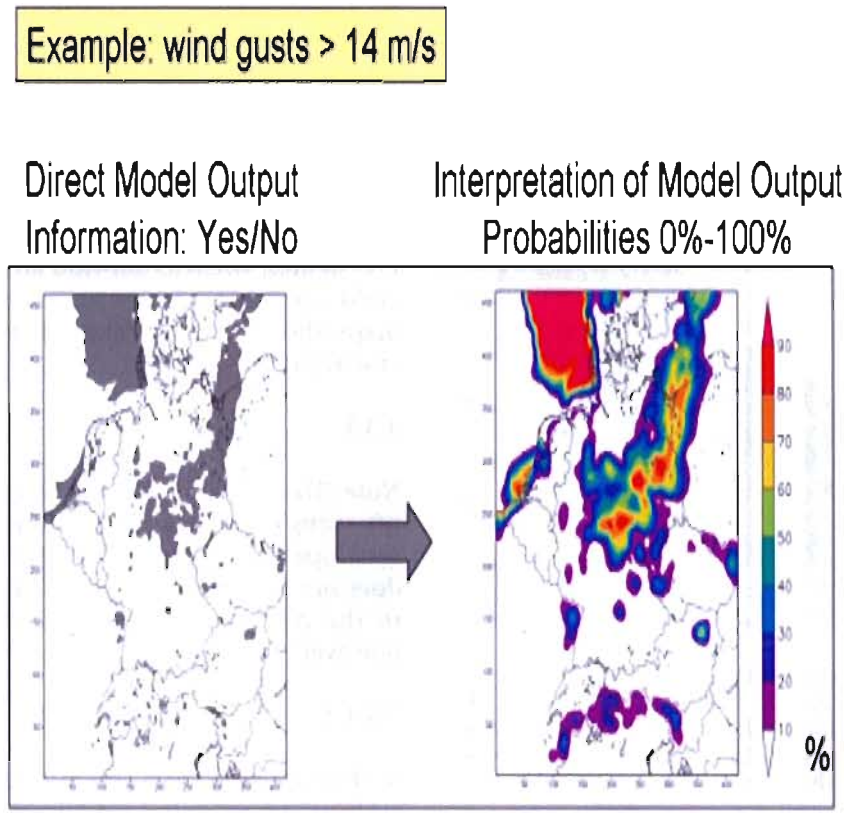

Figure 3.13. Exceedance probabilities derived from the neighbourhood method

end of updraughts should be predicted with a precision of 30 minutes, while the strength and the height of the lift require a resolution of 0.1 m/s and 100 m, respectively. Isolated and aligned types of lift should be distinguished. Since visual meteorological conditions are required for gliding, predictions of clouds and precipitation are needed.

The precise location of the lift is of minor importance in a forecast, as the horizontal spacing between the updraughts is usually well below the glide range. Given the performance of modern sailplanes, a selection of the best updraughts by pilots is possible, and not every thermal encountered must be used. Paragliders and hang-gliders are more limited in their options.

This chapter lists methods that are available for the preparation of soaring forecasts. Diagnostic and prognostic techniques are currently used. The methods are described briefly. If the reader wishes to use a particular method, necessary references are provided.

In general, NWP LMs do not contain the strength of the updraughts as predictive variables. The strength and the altitude of the updraughts, the depth of the CBL and cloud cover are then obtained from an interpretation of the direct model output. Diagnostic techniques have been developed for this purpose for convective, ridge and wave lift. Convective lift may be either isolated (thermals) or aligned (horizontal convective rolls); ridge lift and wave lift are aligned types of lift.

In high-resolution three-dimensional models (that is, the LM), the vertical motion is a prognostic variable that resolves aligned updraughts in stationary gravity waves. In one-dimensional and two-dimensional models with a high vertical resolution, the vertical motion of buoyant parcels is a prognostic variable that resolves thermal updraughts and convective cloud formation; complex terrain can be handled as well. High-resolution models can produce soaring forecasts as direct model output.

Presentation

There are two complementary ways to present soaring forecasts in space and time. A first option is to present the diurnal cycle of the updraughts as a time-altitude cross section for a particular location or region. A second option is to show maps, such as maps of climb rates for different times of

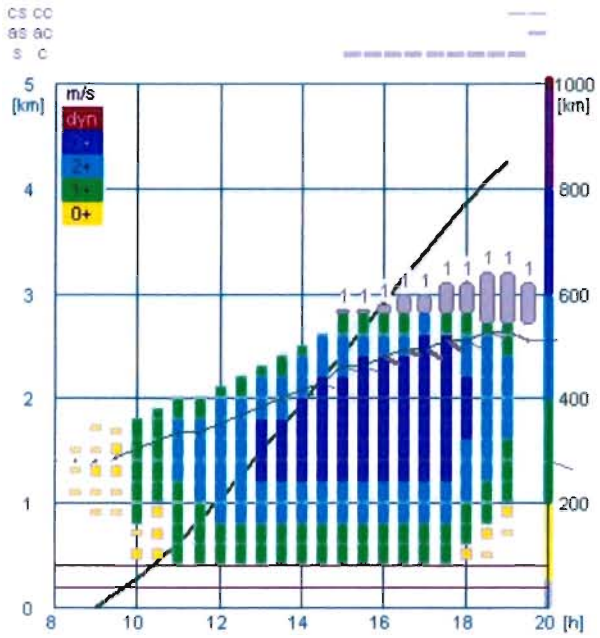

Figure 3.14. Time-altitude cross sections of predicted climb rates in thermals. The potential flight distance (diagonal curve) results from the ground speed for crosswind flight tracks accumulated over the duration of the updraughts.

the diurnal cycle or potential flight distance maps for the full diurnal cycle of the updraughts.

The predicted diurnal cycle of convection is presented as a time-altitude cross section of the climb rates (Figure 3.14) with 30-minute intervals. This shows the duration, strength and depth of convection and may be completed by the expected cloud cover at different levels. As an alternative, averaged climb rates may be shown as uniformly coloured vertical columns throughout the convective boundary layer. The predicted wind is displayed in the upper part of the convective boundary layer, as this is the preferred flight level for soaring in thermals.

Maps of direct or post-processed model output are produced for particular times of the day. Their typical time-interval of three hours is too large for a precise timing of the onset and the end of updraughts. Their horizontal resolution, however, is usually sufficient for soaring forecasts.

Cross sections of predicted climb rates and winds lead to predictions of the ground speed (see section 2.3). The predicted ground speed depends on the performance of the glider and can be accumulated over the diurnal cycle for 30-minute intervals. This results in the potential flight distance (PFD) for the day – an assessment of the day's soaring potential for a particular location (region) and glider (Liechti and Lorenzen, 1998).

The PFD maps (Figure 3.15) provide a comprehensive overview of the predicted soaring conditions. In areas of changing PFD, favourable flight directions are recognized. The accumulation of ground speeds for crosswind tracks leads to intermediate PFD figures, whereas tailwind and headwind tracks yield upper and lower limits, respectively. PFD maps should show intermediate PFD figures for crosswind tracks.

3.3.1 Convective lift

Note: The basic method for diagnosing convective lift using atmospheric soundings is thoroughly developed in WMO/OSTIV (1993), and therefore does not need to be repeated here. Improvements to the method are described in section 3.3.1.6, however.

3.3.1.1 Thermal Index (TI)

A TI is calculated at a specified level by taking the ambient temperature (obtained from a morning sounding) and subtracting the thermal temperature at that level (found by following the dry adiabat upwards from the predicted maximum surface temperature). For example, if the ambient temperature at 800 hPa is 4°C and the thermal temperature at 800 hPa is 7°C, we have:

$$TI\ (800\ hPa) = 4°C - 7°C = -3°C.$$

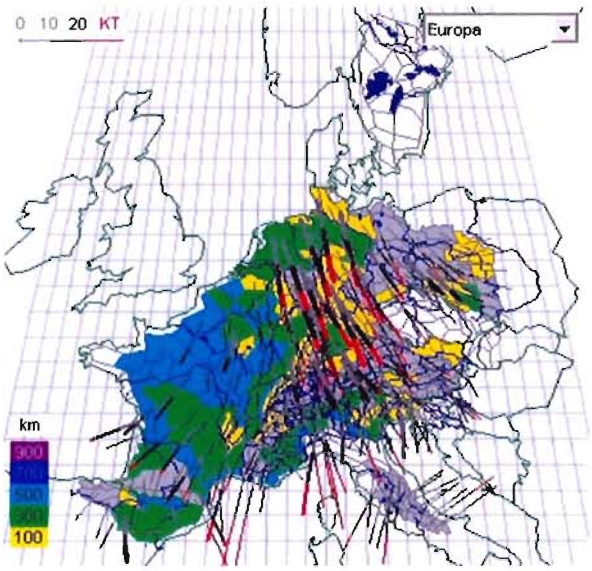

Figure 3.15. Potential flight distance chart using thermals. Wind is shown as flags (streamers).

Larger magnitude negative numbers indicate stronger thermals. The top of the CBL is approximated by the level at which TI = 0. Experience has shown that TI less than –2°C is needed for soaring flight. Note that the TI should not be confused with the Lifted Index (LI) used by meteorologists to predict the probability of thunderstorms.

The TI can be calculated using soundings from either measurements or NWP predictions. Programs such as the rawinsonde observation (RAOB) program (see section 7.3) run on personal computers and automatically analyse the soundings. Some offices of the National Weather Service in the United States produce daily soaring forecasts that are available on their websites, including a calculation of the TI at various levels. This allows the user to estimate thermal strength and maximum height of the thermals. The information, however, is typically for only one location.

Maps of the TI can be created from NWP output. One example is the so-called Soaring Index (simply the TI calculated at 1.5 km AGL) produced at Colorado State University (rams.atmos.colostate.edu/realtime/00z/) using predictions from daily Regional Atmospheric Modelling System (RAMS) forecasts (Figure 3.16).

Joss (1976) reported an adaptation of the TI for use in the Great Basin in the western United States. The empirically derived algorithm forecasts expected thermal strength and is called the Great Basin Soaring Index. The index has been shown to be a function of two parameters: the temperature differential between 4 000 feet AGL and the expected maximum altitude of thermals, and the maximum altitude of the thermals during the time of maximum temperature for the day.

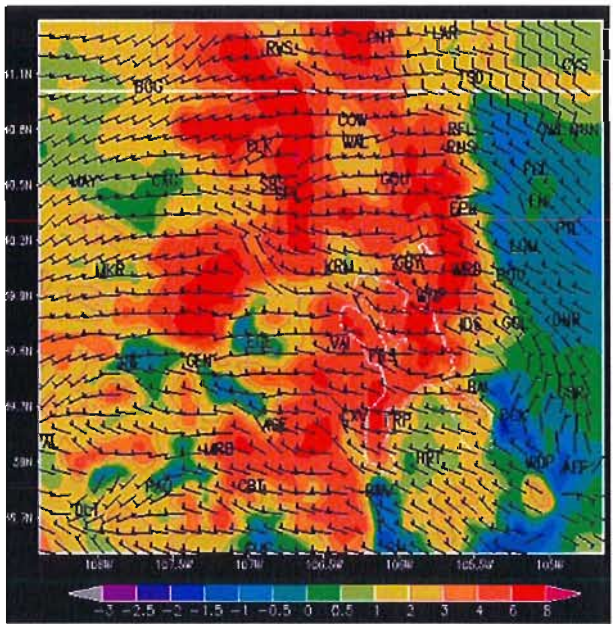

Figure 3.16. Map of the Soaring Index (TI calculated at 1.5 km AGL) on a weak soaring day in north-eastern Colorado, USA. Note that the best conditions (most negative TI) occur in conjunction with convergence of the surface winds.

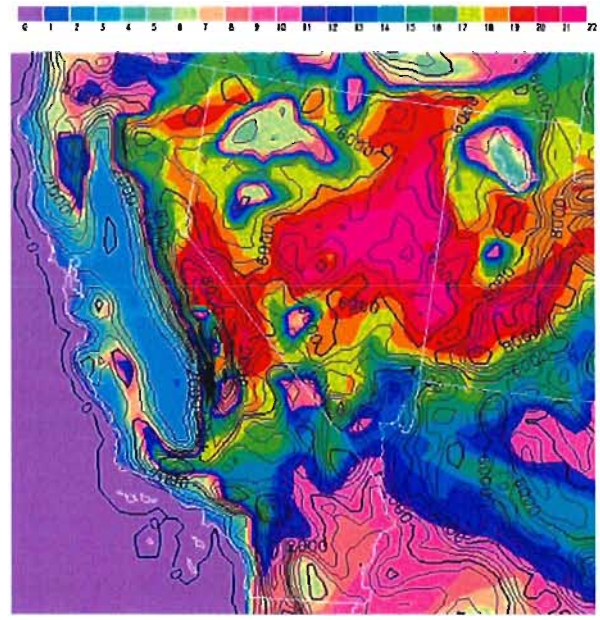

Figure 3.17. Map of the forecasted topography of the CBL height (TI = 0) using a BLIPMAP for the western United States. Ocean areas (far left) feature essentially no CBL. A deeper CBL is seen over elevated terrain (ft MSL/1 000) and desert areas of California, with the highest values over the high desert of Nevada.

3.3.1.2 Boundary Layer Information Prediction Maps (BLIPMAPs)

The BLIPMAPs (Glendening, 2002) are widely used by soaring pilots in the United States. The BLIPMAPs take data from routine numerical prediction models and produce regional-scale Internet-accessible maps displaying a large variety of derived quantities. These include measures of the CBL depth, thermal strength, boundary layer winds (including a buoyancy/shear ratio) and convergence, as well as various cumulus cloud parameters (such as cumulus potential and base, and over-development potential). Products are available for a 24-hour forecast and are displayed at three-hour intervals (www.drjack.info/). An example of model-predicted CBL height produced by BLIPMAPs is shown in Figure 3.17. The use of BLIPMAPs is expanding to the United Kingdom, Germany, Australia and South Africa. The resolution of soaring-weather products

produced by BLIPMAPs in a specific region is dependent upon the resolution of the host NWP model.

3.3.1.3 Olofsson method

Olofsson and Olsson (2006) utilized direct output from the European High Resolution Limited Area Model (HIRLAM) for winds and total cloud cover and diagnostic post-processing of temperature profiles at all grid points for CBL depth, average climb rate and convective cloud formation. Displayed are maps with wind, CBL depth, climb rate and cloud cover at three-hour intervals (Figure 3.18).

3.3.1.4 Hindman method

Hindman and others (2007) utilized direct output from the RAMS NWP model and diagnostic post-processing following Olofsson and Olsson (2006), averaged over all grid points contained in defined forecast regions. Output consists of tables with wind, CBL depth, cloudiness and climb rate at 30-minute intervals for each forecast region. The display of such a table is shown in Figure 3.19).

3.3.1.5 Gold method

Several National Weather Services, as well as self-briefing software in aviation, use the Gold method (Gold, 1930) to analyse convection based on data from radiosondes and atmospheric soundings generated by NWP models (Figure 3.20).

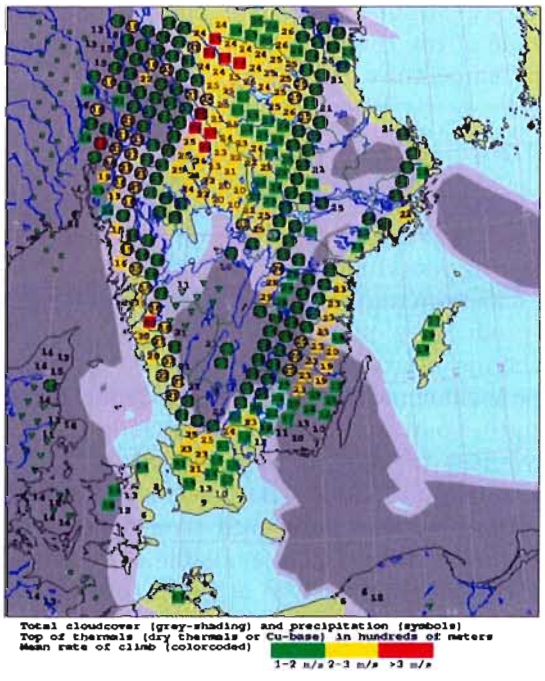

Figure 3.18. Automatic thermal forecast based on the Olofsson method

The Gold procedure calculates the diurnal variation of air temperature based on available radiative energy at a location in central Europe, without taking into account extinction and temperature advection. It assumes flat topography and clear skies. It also predicts the height of the convectively active boundary layer, which is, to first order, equivalent to the base of cumulus clouds, or the top of blue (dry) thermals, respectively.

Empirical corrections for the radiative energy under varying degrees of cloud cover (Table 3.1) or special orographic features (Table 3.2) have been developed. The application of Gold's method in regions outside of central Europe necessitates appropriate modification and adjustment of the parameters. For southern Europe an increase in the radiative energy of 20 to 30 per cent is recommended.

The thermal forecast is derived from the diurnal temperature development and other known predictions of convection. The vertical velocity W [m/s] is given as the product of the height of the convectively active boundary layer H [km] and an empirical factor α:

$$W = \alpha * H$$

$\alpha = 1$ for blue/dry thermals (either before condensation sets in or after the clouds have dried up).

When clouds form, α depends on the depth Hw [m] of the clouds:

$$\alpha = 1.2 + 0.3 * Hw / 1\,600$$

Typical values of α are:

$\alpha = 1.2$ for Cu humulis

$\alpha = 1.5$ for Cu mediocris

For values of Hw above 2 000 m, the calculated climb rate becomes unreliable.

In mountainous terrain, the values of vertical wind speeds are higher by about 0.5 m/s. From experience, thermals are likely to be broken up when the wind speed exceeds 40 km/h at 1 000 m AGL.

The following synoptic effects are not taken into account by Gold's method:

(a) Temperature and humidity advection (stabilizing cold air advection close to the ground, stabilization at altitude);

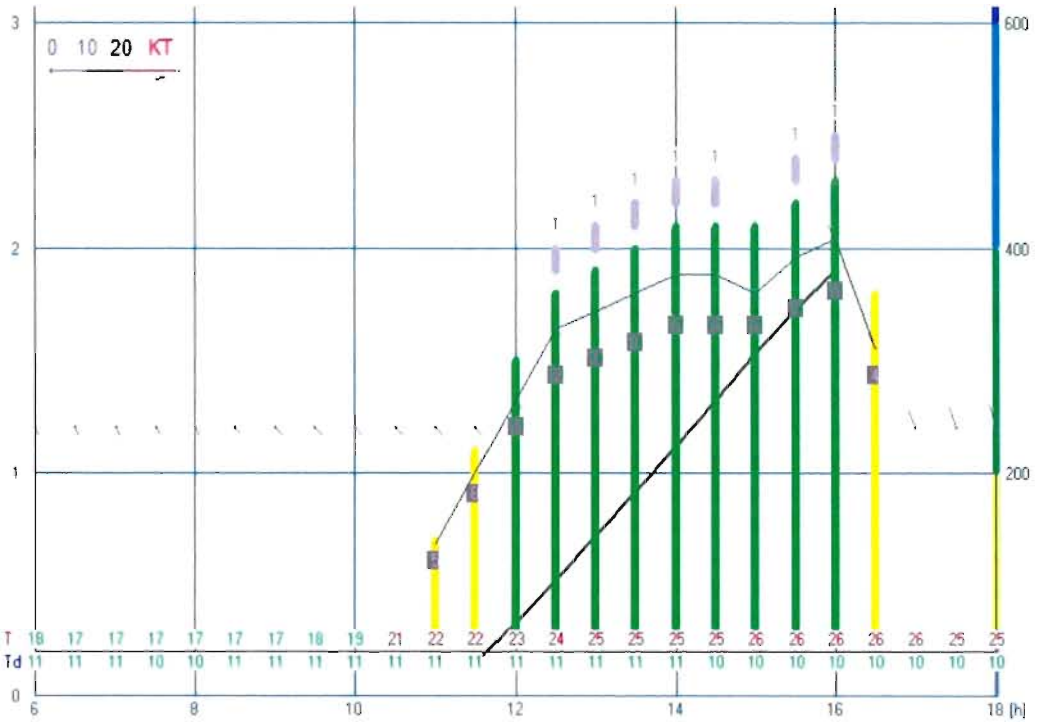

Figure 3.19. Diurnal cycle of the depth of the CBL in a particular region based on the Hindman method. Climb rates are 0–1 m/s (yellow) and 1–2 m/s (green). The potential flight distance is the diagonal green line.

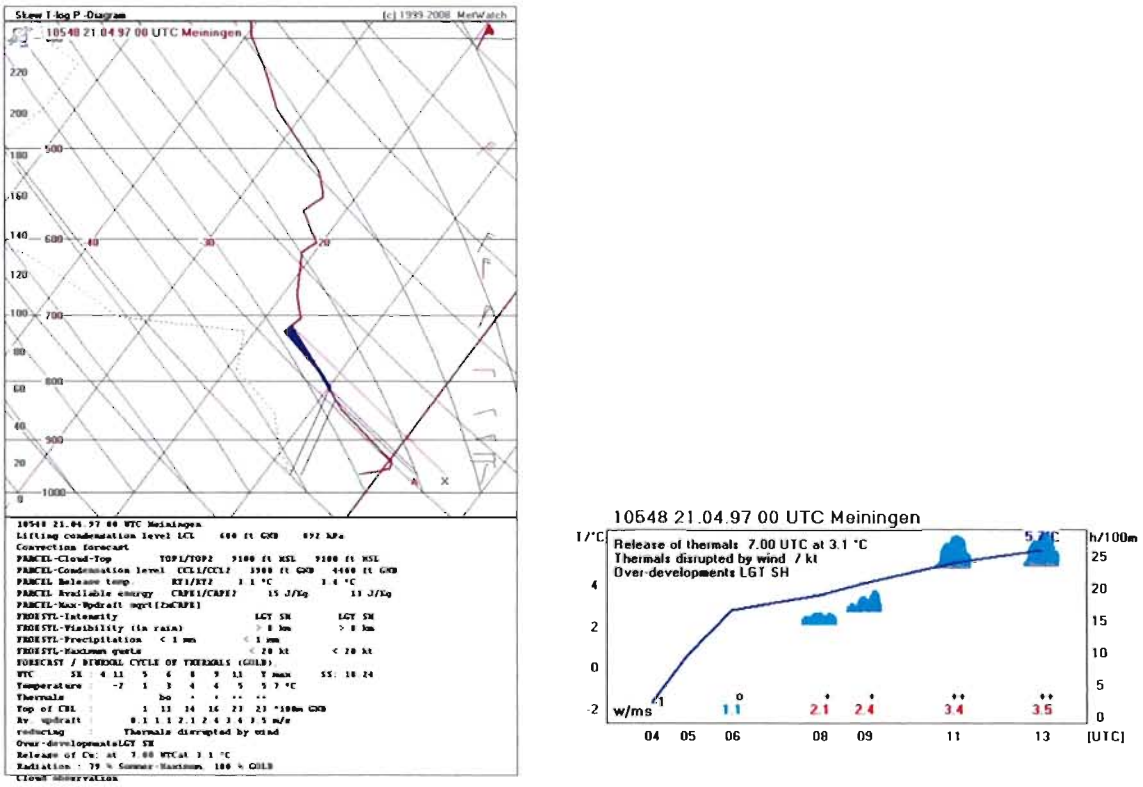

Figure 3.20. The Gold method applied to a nocturnal sounding (left panel, red curve for 0000 UTC) calculates the diurnal cycle (right panel) of the temperature (blue curve), the climb rate (figures) and convective clouds (cloud cover and cloud base). On the left panel the blue lines mark the onset of cloud formation and the maximum temperature, respectively. The observed 1200 UTC sounding is shown for comparison (left panel, blue curve).

(b) Large-scale vertical motion;
(c) Development of clouds at an inversion layer, resulting in reduced thermal activity;
(d) Strong extinction by the atmosphere (sand- and dust storms, haze in inversion layers).

A similar scheme has been developed for the United States by Young (1987).

3.3.1.6 Soundings available on the Internet

In past years, the analysis of thermodynamic diagrams was a time-consuming process. The advent of personal computers, modern graphics packages (such as RAOB, see section 7.3) and the Internet has dramatically simplified the analysis. A great number of Internet websites (Heise, 1999) allow the user to view and analyse soundings from either standard observational or NWP-predicted soundings. Some websites offer interactive soundings, allowing the user to forecast thermal soaring conditions depending on various input surface temperatures. Other websites offer an archive of soundings, allowing the forecaster to analyse weather situations after the fact. A complete treatment of the vast amount of available Internet soundings is beyond the scope of this handbook. Therefore, an example Internet site is listed in section 7.3.

Of the NWP models, the LMs generally give more accurate forecasts of vertical profiles.

Table 3.1. Corrections to the Gold method for cloud cover

Cloud cover	*Available radiation (fraction in %)*
Clear sky	100
High clouds – cirrus (thin, few Ci-patches)	>90
High clouds – cirrostratus, cirrocumulus	80–90
Medium-altitude clouds – altostratus transparent	65–75
Dense medium-altitude clouds (Altostratus opacus) and/or low-altitude clouds	45–65

Table 3.2. Corrections to the Gold method for orography

Orography	*Available radiation (fraction in %)*
Flat lands	100
Hilly terrain	110
Mountains	102–130
High mountains/ alpine regions	104–150

3.3.1.7 Prognostic convection model (TOPTHERM)

ALPTHERM is a prognostic one-dimensional NWP model for parcels with lateral entrainment and detrainment (Liechti and Neininger, 1994). It is applied to observed or predicted soundings for regions with complex terrain. Complex terrain is treated quantitatively by its area-elevation distribution (Figure 1.10, left). The parcel vertical motion and the cloud cover of each layer are prognostic variables (Figure 1.10, right). The model produces the diurnal cycle of the mixing height, the climb rate profile and the cloud base/top/cover. The internal resolution is 100-metre vertical intervals and 2-minute time intervals.

REGTHERM is the two-dimensional horizontal extension of ALPTHERM, with local winds (valley wind) driven by differential heating (Liechti, 2002). TOPTHERM is the application of REGTHERM with external forcing. Profiles from the DWD RM at one-hour intervals are used for initialization and advection above the internally developing CBL. TOPTHERM replaces the high-resolution local model in Figure 3.2 for defined forecast regions and produces regional soaring forecasts as direct model output.

Figure 3.21 shows a TOPTHERM time-altitude cross section for a region with complex terrain that is presented to pilots in the online DWD self-briefing system pc_met. The vertical resolution is 200 m and climb rates are given at 30-minute intervals. The tabular form has a vertical resolution of 100 m and is suitable as input to the flight planning algorithm TopTask (section 4.3). The tabular form includes the RM wind in the upper part of the predicted CBL. Figures 1.5 through 1.10 show ALPTHERM direct model output in a thermodynamic diagram and the corresponding time-altitude cross section of the CBL.

3.3.2 Horizontal convective rolls

Diagnostic methods for the prediction of horizontal convective rolls exist for wind profiles with a vertical shear in the convective boundary layer. In

cases of small directional shear, two characteristics of the wind profile are important: the wind speed must exceed a threshold and the directional shear in the convective boundary layer must decrease with altitude.

According to Müller and others (1985), Müller and Kottmeier (1986) and Weckwerth and others (1998), the wind speed u at the top of the convective boundary layer should exceed a threshold value which increases with the depth h of convection:

$$u >= 40 * h - 4,$$

where u is expressed in km/h and h in km. Deeper convection requires a higher wind speed. A constant wind speed of 36 km/h favours the formation of convective rolls if the depth of convection is less than 1 000 m. The directional shear must be smaller in the upper half of the convective boundary layer than in the lower part.

In cases of large directional shear, two criteria apply:

(a) The directional shear angle must exceed a threshold;

(b) The average wind in the convective boundary layer must exceed a threshold.

The directional shear angle $\beta > 330 * h/u$, where h is the depth of the convective boundary layer in km and u is the average wind in km/h in the convective boundary layer. The value of u must exceed 15 km/h.

Figure 3.22 shows an example of such a diagnosis.

3.3.3 Ridge lift

Currently, quantitative methods are being developed to forecast ridge lift from NWP wind fields interacting with model topography. The most important feature of such diagnostic techniques is that they require a threshold wind speed to indicate ridge soaring conditions. In addition, VMC must be considered.

3.3.4 Wave lift

3.3.4.1 Lester-Harrison nomogram

The use of this empirical method allows one to estimate the probability of lee wave development

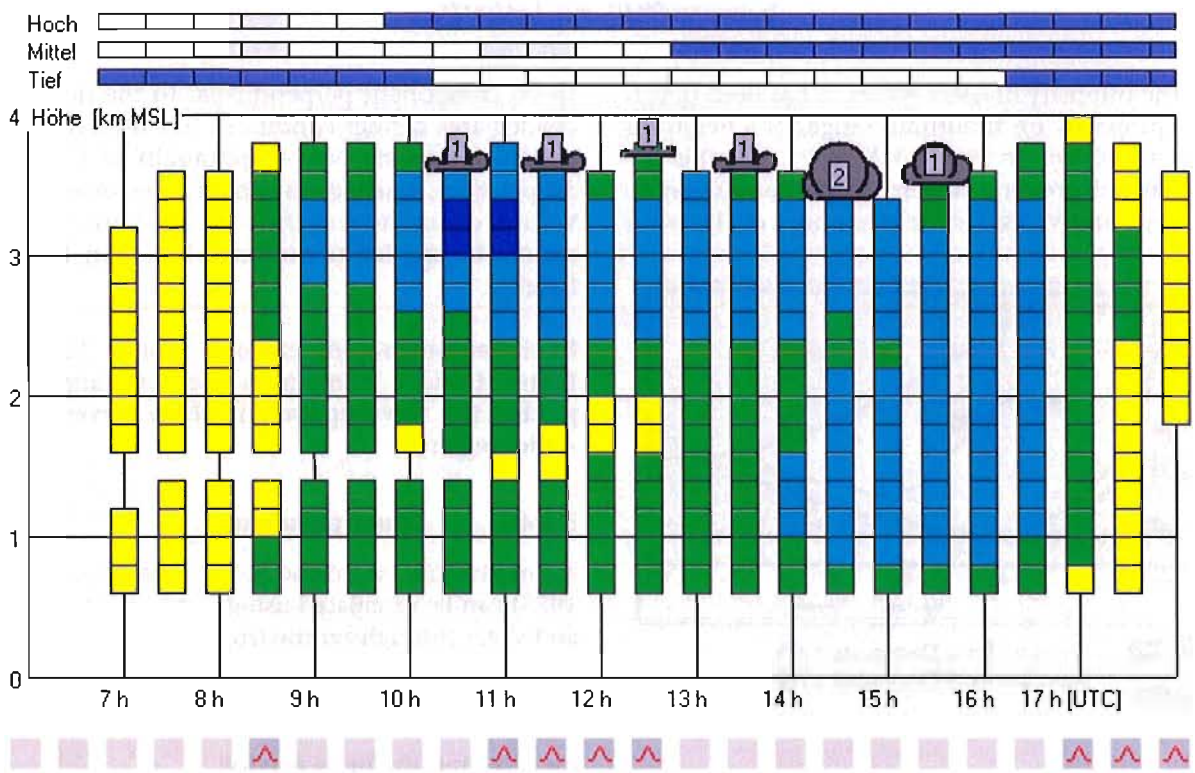

Figure 3.21. Diurnal evolution of the climb rate and of cumulus clouds over complex terrain in the TOPTHERM model. In the example shown, a temperature inversion at 1.5 km between 0700 and 1300 UTC reduces the climb rates of thermals originating from elevations below the inversion. Climb rates: yellow – 0.1 to 0.8 m/s, green – 0.9 to 2 m/s, light blue – 2.1 to 3 m/s and dark blue – greater than 3 m/s.

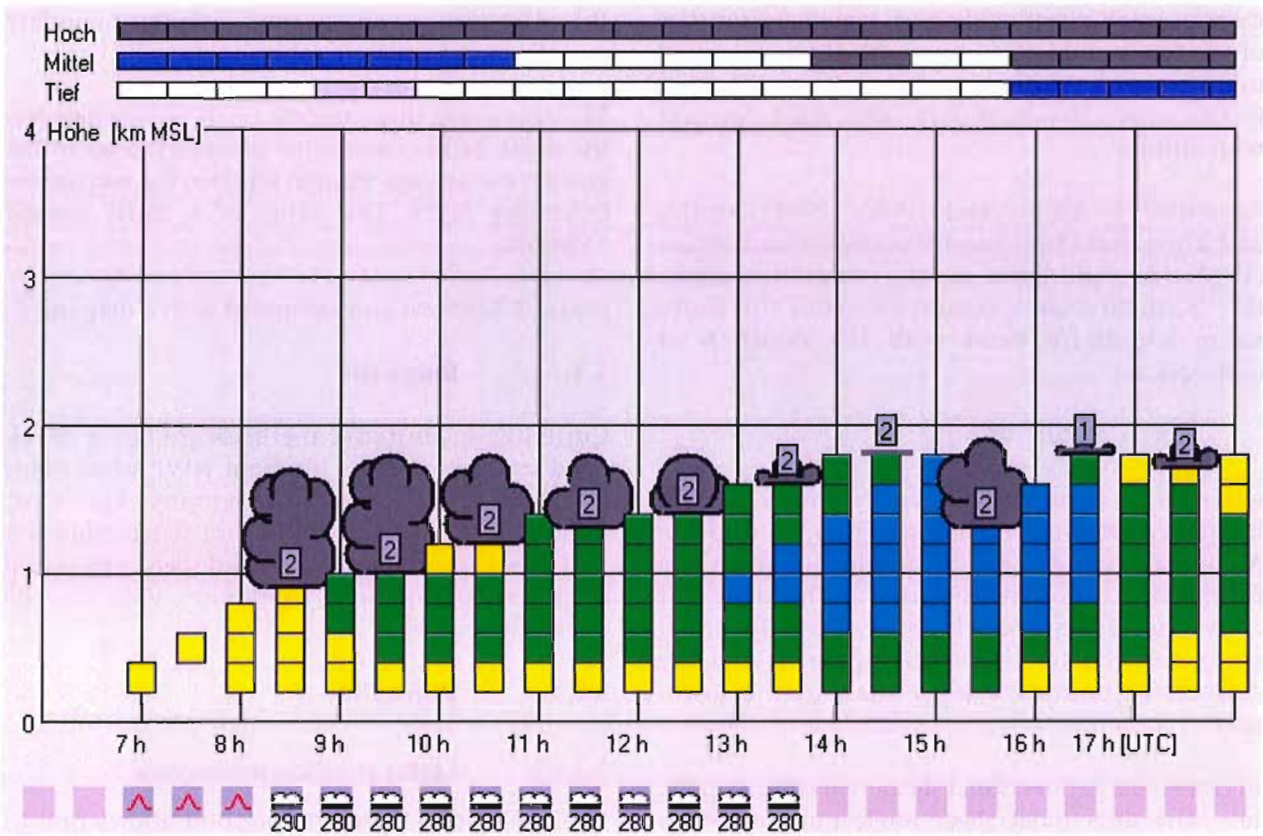

Figure 3.22. Diurnal evolution of the CBL, the climb rate and the cumulus clouds in the TOPTHERM convection model for flat topography. Horizontal convective rolls oriented at 280 degrees are diagnosed between 0830 and 1330 UTC.

and the intensity of these waves. It has been developed primarily for mountain ranges of a height of at least 3 000 m. In Figure 3.23, ΔP_{MSL} (hPa) is the normalized pressure difference perpendicular to the ridge and Vp (kt) is the maximum of the wind speed component perpendicular to the ridge. The shaded area defines conditions in which the probability for usable wave updraught is less than 50 per cent. Dashed lines help in estimating the vertical component of the wave flow. This method cannot be applied to ranges of less than 1 000 m height.

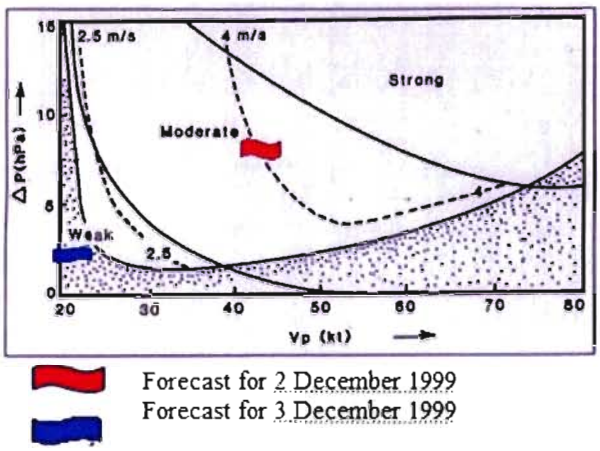

Figure 3.23. Use of the Lester-Harrison nomogram for estimating the lee-wave intensity over the Argentine Andes on 2 December 1999 (moderate intensity) and on 3 December 1999 (weak intensity)

In the accompanying example (Figure 3.23), the Lester-Harrison nomogram has been applied to predict the wave updraught of lee waves in the Andes region.

3.3.4.2 Scorer parameter

A forecast tool called the Scorer parameter (Scorer, 1978) can be calculated using wind speed, stability and shear throughout the troposphere:

$$l^2 = g\,(\gamma^* - \gamma)/(T\,u^2) - 1/u(\delta^2 u/\delta z^2);$$

g = acceleration due to gravity;

γ^* = dry adiabatic lapse rate;

γ = ambient lapse rate of the layer;

T = average temperature in the layer;

u = average wind speed in the layer;

$\delta^2u/\delta z^2$ = curvature term, specifically, the vertical derivative of the vertical wind shear.

If the Scorer parameter decreases with height (Figure 3.24), trapped waves are likely. The Scorer parameter will decrease with height if: stability decreases with height, wind speed increases with height and vertical shear increases with height. An inversion above the mountaintop layer often separates lower-level air with a high Scorer parameter from upper-level air with a low Scorer parameter. In order to obtain smooth profiles, the data can be averaged over layers of 500 m (Forstner and Prodinger, 2000).

Rules:

(a) A sharp decrease of l^2 with altitude indicates lee waves;

(b) A sharp increase of l^2 with altitude indicates rotors.

3.3.4.3 Mountain Wave Project (MWP) forecasting tool

Together with the German Military Geophysical Service, the MWP developed a numerical forecast tool to predict orographically generated turbulence. The objectives of this development were an operational forecast of turbulence originating in the rotor-wave system for all branches of aviation, as well as a global scan of regions with frequent wave occurrences and their evaluation with respect to long-distance soaring flight.

As a first step, the MWP tool selects those grid points of a numerical forecast model for which the slope of the orography exceeds a minimum value. Then it calculates at these grid points the component of the wind velocity along the slope and uses it together with the stability indices of the air mass to check the Scorer rules for wave development. For all grid points at which the Scorer condition is met, a two-dimensional stationary linearized lee-wave flow pattern across an obstacle with an idealized (Gaussian) shape is calculated, neglecting effects of the Coriolis force.

The input parameters (such as vertical wind profile) for the model, which calculates the deflection of the streamlines across the obstacle, are extracted from the numerical model as well. It is the vertical deflection of the streamlines that determines the classification in weak, moderate and strong waves. Figure 3.25 provides an example of an MWP wave forecast for the Argentine Andes.

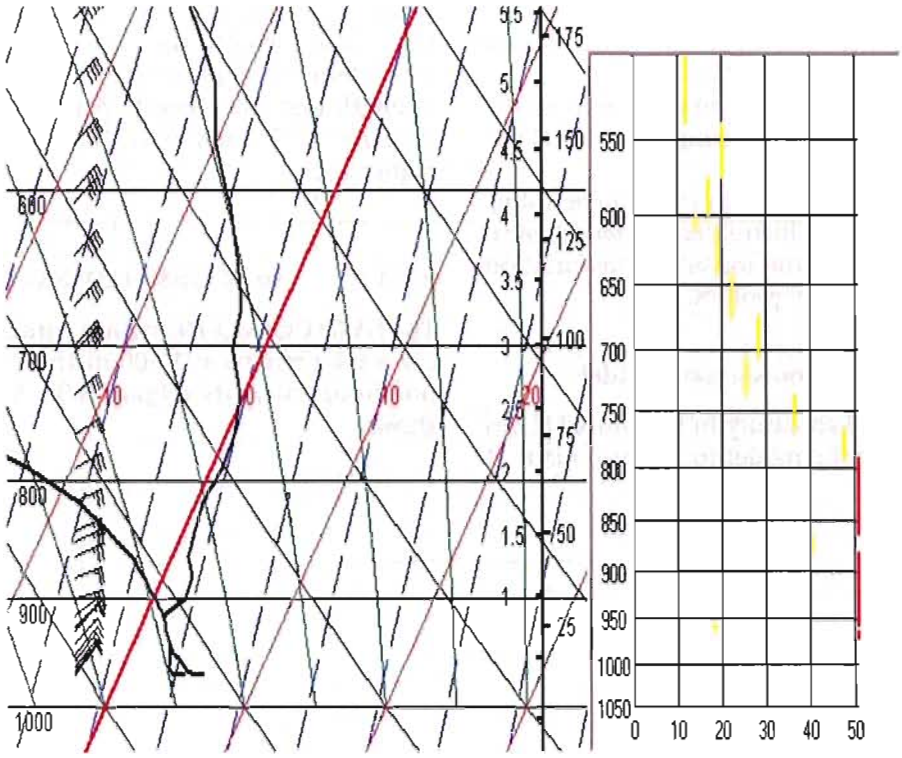

Figure 3.24. Predicted sounding (left) with a profile of the Scorer parameter (right) favourable for wave activity

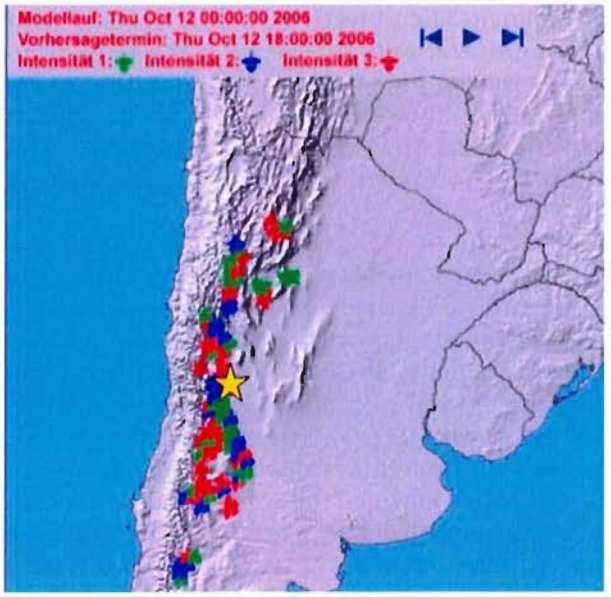

Figure 3.25. MWP Wave forecast for the region of the high Cordillera in the Andes on 12 October 2006. The star indicates the location of Mendoza. Note: Modellauf = model run, Vorthersagetermin = end of forecast and intensitaet = intensity.

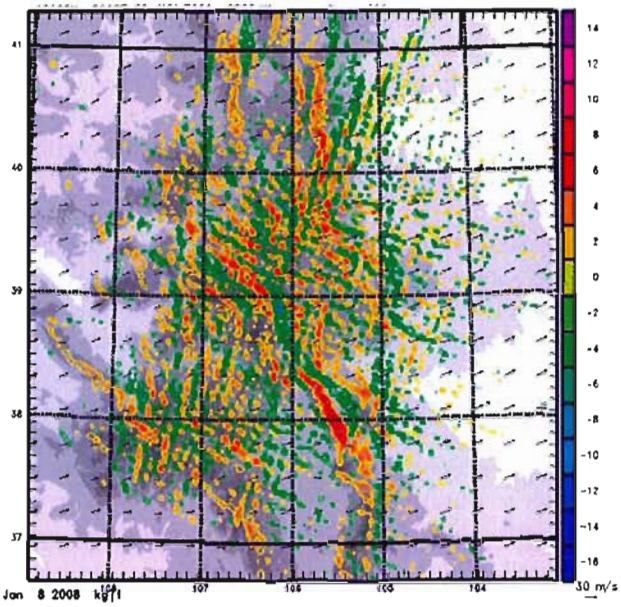

Figure 3.26. Vertical velocity at 5.5 km from the linear wave model at the Naval Research Laboratory. The area shown approximately encompasses the State of Colorado in the USA. The strongest wave lift appears downwind of the Sangre de Cristo Mountains, which are known to favour waves in south-westerly flow.

When using the MWP wave forecast, the following aspects/caveats have to be taken into account:

(a) A generalization of the orography used in numerical forecast models (smoothing of valleys, reduction of the height of mountains, approximated values of slopes);
(b) Coarse resolution of small-scale phenomena (low-level jets and convergences);
(c) Inadequate modelling of anabatic flow in the NWP, which causes a disruption of realistic wind profiles;
(d) No differentiation between visual meteorological conditions and instrument meteorological conditions due to the missing representation of vertical humidity profiles.

3.3.4.4 Linear diagnostic wave model

The Naval Research Laboratory in the United States uses a linear diagnostic model to produce maps at several levels and cross sections of vertical velocity and potential temperature for two regions of the country. The linear model is initialized with output from the Coupled Ocean Atmospheric Mesoscale Prediction System (COAMPS) at three-hour intervals, from which the soaring pilot can infer mountain-wave parameters such as updraught strength and wavelength. An example of vertical velocity at 5.5 km over Colorado is shown in Figure 3.26.

3.3.4.5 Local model (COSMO-DE)

The DWD COSMO-DE vertical winds reveal stationary wave patterns at 1 500 m and 3 000 m MSL in one-hour intervals (Figure 3.8). Moisture is not shown.

CHAPTER 4

METEOROLOGICAL SUPPORT FOR SOARING FLIGHT

4.1 SELF-BRIEFING

The rapid development of the means of communication over the past decade has resulted in many different information sources with a vast array of meteorological data and products useful for soaring purposes. The individual retrieval and analysis of this weather information from the Internet or via special briefing facilities is called "self-briefing" or "home-briefing".

The nearly unlimited sources of weather information often lead to more confusion than help for meteorologists and pilots in the decision-making process. With a view to addressing this problem, a possible scheme for glider pilots' self-briefing is provided below (Table 4.1). This recommended scheme is the result of discussions with glider pilots during meteorological seminars and it is employed in pc_met, the DWD online self-briefing system that is widely used in Europe. It should be stressed that this scheme is one possible guideline for the self-briefing of glider pilots for soaring activities, especially in central Europe. Depending on local conditions (weather, available data and products), another scheme may be better for other areas.

4.2 PERSONAL BRIEFING

In this context "personal briefing" is defined as providing, in person, tailored meteorological information in a short and concise way to glider pilots. Despite today's highly sophisticated model forecasts, personal briefings are still a benefit for planning flight tasks. There are different requirements, of course, depending on the event (such as competitions, camps or safaris). For competitions in particular it is valuable to have a meteorologist on site, preferably someone who is familiar with gliding weather of the local area. The competition meteorologist plays a key role in:

(a) Supporting operations with forecasts of surface wind for the expected runway to use;
(b) Planning the tasks and supporting the task-setter with detailed information;
(c) Preparing and presenting the weather briefing for the competitors;
(d) Monitoring the meteorological conditions, especially hazardous weather.

4.2.1 Meteorological support for competitions

A possible timetable of preparations for a competition may look like this:

t–180 min Analysis of the latest surface and upper-air charts and of the current weather situation (radar, satellite, webcams, mesonet stations)

t–160 min Checking the models: limited area models (two-dimensional charts, sounding forecasts), special local models

t–140 min Forecast of the surface wind for the expected runway to use (gridding of the gliders), first guess of the tasks with task-setter(s): flyable area and duration of flyable conditions

t–120 min Comparison of models with the actual conditions and identification of corrections

t–100 min Coordinating the meteorological conditions with the provisional tasks set by the task-setter, preparing alternatives, if necessary

t–75 min Monitoring the conditions for the prepared task(s) and feedback loop with the task-setter

t–60 min Preparation of the weather briefing using, for example, the PowerPoint program

t–0 min Weather briefing for pilots

t–take off Monitoring: unexpected changes, hazards – communication with the organizer

4.2.2 Preparation of soaring forecasts

Successful forecasting for soaring is a major challenge for meteorologists and depends on detailed analysis concentrated upon a relatively small area. The necessary work consists mainly of three parts: the synoptic analysis of the actual weather at the surface and the upper air, the interpretation of the numerical model outputs and their comparison with the actual weather situation.

Table 4.1. Self-briefing products and data that may be available/valuable for soaring activities

Day	*Basic data and products*	*Additional products*	*Special products*
0	Analysis 0000 UTC: • Surface • 850 hPa • 700 hPa • 500 hPa Forecast H+12 (regional model): • Surface • 850 hPa • 700 hPa • 500 hPa	(Last available) data: • HR satellite picture • Radar data • Lightning data • METARS, SYNOPS, TAFs Vertical soundings: • Analysis 0000, 0600 UTC • Forecast (RM, LM 0600, 1200 UTC	Soaring forecasts tools: • TOPTHERM/TopTask (D) • SkyView of COSMO (D) • Olofsson's method (S) • Dr Jack's method (US) Text forecasts for soaring activities: • Soaring forecast (D) DMD outputs of regional or local models: • COSMO – wave forecast • Scorer parameter • Cloud coverage, precipitation, wind field, and so on.
–1	Forecast H+24, H+36 (regional model): • Surface • 850 hPa • 700 hPa • 500 hPa	Vertical soundings: Forecast H+24, H+36 (RM and/or LM)	Output of soaring forecasts tools, such as: • TOPTHERM/TopTask (D) • SkyView of COSMO (D) • Olofsson's method (S) • Dr Jack's method (US) Text forecasts for soaring activities: • 3-day forecast (D) DMD outputs of regional or local models: • COSMO – wave forecast • Scorer parameter • Cloud coverage, precipitation, wind field, and so on
–2	Forecast H+48, H+60 (regional model): • Surface • 850 hPa • 700 hPa • 500 hPa	Vertical soundings: Forecast H+48, H+60 (RM and/or LM)	Output of forecasts of global models, such as: • SkyView of COSMO (D) • Dr Jack's method (US) Text forecasts for soaring activities: • 3-day forecast (D) DMO outputs of regional models: • COSMO – wave forecast • Scorer parameter • Cloud coverage, precipitation, wind field, and so on
–3 (–4)	Forecast H+72 (96), H+84 (108); (global model): • Surface • 850 hPa • 700 hPa • 500 hPa	Vertical soundings: Forecast H+72 (96), H+84 (108); (GM)	Output of forecasts of global models, such as: • Cloud coverage • Precipitation • Wind field • Vorticity

4.2.2.1 Analysis

A detailed analysis of the current weather situation is important to get an overall view of the weather. If there is no way to analyse surface and upper-air charts, charts issued by major meteorological services may help and save time. The following are important weather features to look for in the various sources of data:

(a) Latest surface chart:
  (i) Pressure field, isallobaric fields, pressure centres and their movement;
  (ii) Frontal zones with or without precipitation, convergence lines and their movement;
  (iii) Observed cloud types in different levels (for example, Ac cas as an indication of an upper air destabilization, Ac len for mountain waves);
  (iv) Rainfall amount of the previous day in the surrounding area;
  (v) Dewpoint analysis;
  (vi) Hazards (thunderstorms, squall lines, hail) in the upstream area;
(b) Upper-air charts (0000 and 1200 UTC):
  (i) Jet stream positions at 300 hPa (left or right exit of jet streaks) and movement;
  (ii) Geopotential field, trough and ridge positions and their movement at 500 hPa;
  (iii) Air mass analysis: temperature gradients and advection at 850 and 700 hPa;
  (iv) Wind and humidity fields at 850 and 700 hPa;
(c) Satellite, radar pictures, webcams, wind profiler and mesonet stations:
  (i) Development and formations of clouds, frontal structures and associated movement;
  (ii) Radar echoes, weakening or intensifying of rain bands or convective systems;
  (iii) Current wind and temperature distribution;
(d) Soundings:
  (i) Nearest station;
  (ii) Upstream soundings;
  (iii) Making a local sounding by plane or model plane could be helpful;
(e) Special observations:
  (i) METAR (current weather);
  (ii) AIRMET, GAMET, SIGMET (current and forecast hazardous weather);
  (iii) PIREPS (Pilot reports).
  (iv) Numerical model output

The model output should be checked critically. The important features to look for are:

(a) Development of troughs and ridges (large-scale vertical motion and vorticity advection);
(b) Influence of jet streams;
(c) Movement of frontal systems;
(d) Advection of temperature and humidity, clouds at different levels;
(e) Wind fields at different heights;
(f) Change in surface pressure;
(g) Stability of the atmosphere (forecast soundings);
(h) Identification of mesoscale structures (meso low, low-level jet).

4.2.2.2 Comparison

Numerical forecasts need to be compared with the analyses, if possible by employing the NWP LM and special tools (such as TOPTHERM) that use boundary conditions of the LM. If the model forecasts fit well to the latest analysis (for example, the 0000 UTC model run valid at 0600 UTC fits the actual 0600 UTC analysis), then you can trust the model.

Special attention should be paid to:

(a) More or fewer layer clouds than forecasted that could weaken or strengthen the convection;
(b) Earlier or later development of convection and its strength;
(c) Reinforcement or weakening of nearby fronts;
(d) Change of wind direction and/or speed at different levels;
(e) Higher or lower temperature at the surface (which affects the start time of convection);
(f) Existence of inversions not forecast (local effects, in mountainous areas especially).

If any of the features mentioned above, determined from prevailing conditions, are different from the model forecast, adjustments are necessary.

In the unlikely event of a communication failure, which would mean that no forecast soundings from models are available, the "classic" analysis and forecast method using actual soundings (perhaps from a tug aircraft) is required to assess the impact of horizontal advection of temperature and/or humidity. There is software available that easily calculates and displays the change of the vertical profile in time (see section 3.3.1.1).

4.2.3 Meteorological support for the task-setter

Setting good tasks in terms of direction and distance is a challenging job. Depending upon the weather situation, the orographic conditions and the performance of the gliders, the task-setter has to

choose tasks that are neither too easy nor too difficult to complete.

After a detailed analysis and a first check of the numerical weather models, a potential task area can be chosen. Thus, the task-setter is able to prepare a draft of several tasks using flight planning software with geographical information (Figure 4.1). After the detailed study of the forecast models and the actual weather conditions, a set of provisional tasks can be worked out. The competition meteorologist gives a short briefing to the task-setter to enable him to finalize the tasks.

In cases of uncertain weather forecasts, a primary and a reduced secondary task should be prepared for each performance class, taking into consideration the planned take-off sequence.

There are tools for the simulation of tasks with the predicted weather to demonstrate their feasibility (see section 5.3).

4.2.4 Documentation for pilots

Most pilots like to have documentation of the expected meteorological conditions for the task. There are several ways to provide this service:

(a) A weather board;
(b) The competition website;
(c) Handouts (a sample can be found in WMO/OSTIV, 1993).

The competition website might be the best way to provide weather information to the pilots, because it can be updated and animations can be included.

4.2.5 Competition briefing

A PowerPoint presentation is a common and useful form for a competition briefing; it easily combines text with illustrations such as pictures, movies or diagrams. The presentation should be as short and as clear as possible and should contain all the meteorological information needed for the competition day.

In general, there are two basic concepts for giving a presentation. One is to start with the big picture and move step by step into greater detail, ending with the local picture. The other approach is to start with local phenomena and then explain how these fit, step by step, into the bigger meteorological picture.

The contents of a briefing are listed in Table 4.2.

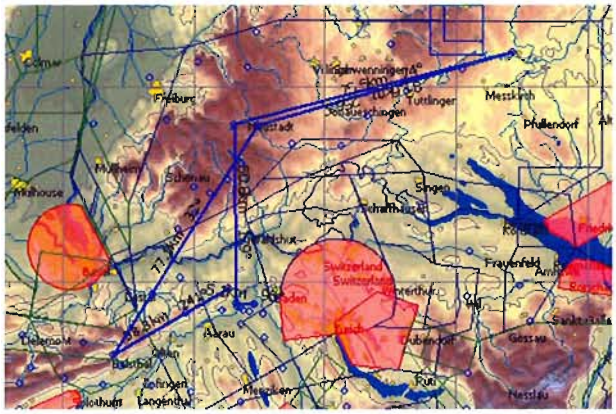

Figure 4.1. A 328-km task out of Birrfeld (Switzerland)

Table 4.2. Contents of a competition briefing

Goal	*What to present/show*
General synoptic weather situation and development, comparison to the day before and outlook Air mass	Analysis: Upper-level and surface chart Numerical forecasts Satellite images (animation) Radar images (animation)
Thermals and relevant phenomena for the competition area Height, duration and strength of thermals during the day, convective clouds with base and tops, stratiform clouds, inversions, advections, freezing level Special remarks, such as low-level outflow of cold air, and so on	Vertical soundings (measured and predicted) influencing the competition area Time-altitude cross section for thermals and weather phenomena Fixed-time forecast chart for a specified area
Wind	Wind fields in different levels: sfc, 850, 700 (500) Wind profile
Special phenomena, depending on the situation	Cloud cover and precipitation analysis and forecasts Meteogram Webcams
Warnings: Hazards in flight and on the ground	Any supporting material that indicates dangerous phenomena
Additional information	Sunset, minimum QNH, maximum of temperature

4.2.6 Monitoring the weather

Nowcasting is an important process after the briefing. The competition meteorologist should provide, as needed, the task-setter(s) and/or the organizer with actual weather information during the ongoing competition. Deviations from the forecast, especially information about hazards, may influence the competition significantly; for example, unforecasted weather may develop. Hazard alerts must be issued as soon as possible. Warnings are to be distributed to the crew and to the pilots by radio or cell phone. If hail or strong winds are expected, warnings for ground operations are also necessary.

4.2.7 Pilot support

In the past, direct support by a meteorologist was the only way to receive serious meteorological information at soaring competitions. Therefore, many national teams had a meteorologist. With today's communication and self-briefing facilities (such as the Internet and dedicated software tools), individual pilots or national teams can find the meteorological information needed for successful competition flights. Therefore, the question arises: are team meteorologists still needed or are they a vanishing species? The tasks of a team meteorologist are listed below. Extra profit for the pilots can be expected from a team meteorologist.

The daily tasks of a team meteorologist during competitions include:

(a) Familiarization with the weather situation (analysis, forecast, warnings);
(b) Participation in the official competition briefing;
(c) Execution of the meteorological part of the daily team briefing with:
    (i) Advice regarding possible differences to the official competition briefing;
    (ii) Information on special weather conditions (showers, thunderstorms, outspreading clouds, cloud streets, waves);
(d) Adaptation of the competition forecast to the tasks in the different classes;
(e) Before the start: obtaining the latest weather information, especially new data for a decision regarding the best "meteorological period" for the task;
(f) After departure and during the flight:
    (i) Monitoring of the weather conditions based on a comparison of observational data (METARS, SYNOPS, Temps, radar and lightning data, high-resolution satellite pictures) with model forecasts;
    (ii) Interactions with pilots and the team captain with regard to special or adverse weather conditions (use of nowcasting tools in marginal/changing weather conditions);
(g) During the final glide:
    (i) Informing the pilots and the team captain of weather conditions along the final glide and at the airport;
(h) Analysis of the daily conditions:
    (i) Verification of weather conditions and forecasting (pilot feedback and hindcasting).

The experience of the German team shows that a team meteorologist contributes to successful competition results if the meteorologist has a comprehensive knowledge of soaring and soaring meteorology and he has a general overview of the geographical and climatological conditions of the competition area. To accomplish their tasks, team meteorologists should be equipped with a wireless laptop computer. Keep in mind, however, that the meteorologist is only a supporter. The final decisions are to be made by the competition pilots.

4.3 METEOROLOGICAL FLIGHT PLANNING

Simulations of planned flight tasks with the predicted weather (Liechti and Lorenzen, 2004) are useful for the selection of:

(a) The task area;
(b) The task length;
(c) The departure time.

A task is defined by a sequence of turnpoints that form the legs of a polygon. Meteorological predictions of the glider climb rates, the spatial distribution of thermals and the wind can be converted to ground speed along the task legs. This conversion is affected by the performance of the glider and the deviations from the shortest track required to locate these updraughts. The resulting task speed depends on the departure time and also to some extent on the departure altitude and the arrival altitude (Figure 4.2).

The temporal and spatial resolutions of the meteorological predictions are related by the task speed. Typical task speeds are around 100 km/h. Thus, a 30-minute temporal resolution of the forecast is matched by a 50-km spatial resolution.

Flight planning can be used to maximize the task distance for individual flights and to optimize the departure time of short tasks for best speed from the meteorological point of view. Task-setting is supported by indicating the possible departure times that allow for feasibility of the task.

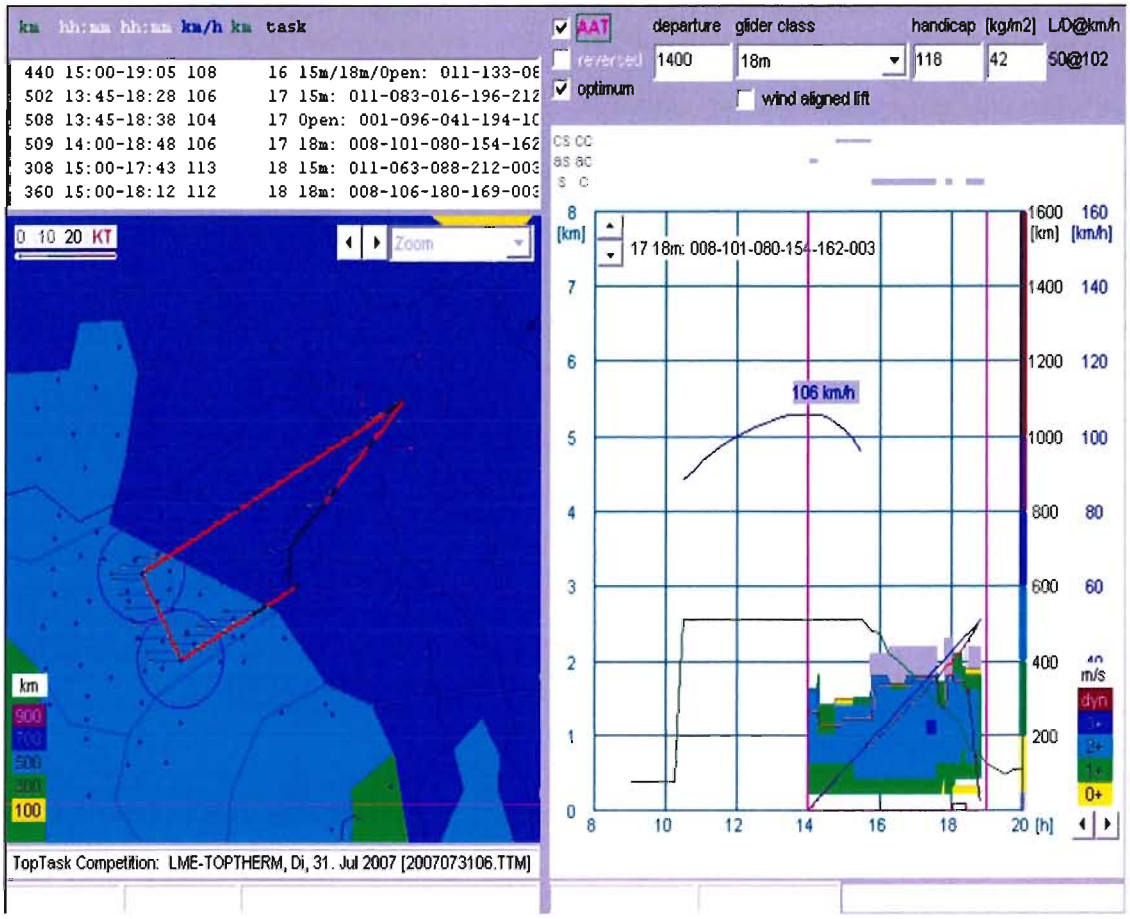

Figure 4.2. Meteorological flight plan of a 500-km task in central France for an 18 m class glider. Map (left): the first leg to the SW is in dry thermals with a tailwind component, the third leg to the NE is under cumulus clouds into a headwind. The final glide (black) starts on the fourth leg. Barogram (right): the task is feasible with a departure time between 10.30 a.m. and 3.30 p.m. (green curve and scale). The predicted task speed is 86 km/h to 106 km/h, depending on the departure time (blue curve and scale).

CHAPTER 5

FLIGHT DATA

5.1 FLIGHT DOCUMENTATION

5.1.1 Flight recorder

For all badge, competition and record flights, an International Gliding Commission (IGC)-approved documentation of the flight is mandatory. This is usually accomplished by using a "secure" GPS-based flight recorder that stores three-dimensional position data and additional barometric pressure in a secure data file called an IGC-file. An on-board navigation (NAV) computer derives real-time ground speed, as well as the wind component along the direction of flight, from these data. If heading information is available, full-vector wind determination becomes feasible. Some NAV/final-glide computers use temperature sensors to calculate true airspeed at altitude and potential temperature.

5.1.2 Flight data analysis

The data from the IGC-file allow for some post-flight analysis. Various visualization tools are available to plot, for example, an altitude trace versus time or a two-dimensional flight track. A full three-dimensional representation of the flight data also can be displayed using the popular Google Earth software, which accepts the IGC data format. Flight data are also a rich source of information on meteorological processes.

5.1.3 Flight data sources

The relevant IGC-files can be used to compile statistics of achieved distances and speeds of a number of flights in a given area or over a given period. These are available from the international Online Contest (OLC) for most active gliding regions around the globe, or, for localized events, from the main national and international competition sites. The latter, in particular, are suitable for verification of the forecasts given.

5.2 POSITION OF UPDRAUGHTS

Updraughts can be identified in recorded flight data and atmospheric lift patterns can be recognized. The positions of thermal lift, ridge lift and wave lift are a result of the solar irradiation and the horizontal airflow interacting with the terrain. The analysis of these positions reveals the meteorological processes at work.

5.2.1 Thermal lift

The combination of high-resolution topographical data and the diurnal and seasonal variation of solar irradiation has been visualized by Heise (1999) and refined by Sigrist (2006) as TherMaps. These maps are calculated for fixed times and dates. Clear sky is assumed and seasonal variations in the surface parameters controlling the albedo (snow line) and the evapotranspiration (vegetation) are included. Furthermore, the significant phase shift of several hours between the irradiation and the resulting updraughts is modelled. In mountainous areas such as the Alps, the Pyrenees and the Apennines, a TherMap analysis of flight data reveals that ascents in thermal lift are located above computed hot spots in numerous cases.

The visualization of flight tracks on TherMaps confirms that slopes significantly affect the spatial distribution of lift used for thermal soaring (Figure 5.1). It suggests that high-resolution fore-

Figure 5.1. Recorded flight track on a TherMap rendered in 3D. The climbing segments (red portion of the flight track) are confirmed by the computed hot spots (brown-to-red surfaces).

casts of thermal lift positions should be possible if thermal predictions at lower resolution are combined with high-resolution topography. Patterns of aligned thermal lift may be identified and related to aligned surface characteristics, such as significant changes in the albedo across the snow line. Pilots may use TherMaps for strategic route planning in mountain areas and for questioning their habits.

5.2.2 Ridge lift

The combination of high-resolution topographical data and a uniform horizontal airflow has been visualized in WindMap by Sigrist (see section 7.3.). These maps, calculated for fixed wind directions and dry air, include sheltering and channelling effects. The WindMap analysis of flight data reveals that ascents in ridge lift are located above computed updraughts in numerous cases.

The visualization of flight tracks on these maps confirms that high-resolution forecasts of ridge lift positions should be possible if airflow predicted at lower resolution is combined with high resolution topography (Figure 5.2). Pilots may use WindMap for strategic route planning in ridge and wave soaring and for questioning their habits.

5.2.3 Wave lift

The combination of recorded flight data (position, time, pressure, temperature and the three-dimensional wind field) and the pilot's observation from the cockpit provides the meteorologist with a realistic picture of small-scale phenomena. A series of flight tracks between 6 000 m and 1 500 m in tailwind and headwind (330 degrees and 150 degrees) on the lee side of a mountain in a stationary lee wave were the data source for Figure 5.3.

Wave positions can be obtained from flight log data. Figure 5.4 (Forstner and Prodinger, 2000) shows the positions of lee waves in the Austrian Alps for a particular south foehn case as deduced from the climb rate of several recorded flights.

5.3 STATISTICAL ANALYSIS

The statistical analysis of flight data from competing gliders reveals characteristic properties of the atmospheric lift patterns and how they are explored by pilots for the optimization of the task speed. Such properties and their correlations can be used for the design of forecasting techniques for soaring

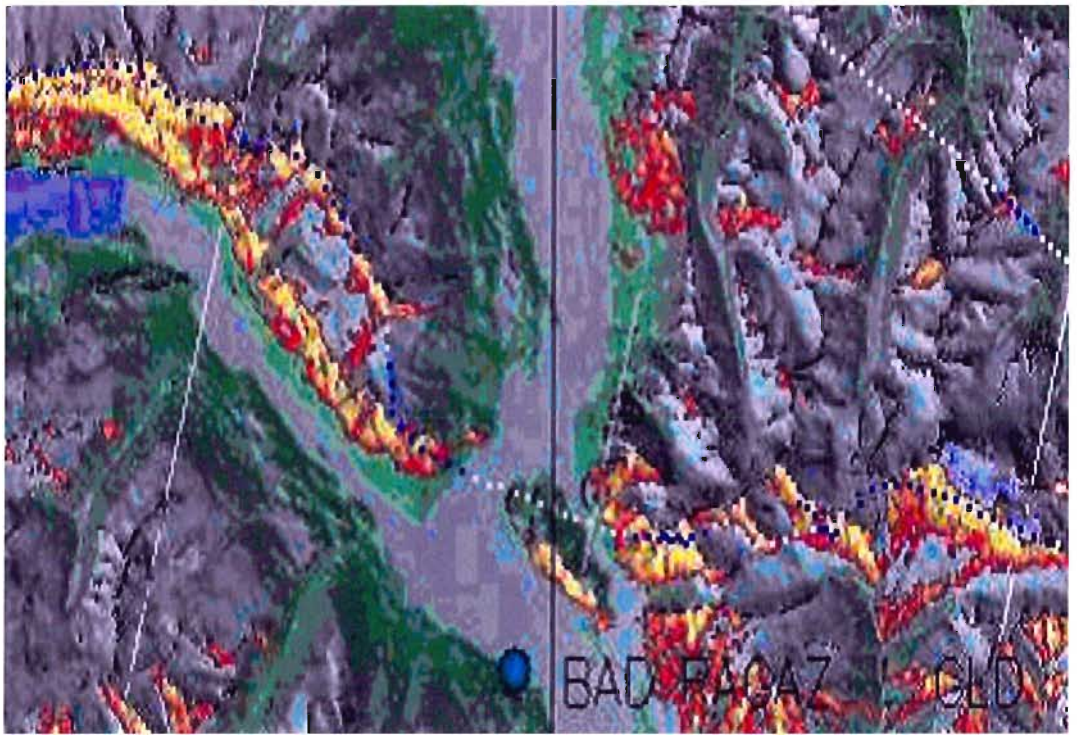

Figure 5.2. Recorded flight track on a WindMap rendered in 2D. The climbing segments (blue dots) of the flight track are confirmed by the computed updraughts (yellow surface).

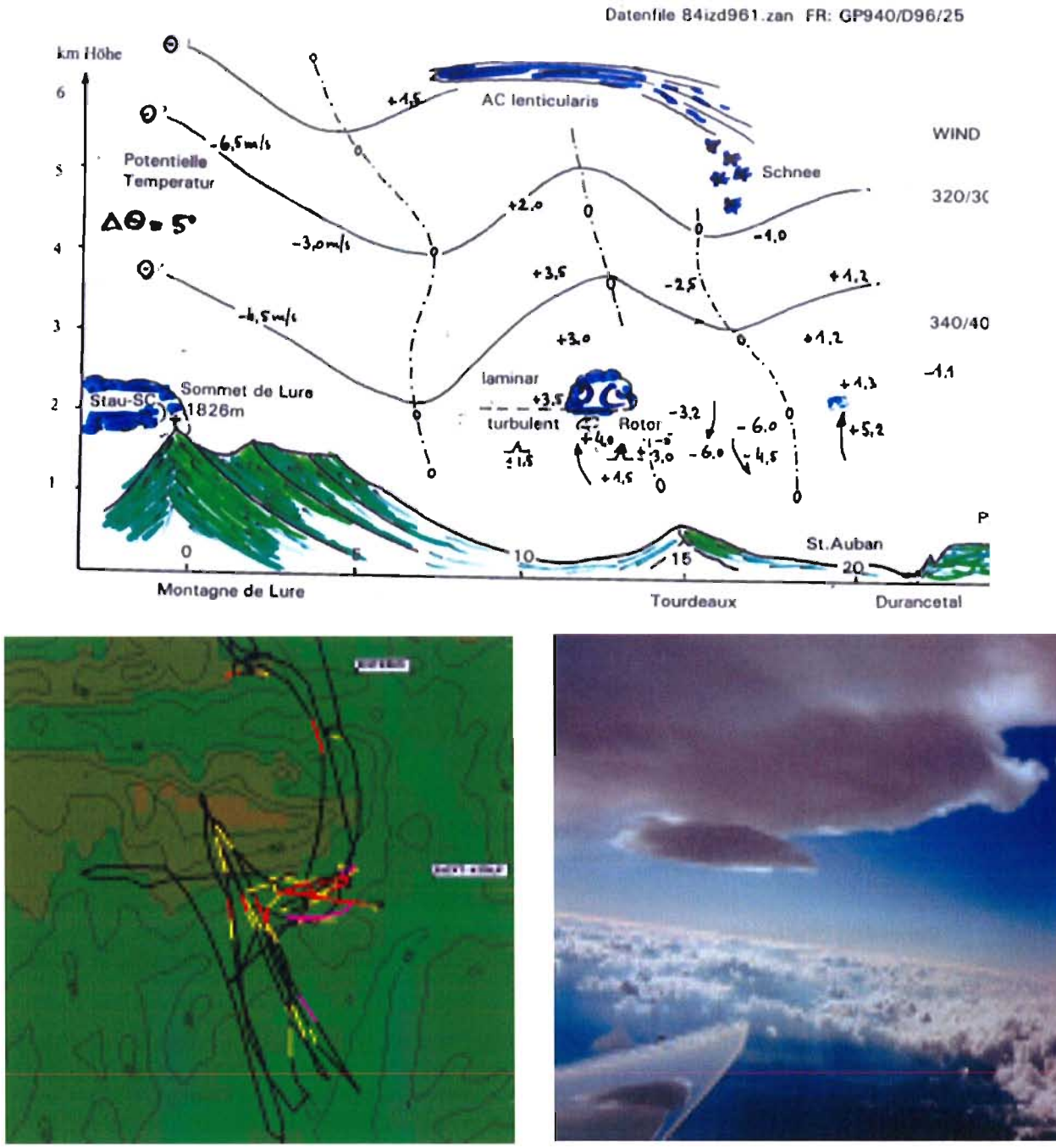

Figure 5.3. Cross section of the observed and measured flight data (top) on the lee side of Montagne de Lure in southern France on 18 April 1998. The flight trace and the pilot's view are shown in the left and right panels, respectively.

through the interpretation (post-processing) of direct model output. In addition, such correlations reflect inherent properties of the CBL.

In a study by Maul (2008) on Lilienthal Glide 2007 (July) out of Lüsse, Germany (latitude 52°N), the competition flight data were cleaned of pre-start and post-finish data points. Then, in order to reduce the number of points without losing relevant information, the minimum time interval between adjacent data points was set to 24 seconds, that is, about the circling time of gliders. The barometric altitude information was used for the calculation of vertical speeds w. It was necessary to average over two neighbouring points to obtain a reasonably smooth result for the deduced vertical speed distribution $f(w)$. From 87 completed flights, some 45 000 data points were typically obtained for a competition day. Each data point is a

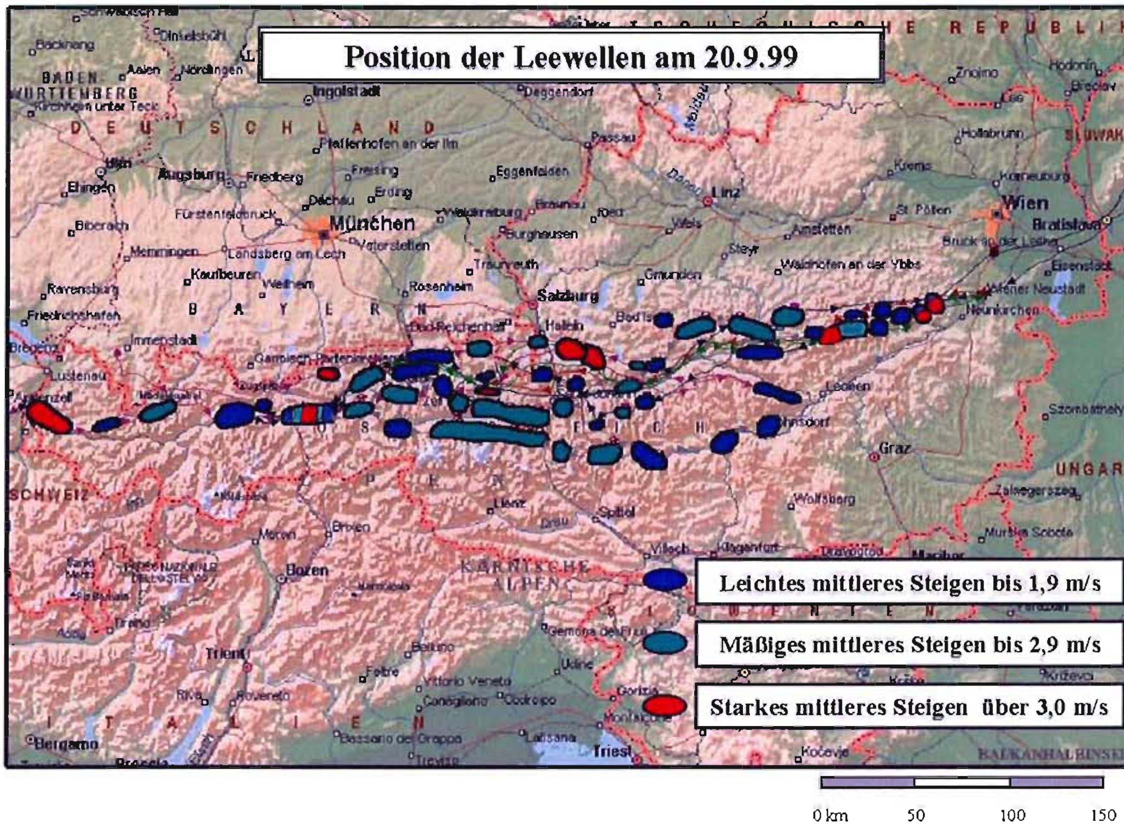

Figure 5.4. Positions of wave lift during a south foehn case on 20 September 1999 over the eastern Alps

vector containing information on time, latitude, longitude, barometric altitude *z* and barometric vertical speed *w*.

5.3.1 Recorded climb rate

The *w* components were binned into intervals of 0.2 m/s width, ranging from –10 m/s to +10 m/s, to obtain the vertical speed distribution *f(w)*. Gliders competing using thermal lift show a bimodal distribution of vertical speeds (Figure 5.5). The two dominant modes consist of normally distributed climb and sink rates. On average, winning pilots manage to climb faster than the crowd. Spending more time in weaker lift leads to slower task speeds.

5.3.2 Recorded altitude

The *z* components were binned into intervals of 50 m width, ranging from 0 m to the top of the CBL, to obtain the altitude distribution *f(z)*. Gliders competing in thermal lift prefer to climb in the upper half of the CBL (Figure 5.6). On average, winning pilots manage to fly at higher altitudes than the crowd. Having to spend more time at lower altitudes results in slower task speeds. The most likely flight level is typically found at 67 per cent of maximum flight level, which represents the maximum CBL depth of the day.

5.3.3 Convective boundary layer depth and climb rate

The most likely climb rate *w* and the most likely flight altitude *z* were determined from *f(w)* and *f(z)* for eight competition days (Table 5.1). The maximum flight altitude was arbitrarily set to the 99.75 percentile of the distribution. On the first two days the CBL depth jumped significantly in both space and time during the competition. These changes were much smaller and smooth, however, on the remaining six days. The most homogeneous day was 26 July 2007.

Figure 5.7 indicates that the daily maximum flight level and the most likely climb rate of the six days with a small and smoothly growing CBL depth during the flights (large symbols) are correlated in a linear way. The two days with clearly heterogeneous conditions (small symbols) have been omitted for the calculation of the linear regression line.

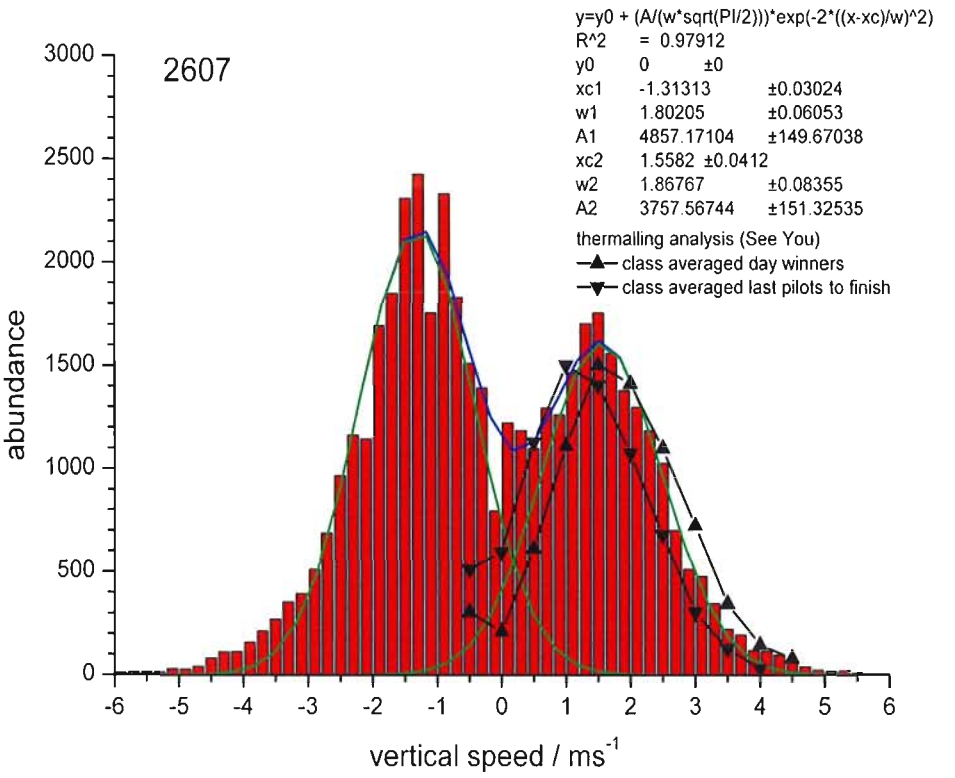

Figure 5.5. Recorded vertical speeds of 87 gliders flying a competition task with thermal lift over flat terrain on a day with spatially rather homogeneous and smoothly varying temporal conditions. First and last finishers use different climb rates.

The correlation between the most likely climb rate and the daily maximum altitude (that is, the maximum depth of the CBL) is useful for the interpretation of direct model output: if the CBL depth can be assessed from direct model output, it can be converted to the most likely climb rate for a thermal forecast. Table 5.2 contains the Lüsse results extrapolated to both deeper and more shallow CBLs (that is, stronger and weaker climb rates). The result is systematically different from existing methods (WMO/OSTIV, 1993; Hindman and others, 2007) and the tentative linear extrapolation needs to be confirmed by the evaluation of further flight data. Certainly, the relation between climb rate and CBL depth depends on the types of flight considered (section 2.2) and it might be different in mountain areas.

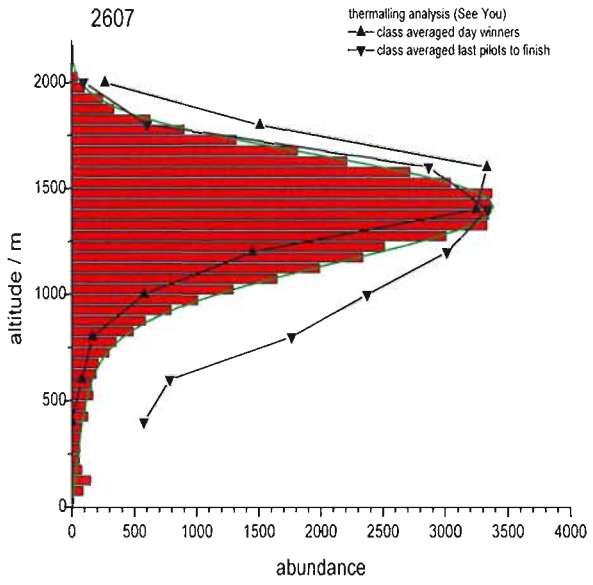

Figure 5.6. Recorded flight levels of gliders flying a competition task with thermal lift over flat terrain on a day with spatially rather homogeneous and smoothly varying temporal conditions. First and last finishers fly at different altitudes.

As the sink rate of gliders in steady turn is 1.0 m/s (section 2.2), the updraughts have a higher vertical speed than the recorded climb rates. In Figure 5.7 the top and the bottom axes are offset by this value. A linear scaling between the updraughts (top axis) and the height (right axis) of the CBL is indicated by the extrapolated (full) lines. This scaling suggests that the rise time of thermal updraughts is on the order of 700 s – independently of the absolute depth of the CBL. Such a scaling is in agreement with theoretical concepts of the CBL.

Table 5.1. Most likely climb rate *w* and most likely flight altitude *z*

Day	*Maximum altitude [m MSL]*	*Most likely altitude [m MSL]*	*Most likely climb rate [m/s]*
15.07	**2 647**	**1 150**	**1.67**
16.07	**2 777**	**1 756**	**2.15**
18.07	**2 267**	**1 490**	**2.02**
19.07	**1 853**	**1 220**	**1.36**
21.07	**1 708**	**1 135**	**1.24**
23.07	**1 831**	**1 120**	**1.40**
10.30–11.00	1 531	1 050	1.69
11.00–11.30	1 654	1 040	1.42
11.30–12.00	1 769	1 190	1.36
12.00–12.30	1 895	1 240	1.46
12.30–13.00	1 779	1 210	1.38
13.00–13.30	1 809	1 120	1.63
26.07	**1 970**	**1 410**	**1.56**
12.00–12.30	1 752	1 330	1.72
12.30–13.00	1 787	1 340	1.67
13.00–13.30	1 847	1 430	1.79
13.30–14.00	1 992	1 410	1.91
14.00–14.30	2 020	1 540	1.74
14.30–15.00	2 000	1 500	1.26
27.07	**1 855**	**1 100**	**1.44**

5.4 VERIFICATION OF SOARING FORECASTS

Recorded flight data are useful for checking the quality of weather predictions for soaring. Predicted climb altitudes and climb positions can be verified in great detail, as the spatial and temporal resolution of the available flight data is usually higher than that of the numerical predictions. Taking the speed polar of the glider into account allows for the verification of the predicted updraughts from recorded climb rates, and the predicted wind from recorded ground speeds. Verification of the flight distance of the longest flights includes the predicted duration of the updraughts.

5.4.1 Thermal lift

The predicted depth of convection can be compared to flight levels, and the predicted climb rates and horizontal winds to the observed ground speed,

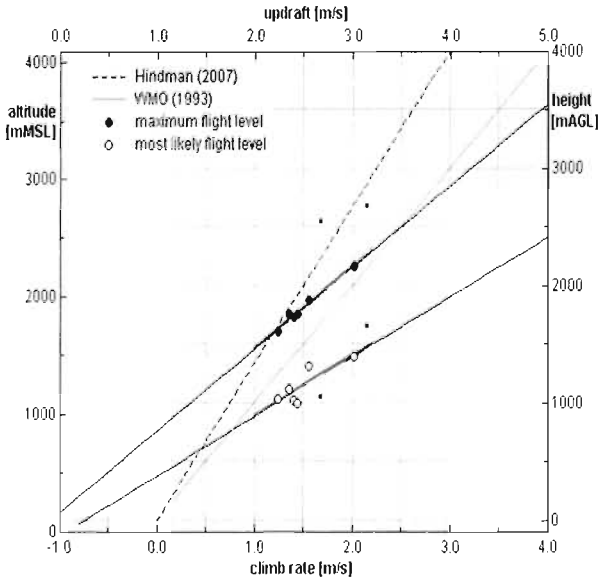

Figure 5.7. The daily maximum flight level and the most likely flight level are linearly related to the most likely climb rate. The updraughts (top axis) are proportional to the height of the daily maximum flight level (right axis). The data points were obtained from a statistical analysis of recorded competition flight data (Lilienthal Glide 2007 in Lüsse, Germany) and indicate a systematic deviation from previously used relations between climb rate and CBL depth.

Table 5.2. CBL depth and corresponding climb rate. Analysed values are set in bold face, extrapolated values in standard face.

CBL depth [m AGL]	*Climb rate [m/s]*	*Updraught [m/s]*
767	0.00	1.00
1 116	0.50	1.50
1 464	**1.00**	2.00
1 812	**1.50**	2.50
2 160	**2.00**	3.00
2 508	**2.50**	3.50
2 856	3.00	4.00
3 204	3.50	4.50
3 552	4.00	5.00

500	–0.38	0.62
1 000	0.33	1.33
1 500	**1.05**	2.05
2 000	**1.77**	2.77
2 500	**2.49**	3.49
3 000	3.21	4.21
3 500	3.93	4.93
4 000	4.64	5.64

while predictions of the potential flight distance can be compared to the length of the flight traces. The predicted speed for flight tasks can be compared to the scored speed in competitions (Liechti and others, 2007). The simulation of actual flights with the predicted weather is the ultimate test of forecasting skill (Hindman and others, 2007). Figure 5.8 shows a recorded flight in thermal lift and its simulation with regional predictions of thermal lift.

Verification of the predicted flight levels is useful for the tuning of the surface parameters (albedo, latent and sensible heat flux) in the boundary layer models. Their spatial and seasonal variation is of particular importance for soaring forecasts. The verification of the predicted ground speed is useful for the tuning of the climb rate calculations.

5.4.2 Wave lift

Soaring flights in wave lift have been compared with forecasts of the Lester-Harrison nomogram (Lindemann and others, 2008) and the MWP tool for the Argentine Andes. Figure 5.9 shows the vertical velocity measured with high-resolution sensors on a day with waves predicted to be of moderate intensity by the Lester-Harrison nomogram (Figure 3.23). The measurements confirmed the formation of waves. The wavelengths and the vertical velocities were found to change with altitude. Figure 5.10 shows a wave flight that reached the stratosphere with an altitude of 12 500 m on a day with waves predicted to be strong by the MWP tool (Figure 3.25). Hindman and others (2004) present extremely high-resolution, in space and time, simulations of an unusual lee-wave event downwind of the Catskill Mountains of New York State, in the United States. The simulations were motivated by a glider reaching the maximum permissible altitude (about 5 200 m MSL) under VMC conditions. The glider was equipped with a GPS flight recorder. The predicted wave locations were compared to the flight record and remarkable consistency was achieved (Figure 5.11). This result indicates the possibility of using such a model to predict the locations and strengths of lee waves for glider flights.

Figure 5.12 shows recorded flight tracks compared to the vertical motion predicted by the DWD LM (Thehos, 2007). The remarkable consistency indicates the possibility of using such a model to predict the locations and strengths of lee waves for glider flights.

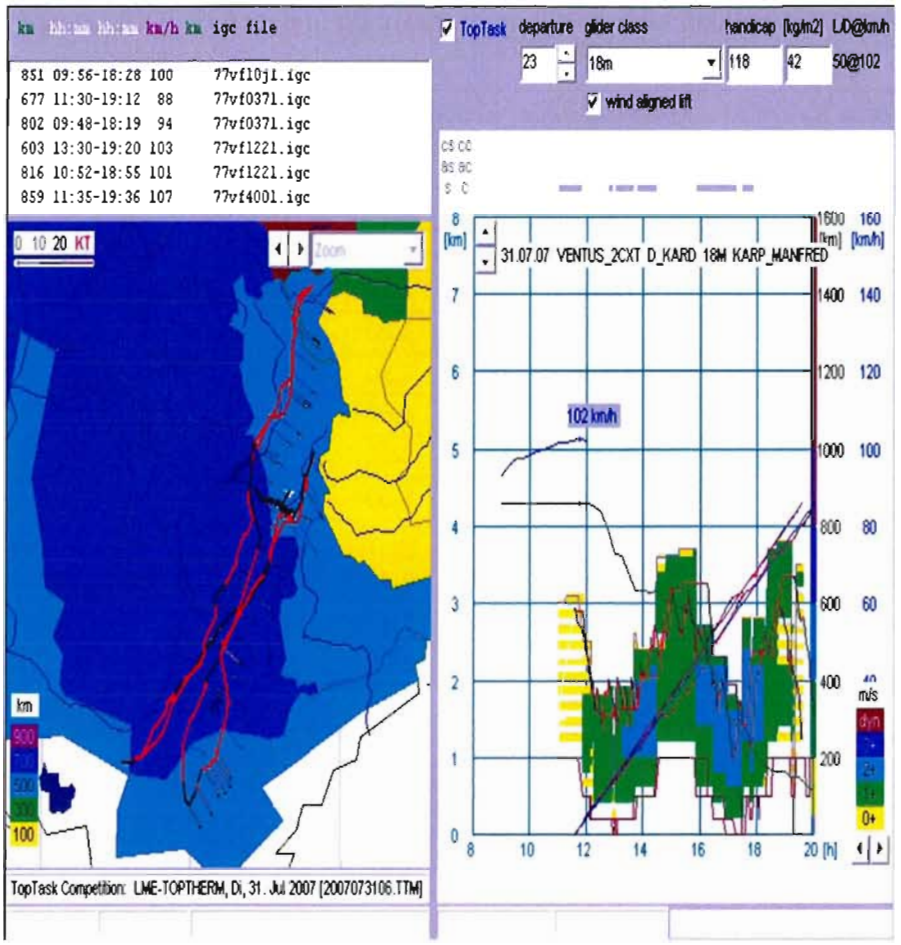

Figure 5.8. Simulation of a glider flight with predicted weather in south-eastern France. Left: the 800-km flight trace begins in the centre. The first turnpoint is in the SSW, the second in the far N, the third again in the WSW and the fourth turnpoint slightly NE of the departure point. The four flight legs are oriented almost perpendicularly to the predicted wind. Right: the simulation begins at 2 900 m MSL at 11.35 a.m. and uses both thermal and dynamic lift. The simulated flight altitude is at 80 per cent of the predicted convective depth, which changes with topography between the flat regions in the SW and the complex terrain of the French Alps in the NE. The diagonal lines represent the recorded and simulated flight distance. Their slopes reflect, respectively, the average ground speed of 107 km/h and 102 km/h.

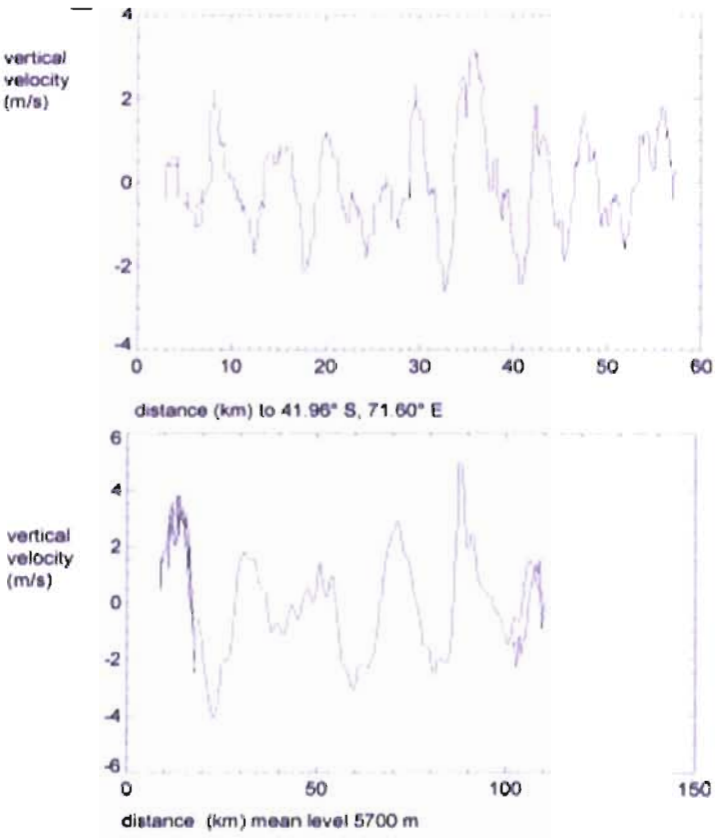

Figure 5.9. Verification of the Lester-Harrison nomogram (Figure 3.23) for estimating the lee-wave intensity over the Argentine Andes. The verification of the 2 December 1999 forecast (moderate intensity) along the San Martin cross section (bottom) shows stronger vertical motion and a longer wavelength than the verification of the 3 December 1999 forecast (weak intensity) for the Chapelco lee wave (top).

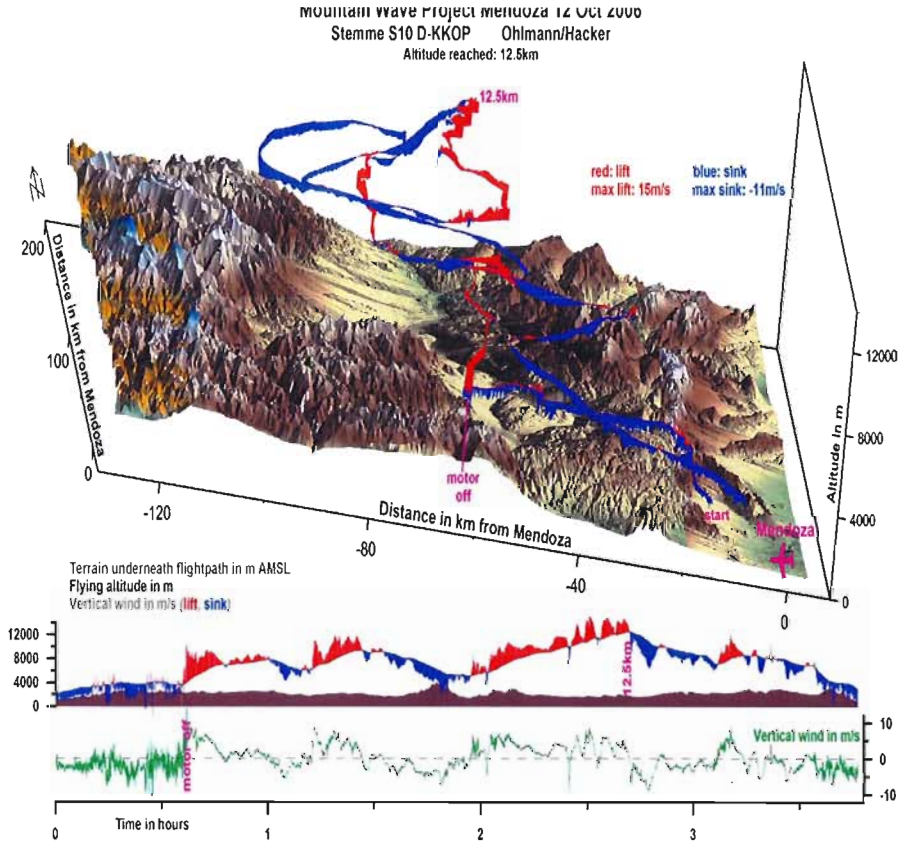

Figure 5.10. Measured vertical velocity from the wave flight (up to 12 500 m MSL) on 12 October 2006. Flight altitude and climb rates compare favourably to the MWP tool forecast (Figure 3.25).

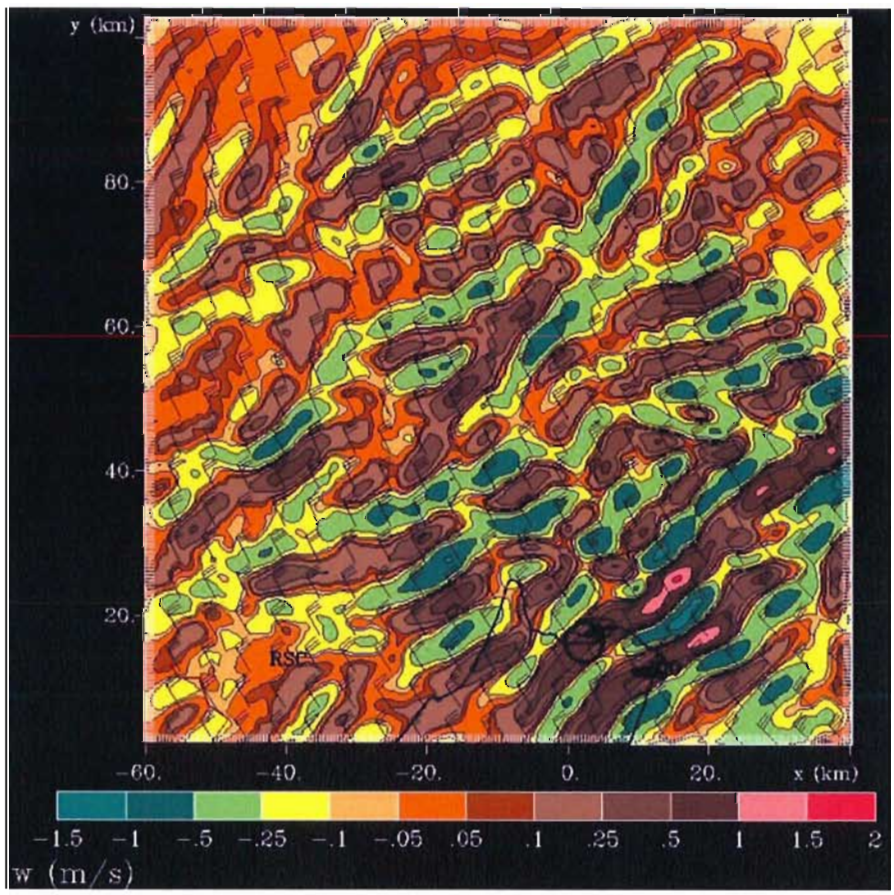

Figure 5.11. Recorded flight track (black irregular line) in wave with positions of updraughts (wave pattern). The circle indicates the region where the glider achieved the highest altitude.

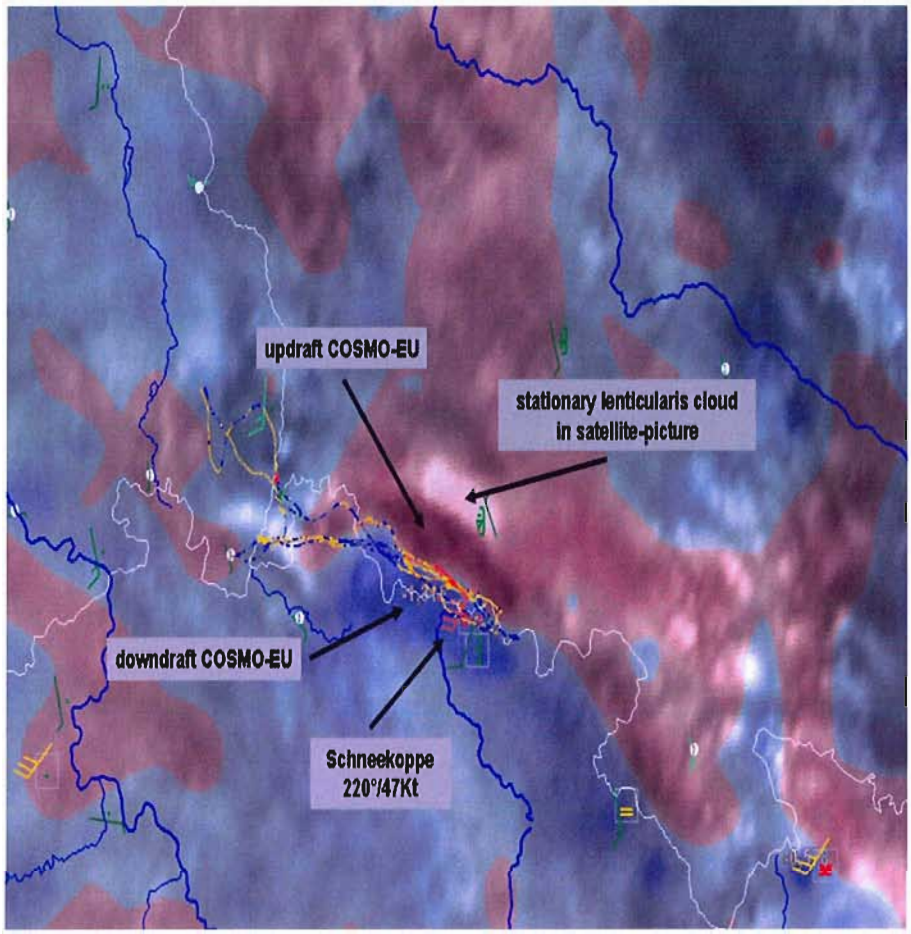

Figure 5.12. A superposition of a flight trace (coloured), a satellite image (grey shades) and the predicted vertical motion (brown denotes regions of updraughts and blue denotes regions of downdraughts). Schneekoppe is a mountaintop station.

CHAPTER 6

EPILOGUE

This publication is for all who are concerned with the meteorological support for gliding. It records the significant progress in weather forecasting for soaring flight since the 1993 edition of WMO Technical Note No. 158 *Handbook of Meteorological Forecasting for Soaring Flight*.

In Chapter 1, the three main types of lift enabling soaring flight – convection, ridge and wave lift – were described. The physical basis for each was given, providing the meteorologist with the understanding to produce meaningful soaring forecasts. Pilot stories describing flights in the three types of lift illustrated the intimate connection, in the cockpit, between theory and practice.

The technical description of gliding and soaring flight in Chapter 2 illustrated the impact of weather on feasibility, timing, range of operations and safety. The connection between glider aerodynamics and meteorology was detailed and used to explain the remarkable flight speeds gliders achieve.

Chapter 3 contained a summary of the essential basics of numerical weather predictions, which are the foundations of current meteorological practice. Explanations of data input, parameterization schemes, scale separations, model outputs and interpretation and verification of forecasts provided insight regarding model successes and limitations. Soaring forecasts for convection, ridge and wave lift based on numerical models were shown to have significant spatial and temporal detail.

In Chapter 4, the weather analyses and forecasts necessary for supporting soaring flights were identified. The role and benefits of the team meteorologist were described. An NWP-based flight planning tool was illustrated; a glider was essentially "flown" through the prediction to estimate the feasibility of a task.

The GPS flight data recorded aboard most sailplanes were described in Chapter 5. Validation of forecasts using these data supports the underlying NWP forecasts, thus demonstrating the usefulness of the glider as an atmospheric probe. New relationships involving climb rate versus convective boundary layer depth were developed.

The major advance in weather forecasting for soaring flight has been the prediction by numerical models of climb rates and altitudes in convection. NWP-based flight planning also would benefit from such predictions for ridge and wave lift. A particular challenge with these types of lift is their spatial alignment. Current studies address these issues.

In spite of this progress, our knowledge concerning lift is incomplete. Over the past 80 or 90 years, soaring pilots have identified lift sources that can be categorized as convection, convergence, ridge, wave or some combination of these. It is not uncommon, however, for the soaring pilot to report lift with characteristics, or in a background environment, that do not fit our current conceptual models. It is possible that in the future, reports from soaring flights, combined with atmospheric research, will identify other, as yet unknown, lift sources.

CHAPTER 7

REFERENCES

7.1 ARTICLES

Baldauf, M., 2004: The Lokal Modell (LM) of DWD/COSMO. *Proceedings of ECMWF: Recent developments in numerical methods for atmospheric and ocean modelling*, 6–10 September 2004:41–52. (http://www.ecmwf.int/publications/library/do/references/list/161)

Doernbrack, A., R. Heise and J. Kuettner, 2006: Wellen und Rotoren. *Promet*, 32(1-2):18–24.

Forstner, B. and R. Prodinger, 2000: *Untersuchung von Gebirgswellen durch Auswertung von Segelflug- und Radiosondendaten*. Diplomarbeit Universität Wien, http://www.streckenflug.at/gebirgswellen/

Glendening, J., 2002: BLIPMAPs, *Soaring*, 66(7):30.

Gold, E., 1933: Maximum day temperatures and the tephigram. *Prof. Notes Met. Office*, London, 63.

Heise, R., 1999: Future aspects of meteorological support for competition flights. *Technical Soaring*, 23(1):13–16.

Hindman, E., R. McAnelly, W. Cotton, T. Pattist and R. Worthington, 2004: An unusually high summertime wave flight. *Technical Soaring*, 28(4):7–23.

Hindman, E., S. Saleeby, O. Liechti and W. Cotton, 2007: A meteorological system for planning and analyzing soaring flights in Colorado, USA. *Technical Soaring*, 31(3):68–78.

Joss, J., 1976: *Soar Sierra*, Los Altos, CA, Soaring Press.

Kalman, R. E., 1960: A new approach to linear filtering and prediction problems. *Trans. ASME J. Basic Eng.*, 82D(1): 35–45.

Kuettener, J. P., P. A. Hildebrand and T. L. Clark, 1987: Convection waves: observations of gravity wave systems over convectively active boundary layers. *Quart. J. R. Meteorol. Soc.*, 113:445–467.

Liechti, O. and B. Neininger, 1994: Alptherm – a PC-based model for atmospheric convection over complex topography. *Technical Soaring*, 18(3):73–78. Reprint in *Technical Soaring*, 29(2):55–62.

Liechti, O. and E. Lorenzen, 1998: A new approach to the climatology of convective activity. *Technical Soaring*, 22(2):36–40.

Liechti, O., 2001: Handicaps and Polars. *Technical Soaring*, 25(4):216–220.

Liechti, O., 2002: Regtherm. *Technical Soaring*, 26(1):2–5.

Liechti, O. and E. Lorenzen, 2004: TopTask meteorological flight planning for soaring. *Technical Soaring*, 28(4): 1–6.

Liechti, O., E. Lorenzen, R. Thehos, B. Olofsson and E. Olsson, 2007: Verification of thermal forecasts with glider flight data. *Technical Soaring*, 31(2):42–51.

Liechti, O., 2007: *Operational predictions of the potential flight distance for soaring in wind and thermals*. Presented at OSTIV Meteorological Panel Meeting, St Auban, France, September 2007.

Lindemann, C., R. Heise and W.-D. Herold, 2008: Lee waves in the Andes Region. *Technical Soaring*, 32(3):93–96.

Lissaman, P., 2007: Fundamentals of energy extraction from natural winds. *Technical Soaring*, 31(2):36–41.

Maul, C., 2008: Statistical analysis of competition flights. *Technical Soaring*, 32(3):97–106.

Müller, D. and C. Kottmeier, 1986: *Meteorologische Aspekte des Streckensegelfluges* (Hannover, self-published).

Müller, D., D. Etling, C. Kottmeier and R. Roth, 1985: On the occurrence of cloud streets over northern Germany. *Quart. J. R. Met. Soc.*, 111:761–772.

Olofsson, B. and E. Olsson, 2006: Automatic thermal forecasts from the Swedish HIRLAM model. *Technical Soaring*, 30(4):101–104.

Pretor-Pinney, G., 2006: In search of the Morning Glory, *Weatherwise*, Jan/Feb:20–25

Ragot, F., 2004: Best speed story. *Technical Soaring*, 28(1-2):1-54.

Sigrist, B., 2006: Use of topographic elevation models to identify thermal hotspots in Alpine areas. *Technical Soaring*, 30(3):53–60.

Steinacker, R., 1984: Area height distribution of a valley and its relation to the valley wind. *Beitr. Phys. Atmosph.*, 57:64–71.

Thehos, R., 2007: Wo steht die lange Welle? *Aerokurier*, 2/2007.

Trimmel, H. 1999: *Possible contributions of glider pilots with logger data to the knowledge of small and mesoscale weather phenomena*. Poster presented at the Mesoscale Alpine Project Appenzell meeting.

Young, G., 1987: The structure and prediction of thermals, *Soaring*, 51(8):37–49.

Weckwerth, T.M., J.W. Wilson, R.M. Wakimoto and N.A. Crook, 1997: Horizontal convective rolls: determining the environmental conditions supporting their existence and characteristics. *Mon. Wea. Rev.*, 125:505–526.

7.2 BIBLIOGRAPHY

Baines, P. G., 1995: *Topographic Effects in Stratified Flows*. Cambridge, Cambridge University Press.

Brigliadori, L. and R. Brigliadori, 2006: *Competing in Gliders – Winning with Your Mind*. Spettacolo, Bellavite. Blanchard, A., 1994: Les Pyrénées en planeur. Éditions Odyssée.

Bradbury, T., 2000: *Meteorology and Flight*. London, A & C Black.

Fièque, J. P., 2007: *Météo du vol à voile et du vol libre*. Toulouse, Cépaduès.

Hack, K. H., 2003: *Flugwetter*. Aviamet.

Hafner T., 1999: *Handbuch der Flugwettervorhersagen für die Luftfahrt, Vorabdruck zu den 26. Segelflugweltmeisterschaften 1999 in Bayreuth*.

Hertenstein, R., 2005: *Thermals*. Minneapolis, Bob Wander Books.

Irving, F., 1998: *The Paths of Soaring Flight*. London, Imperial College Press.

Kalkreuth, J.,1972: *Segeln über den Alpen*. Stuttgart, Motorbuch Verlag.

Kreipl, M., 1993: *Das Thermik-Handbuch*. Stuttgart, Motorbuch Verlag.

Lindsay, C. and S., Lacy, 1972: *Soaring Meteorology for Forecasters*. National Oceanic and Atmospheric Administration, National Weather Service, USA.

Palmer, M., 2004: *Practical Wave Flying*. Minneapolis, Bob Wanders Books.

Piggot, D., 2004: *Understanding Flying Weather*. London, Adlard Coles Nautical.

Reichmann, H., 1988: *Cross-country Soaring*. Stuttgart, Motorbuch Verlag.

Scorer, R., 1978: *Environmental Aerodynamics*. Chichester, Ellis Horwood.

Stull, R., 1988: *An Introduction to Boundary Layer Meteorology*. Springer.

Thomas, F., 1999: *Fundamentals of Sailplane Design*. Silver Spring, College Park Press.

Whelan, R., 2000: *Exploring the Monster*. Wind Canyon Books.

Whiteman, C. D., 2000: *Mountain Meteorology*. Oxford, Oxford University Press.

World Meteorological Organization and Organisation Scientifique et Technique Internationale du Vol à Voile, 1993: *Handbook of Meteorological Forecasting for Soaring Flight*. WMO Technical Note No. 158. Second edition (WMO-No.495). Geneva.

World Meteorological Organization, 1973: *The Airflow over Mountains*. WMO Technical Note No. 27. Geneva.

7.3 WEBSITES

BLIPMAP
http://www.drjack.info/

Digital elevation data
http://srtm.csi.cgiar.org/

FAI
http://www.fai.org/

METWATCH – Software
http://www.metwatch.de

Mountain Wave Project
http://www.mountain-wave-project.de

OSTIV
http://www.ostiv.fai.org

OSTIV Meteorological Panel
http://www.pa.op.dlr.de/ostiv/

RAOB
http://www.raob.com

TherMap
http://www.aerodrome-gruyere.ch/thermap

Thermal index maps
http://rams.atmos.colostate.edu/realtime/00z/index.php3

Thermal index tables
http://www.soarforecast.com/

WindMap
http://www.aerodrome-gruyere.ch/windmap

Worldwide forecasted and archived soundings
http://www.arl.noaa.gov/READY.html

APPENDIX

In general international standard units are used throughout this manual. In practice, and in some figures in this manual, other units are still used. Some basic conversion formulas shall be given here:

Nautical miles (nm):

1 nm = 1.853 km
1 km = 0.540 nm

Knots (kt):

1 kt = 1.853 km/h
1 km/h = 0.540 kt

1 kt = 0.514 m/s
1 m/s = 1.942 kt

Feet (ft):

1 ft = 0.3048 m
1 m = 3.2808 ft

Feet per minute (ft/min):

100 ft/min = 0.508 m/s
1 m/s = 196.9 ft/min

Degree Fahrenheit (°F):

Temperature (°C) = (Temperature (°F) 32) • 5/9
Temperature (°F) = Temperature (°C) • 9/5 + 32

Kelvin (K):

Temperature (°C) = Temperature (K) 273.15

Note: In this handbook Kelvins are only used to indicate temperature differences.

Hectopascal (hPa):

1 hPa = 1 mbar

ABBREVIATIONS

AAT	assigned area task with extended turn-point areas
AGL	above ground level
CAPE	convective available potential energy
CBL	convective boundary layer
COSMO	Consortium for Small-Scale Modelling
DMO	direct model output
DWD	German Weather Service
ECMWF	European Centre for Medium-Range Weather Forecasts
GM	global model
GPS	global positioning system
FAI	Fédération Aéronautique Internationale
IGC	International Gliding Commission
LM	local model
LT	local time
MOS	model output statistics
MSL	mean sea level
MWP	Mountain Wave Project
NWP	numerical weather prediction
OLC	Online Contest for soaring
PFD	potential flight distance
QNH	altimeter setting that provides the airfield altitude on landing
RAOB	rawinsonde observation program
RAMS	regional atmospheric modelling system
RASS	radio acoustic sounding system
RM	regional model
TAF	Terminal Aerodrome Forecast
UTC	universal time coordinated
VMC	visual meteorological conditions